

Seismic Design Factors and Allowable Shears for Strawbale Wall Assemblies

by

Sara Jalali

Research Assistant

and

Mark Aschheim, Ph.D. P.E.

Professor and Chair

Department of Civil Engineering
Santa Clara University

with

Martin Hammer, Architect

and

Kevin Donahue, S.E.

Working Draft
September 26, 2013

Contents

List of Figures.....	v
List of Tables	x
Abstract	1
1. Introduction	1
2. Experimental Behavior	3
2.1. Walls B, C, and E tested by Ash et al. (2003)	4
2.2. Slender wall tested by Faurot et al. (2004)	13
2.3. Strawbale infill tests (with post and beam framing) by Ramirez (1999).....	14
2.4. Squat wall tested by Nichols and Raap (2000)	20
3. Derivation of Allowable Shears	22
4. Lateral Stiffness and Compatibility with Light-framed Walls Sheathed with Wood Panels	30
5. Conventional Evaluation of Seismic Design Factors.....	31
6. Seismic Design Parameters Determined by Adjustment Based on Empirical Ductility Capacities.....	37
7. FEMA P695 Overview	41

8. Application of FEMA P695 methodology to the quantification of seismic performance factors to one and two-story strawbale wall buildings	47
8.1. System Design Requirements	48
8.2. Test Data Requirement.....	48
8.3. Adjustments for Allowable Shears and Seismic Mass	50
8.3.1. Adjustments made in the analyses using the SAWS model	51
8.3.2. Adjustments made in the analyses using the Pinching4 model	54
8.4. Identification of Archetype Configurations	54
8.5. Nonlinear Model Development.....	60
8.5.1. Hysteretic Models.....	60
8.5.2. Modeling Procedure	65
9. Modeling of Archetypes	73
10. Nonlinear Static (Pushover) Analysis.....	74
11. Nonlinear Dynamic Analyses.....	76
11.1. Normalization of the Records	76
11.2. Scaling of Record Sets.....	79
12. Uncertainty Evaluation	86
13. Performance Evaluation	87
14. Effect of different hysteretic model	91

15. Evaluation of overstrength Factor, Ω_0	92
16. Evaluation of the Deflection Amplification Factor, C_d	93
17. Summary and Recommendations	93
References	97
Appendix A	99
Draft Provisions (as proposed for the <i>Oregon Structural Specialty Code</i> on December 17, 2012)	99
Appendix B	112
Load-Deformation Plots of Straw Bale and Light-Framed Plywood Sheathed Wall Assemblies.....	112
Appendix C	120
Index building in three Archetypes	120
Appendix D	123
Unit area load	123
Appendix E	125
Building archetype loading	125
Appendix F	126
Building archetype Design	126
Appendix G	130

Sample OpenSees SAWS data file	130
#Wall B Archetype ID 1.....	130
#Wall B Archetype ID 3.....	132
#Wall E Archetype ID 1.....	134
#Wall E Archetype ID 3.....	136
#Wall E Archetype ID 5.....	138
Appendix H.....	141
Sample OpenSees Pinching4 data file.....	141
Appendix I	145
Sample C# Program File.....	145

List of Figures

Figure 1: Wall B details, from Ash et al. (2003)	6
Figure 2: Wall C details; from Ash et al. (2003)	7
Figure 3: Wall E details; from Ash et al. (2003)	8
Figure 4: Reversed cyclic loading protocol to 5% drift (4.92 inches).....	9
Figure 5: Load-Displacement Plots for Walls B, C, and E	10
Figure 6: Flexural cracks in Wall E (2.5% drift level).....	12
Figure 7: Wall E mesh failure (7.5% drift level)	12
Figure 8: Details of slender wall tested by Faurot et al. (2004).....	13
Figure 9: Load-displacement response of slender wall tested by Faurot et al.....	14
Figure 10: Cross Section of Test Unit 1 (Three-String Straw-Bale Wall), from Ramirez (1999).....	16
Figure 11: Cross Section of Test Unit 2 (Two-String Straw-Bale Wall), from Ramirez (1999)	17
Figure 12: Schematic elevation of wall and test-setup, from Ramirez (1999)	17
Figure 13: Load-displacement response of Test Unit 1 (from Ramirez (1999))	18
Figure 14: Load-displacement response of Test Unit 2 (from Ramirez (1999))	18
Figure 15: Schematic of Damage to Unit 2 at +3% Drift, from Ramirez (1999)	19
Figure 16: Envelope Curves for Units 1 and 2, from Ramirez (1999)	19

Figure 17: Elastic Response and Envelope Curves for Test Units 1 and 2 versus Drift, from Ramirez (1999).....	20
Figure 18: details of the wall from Nichols and Rap report.....	21
Figure 19: First monotonic loading, until failure of load cell attachment	21
Figure 20: First monotonic loading, until failure of load cell attachment	21
Figure 21: Third monotonic loading, until failure of specimen.....	22
Figure 22: Failure of the Raap and Nichols wall in shear	22
Figure 23: Rocking Model.....	25
Figure 24: Sketch defining seismic design factors (from Uang, 1991)	33
Figure 25: Response of Straw Bale Wall B.....	34
Figure 26: Response of Straw Bale Wall C.....	34
Figure 27: Response of Straw Bale Wall E.....	35
Figure 28: Evaluation of Displacement Quantities (adapted from W-13 for evaluation of Δy)	38
Figure 29: Key elements of the Methodology. [adapted from FEMA P695]	42
Figure 30: Idealized nonlinear static pushover curve. [adapted from FEMA P695].....	43
Figure 31: Test data for cement plaster walls reinforced with 2 x 2 by 14 gauge mesh (a) 4 feet long by 8 feet high (Faurot et al. 2004) (b) 8 feet long by 8 feet high (Ash et al. 2003)50	
Figure 32: The simplified backbone curves derived from test data of full-scale reinforced cement plaster walls having lengths of 4 and 8 ft, nominally 8 ft high.....	50

Figure 33: Adjusted experimental data for Wall E, reported by Ash et al (2003).....	52
Figure 34: Adjusted experimental data for Wall B, reported by Ash et al (2003)	53
Figure 35: MCE response spectra required for collapse evaluation of index archetypes designed for Seismic Design Category (SDC) D, FEMA P695	59
Figure 36: Hysteretic model of shear spring element included in SAWS program (Folz and Filiatrault, 2004a, b).....	61
Figure 37: Pinching4 Hysteretic Model	63
Figure 38: Wall B, Hysteretic response for test results and SAWS model.....	65
Figure 39: Wall E, Hysteretic response for test results and SAWS model.....	66
Figure 40: The behavior of model Wall E under earthquake using SAWS model in OpenSees (Archetype one,small-single family house, Imerial Valley 1979 earthquake).....	67
Figure 41: Illustration of negative stiffness in SAWS Model, Wall B.....	68
Figure 42: Illustration of negative stiffness in SAWS Model, Wall E.....	68
Figure 43: Example of correct calibration procedure (Haselton, 2006)	69
Figure 44: Wall E, Hysteretic response for test results and Pinching4 model.....	70
Figure 45: The behavior of model Wall E under earthquake using Pinching4 model in OpenSees (Archetype ID5, Two Story Building, Loma Prieta, Capitola 1989 earthquake)	71
Figure 46: The illustration of Rocking in Pinching4 model for Wall E.....	72
Figure 47: Modeling Straw bale shear wall in SAWS model.....	74
Figure 48: Monotonic Static Pushover curve on one story single family with Cement plaster wall material finishes (Wall E Archetype ID 3), determined using the SAWS model.....	75

Figure 49: Results of incremental dynamic analysis to collapse for the one-story large family building with Cement plaster wall material finishes (Archetype ID 3).....	84
Figure 50: Collapse fragility collapse curve for archetype 3 of Wall E.....	85
Figure 51: Plot showing the trend (and three circled outliers) in the probability of collapse of selected bearing wall systems, building frame systems and moment-resisting frame systems as a function of design period. Representative collapse probability and design period data shown in this figure are based on results of prior studies of FEMA P-695 (FEMA 2009) and NIST GCR 10-917-8 (NIST, 2010). From ATC-84 (2011).	95
Figure 52: Response of Straw Bale Wall B.....	112
Figure 53: Response of Straw Bale Wall C.....	113
Figure 54: Response of Straw Bale Wall E.....	114
Figure 55: Response of Cal Poly Straw Bale Wall.....	115
Figure 56: Response of Light-Framed OSB Sheathed Walls (Test 2) under CUREE Protocol.	116
Figure 57: Response of Light-Framed Plywood Sheathed Walls (Test 6) under CUREE Protocol.	117
Figure 58: A6: Response of Light-Framed Plywood Sheathed Walls (Test 1A) under SequentialPhased Displacement Protocol.....	118
Figure 59: Response of Light-Framed Plywood Sheathed Walls (Test 6A) under Sequential Phased Displacement Protocol.....	119
Figure 60: One-family 1200 ft ² home (Archetype Configuration #1) [NAHB Report].....	120
Figure 61: One-family 2100 ft ² home (Archetype Configuration #2)[NAHB Report].....	121

Figure 62: One-family 3000 ft² home (Archetype Configuration #3) [NAHB Report].....122

List of Tables

Table 1: Development of Allowable Shears for Strawbale Walls	29
Table 2: Evaluation of Secant Stiffness at the Allowable Design Level	31
Table 3: Evaluation of component R factors conventional methods.	36
Table 4: Evaluation of ductility capacities.....	36
Table 5: Evaluation of seismic design coefficients by conventional methods.	36
Table 6: Evaluation of “Design-Level” Ductility Capacities.....	40
Table 7: Proposed allowable shears for plastered strawbale wall assemblies	48
Table 8: Range of Variables Considered for the Definition of Strawbale Frame Archetype Buildings for Wall E (cement plaster)	55
Table 9: Range of Variables Considered for the Definition of Strawbale Frame Archetype Buildings for Wall B (clay plaster)	55
Table 10: Performance group for Wall E.....	56
Table 11: Performance group for Wall B	56
Table 12: Index Archetype Configurations for Straw bale wall Shear	58
Table 13: Structural Properties for Wall B Archetype Designs.....	59
Table 14: Structural properties for Wall E Archetype Designs, using the SAWS model	60
Table 15: SAWS Model Hysteretic Parameters Definitions	62

Table 16:: Pinching4 model hysteretic parameter definitions	64
Table 17: SAWS model parameters for Wall B and Wall E (8'x8')	67
Table 18: Pinching4 hysteretic model parameters for Wall E (8'x8')	71
Table 19: Summary of Earthquake Event and Recording Station Data [FEMA P695]	77
Table 20: Summary of PEER NGA database information and Normalization Factors	82
Table 21: Characteristics of the acceleration records at T=0.25 sec	83
Table 22: Spectral Shape Factor (SSF) for Archetypes Designed using SDC D_{max} (Taken from Table 7-1b FEMA P695)	85
Table 23: Quality rating of test design, modeling and design uncertainties	87
Table 24: Acceptable values of adjusted collapse margin values $ACMR_{10\%}$ and $ACMR_{20\%}$.	87
Table 25: The Summary of collapse results and adjusted collapse margin ratio for Wall B (clay plaster), using the SAWS hysteretic model.....	88
Table 26: The Summary of collapse results and adjusted collapse margin ratio for Wall E (cement plaster), using the SAWS hysteretic model.....	88
Table 27: The Summary of collapse results and adjusted collapse margin ratio for Wall E (cement plaster) using the Pinching4 model	89
Table 28: Results for Performance Group comprising one-story archetypes, Wall E (cement plaster), modeled with the Pinching4 hysteretic model.	90
Table 29: Results for Partial Performance Group comprising a single two-story archetype, Wall E (cement plaster), modeled with Pinching4 hysteretic model.	90

Table 30: Influence of hysteretic model and related assumptions on resulting ACMR for each archetype, for Wall E (cement plaster), for Seismic Design Category D_{max} .	92
Table 31: Unit area load for Wall E	123
Table 32: Unit area load for Wall B	124
Table 33: Building Archetype Loading	125
Table 34: Archetype 1 Small -Single Family 1200 Square feet (30'x40') Wall B	126
Table 35: Archetype 2 Large- Single Family 2100 Square feet (35'x60')Wall B	127
Table 36: Archetype 3 Townhouse- Family 3000 Square feet (30'x50')Wall B	127
Table 37: Archetype 1 Small -Single Family 1200 Square feet (30'x40') Wall E	128
Table 38: Archetype 2 Large- Single Family 2100 Square feet (35'x60') Wall E	128
Table 39: Archetype 3 Townhouse- Family 3000 Square feet (30'x50') Wall E	129

Abstract

Experimental studies relevant to the in-plane response of strawbale wall assemblies resisting seismic loading are summarized. Allowable shears for design are established for use with proposed code provisions. Parameters for seismic design (the response modification factor, R , the overstrength factor, Ω_o , and the displacement coefficient, C_d) are developed on the basis of results obtained using three distinct analytical frameworks: (1) a conventional approach in which the R factor is considered to be the product of terms associated with overstrength and ductility; (2) modification of the seismic design parameters accorded to another seismic-force resisting system, light frame walls sheathed with wood panels, based on relative ductility capacities of the two systems; and (3) application of the FEMA P695 methodology using a model containing mass lumped at the floor level and either the SAWS or Pinching4 element to represent response of the shear walls. Details of the application of these approaches are provided herein, along with a summary and conclusion regarding appropriate values of seismic design parameters.

1. Introduction

Strawbale construction originated in the United States in the late 1800s. A resurgence of interest in strawbale construction beginning in the 1980s has spurred the construction in at least 49 of the 50 states as well as the development of building code provisions and guidelines in at least six cities/counties and three states (California, Nevada, and Oregon). A variety of design and construction practices in existence was addressed in a multi-faceted research study conducted under the direction of the Ecological Building Network. This study brought together engineers, architects, and builders well-versed in straw bale construction, with the goal of establishing best practices informed by field experience and laboratory studies. The results of this study, supplemented by relevant studies conducted by others, provides the basis for work developed herein to establish seismic design factors

and allowable shears that are proposed for inclusion in the International Building Code.

Seismic design factors were developed by three separate approaches: a more conventional treatment following the framework described by Uang (1991) and the 1998 NEHRP Seismic Provisions (FEMA-302, year); application of ductility based adjustments to the seismic design factors determined for light-framed walls with wood shear panels, and application of the recently developed FEMA P695 methodology. Results of these approaches were considered in developing the seismic design factors recommended for use with strawbale construction.

In many regards, strawbale construction is similar to light-frame buildings with wood shear panels. Wood frame buildings have similar occupancy, size (footprint and number of stories), gravity framing systems, and spatial disposition of lateral resisting elements. Thus, assumptions made in evaluation of light-framed walls sheathed with wood panels are often adopted in the present work on strawbale construction (except where a different assumption is more pertinent).

Thus, precedents established in FEMA P695 and the NAHB report (March 2011) for the evaluation of light-framed buildings with wood panels were often adopted in the present evaluation of strawbale construction. Thus, relevant archetypes were selected from among those defined in the NAHB report, even though these had symmetric wall configurations that did not induce a torsional response (in plan). Similar “pancake” models were used even though these do not allow for the explicit consideration of P- Δ effects. No non-structural partitions or gravity framing was modeled. Collapse was defined at wherever the interstory drift exceeded 7% of the height, which invariably was on the horizontal portion of the IDA curves. Although one may always seek higher fidelity models, the acceptance of the FEMA P695 and NAHB efforts would suggest that the assumptions made herein would be acceptable as well.

2. Experimental Behavior

The response of plastered straw bale wall assemblies to in-plane lateral loads has been the subject of several research studies. Of primary interest are the walls tested by Ash et al. [2003]. Six full-scale specimens (nominally 8 ft. high by 8 ft. long) were tested. The specimen designs culminated from a series of small and medium scale tests designed to identify best practices for design and detailing for seismic performance. Of the walls subjected to reversed cyclic inelastic loading, two clay plaster wall assemblies (Wall B, using welded wire mesh reinforcement, and Wall C, using polypropylene mesh reinforcement) and one cement plaster assembly (Wall E, using welded wire mesh reinforcement) were considered to have the best inelastic behavior relative to that obtained using the materials and detailing provided in the other walls that were tested. Test results from these walls are supplemented by results obtained in other research studies, as follows:

Faurot et al. (2004) reported the results of a slender wall (nominally 8 ft. high by 4 ft. long) that, other than its length, had nominally identical materials and details as Wall E.

Ramírez (1999) reports the results of two 8 ft. high by 8 ft. long specimens built using a cement plaster (stucco) on one side of the wall and gypsum plaster on the other side. In each case the plaster was reinforced with 17-gauge galvanized woven wire stucco netting. Each wall was bounded by post and beam framing; in Unit One, three-string bales were used and only the bales were directly confined by the post and beam framing; for Unit Two, two-string bales were used and the plaster facings were directly confined (in bearing) by the post and beam framing.

Nichols and Raap (2000) report a test in which a shear failure was observed. This nominally 8 ft by 8 ft wall was built using cement plaster (stucco) reinforced by a 2" by 2" 16-gauge welded wire mesh. A post and beam frame ran along the perimeter of the wall, and lag screws protruding from the post and beam frame provided for mechanical transfer of shear between the plaster and frame. Unlike the preceding tests, loads were applied

monotonically. However, the test had to be repeated several times to finally reach the load causing failure. Salient aspects of these tests are described in the following.

2.1. Walls B, C, and E tested by Ash et al. (2003)

Ash et al. report on the tests of six full-scale walls, each nominally 8 ft high by 8 ft. long. The walls were made with three-string rice bales. Three were made using a clay plaster, and three were made using a cement plaster. Each series of three walls was conceived to represent a range of details derived from the preferences of a variety of builders combined with the results of small and medium scale tests conducted earlier, as part of the same coordinated and comprehensive test program that the in-plane tests were part of. The plasters themselves represent the range of relatively weak to relatively strong plasters, while the details represent “low”, “medium” and “high” levels of detailing. One objective of the tests was to discern the degree to which improved details resulted in improved hysteretic response (e.g. stiffness characteristics and ductility). The tests indicated that clay plaster walls B and C performed well, along with cement plaster wall E. Thus, these walls and their respective detailing requirements form the basis for the proposed code provisions, with consideration given to results from other tests, typically more limited in breadth and in some cases having details that differ from those proposed. Construction details for walls B, C, and E are presented in Figure 1 , Figure 2 and Figure 3 respectively.

The clay and cement plasters were each nominally 1-1/2 inches thick. The clay plaster is comprised of clay, sand, water, and straw fibers. Compression tests of 2” cube samples yielded an average compressive strength of 290 psi after curing for 44 days in the laboratory.

The cement plaster (or stucco) was mixed in a mortar mixer using the following quantities (by volume measure): 30 gallons of sand, 8 gallons of cement, 2 gallons of slaked lime, and 6-1/2 gallons of water. The lime had been hydrated prior to mixing by mixing in 6 gallons

of water per 50-pound bag of slaked finish lime. This mixture was allowed to hydrate for five days until the lime ceased absorbing water. At 7 days, a three cube set of cement plaster had an average strength of 1850 psi. At 36 days, three cubes from the same batch had an average strength of 2210 psi, while another set of three cubes from the same batch had a strength of 2200 psi at 95 days.

The walls were loaded laterally by a hydraulic actuator. Vertical load was applied at the top of the walls to approximate a uniform load along the top of the wall equal to 200 plf. This is considered to be on the light side of the dead load to be expected from a roof in single story construction. Because the lateral load was applied by means of a heavy steel tube section running along the top of the beam, a system of counterweights was devised such that the net load applied to the beam would be approximately 200 plf.

Each of these wall specimens was subjected to reversed cyclic loading as defined in Figure 4, which plots drifts of up to 5% (4.92 inches at the top of the wall). The lateral force applied at the top of the wall and corresponding displacement, for the each wall, is plotted in Figure 5. It should be noted that two complete cycles of displacement to 7% drift were applied subsequently, under manual control.

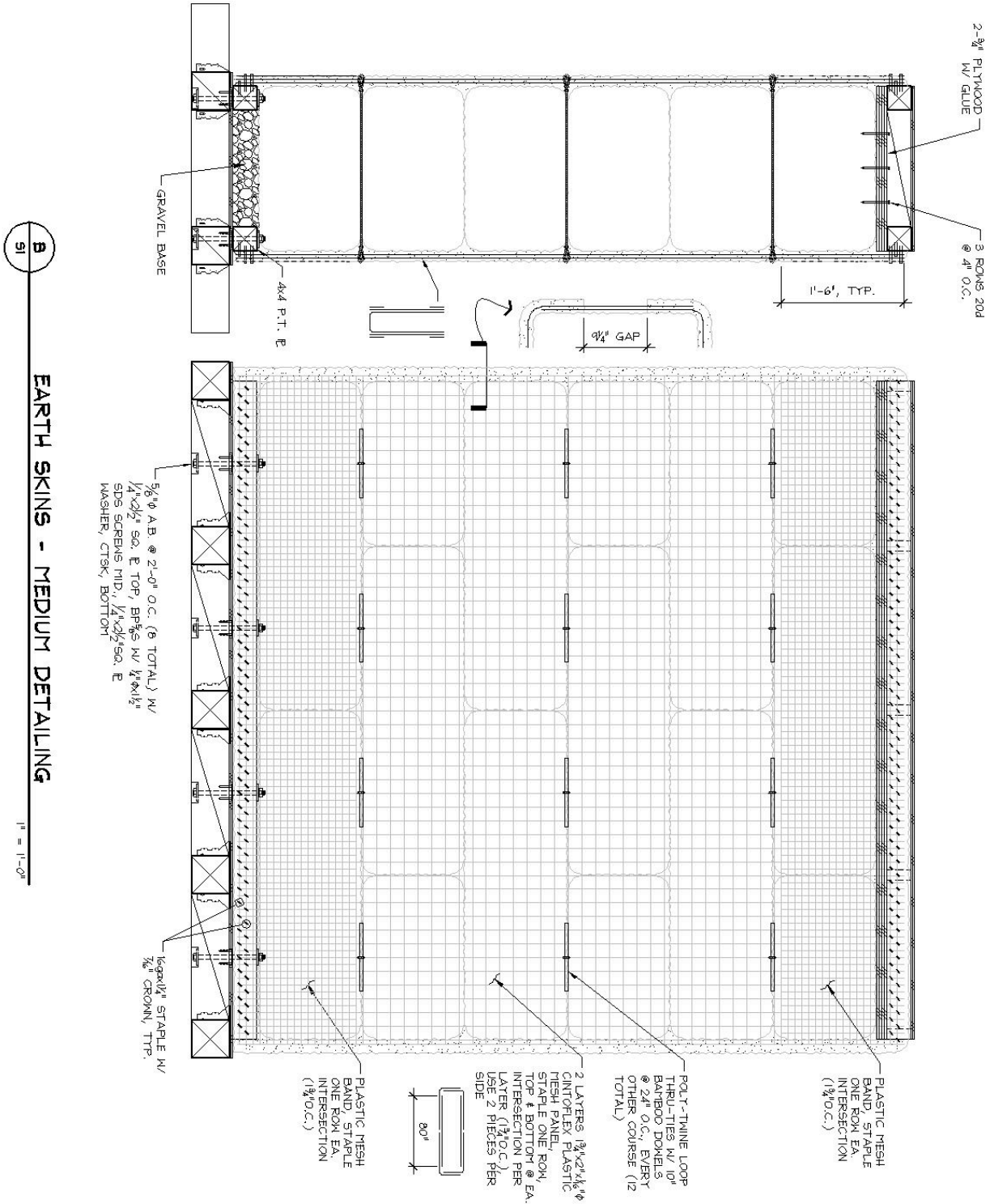


Figure 1: Wall B details, from Ash et al. (2003)

E
SI

CEMENT STUCCO SKINS - MEDIUM DETAILING

1" = 1'-0"

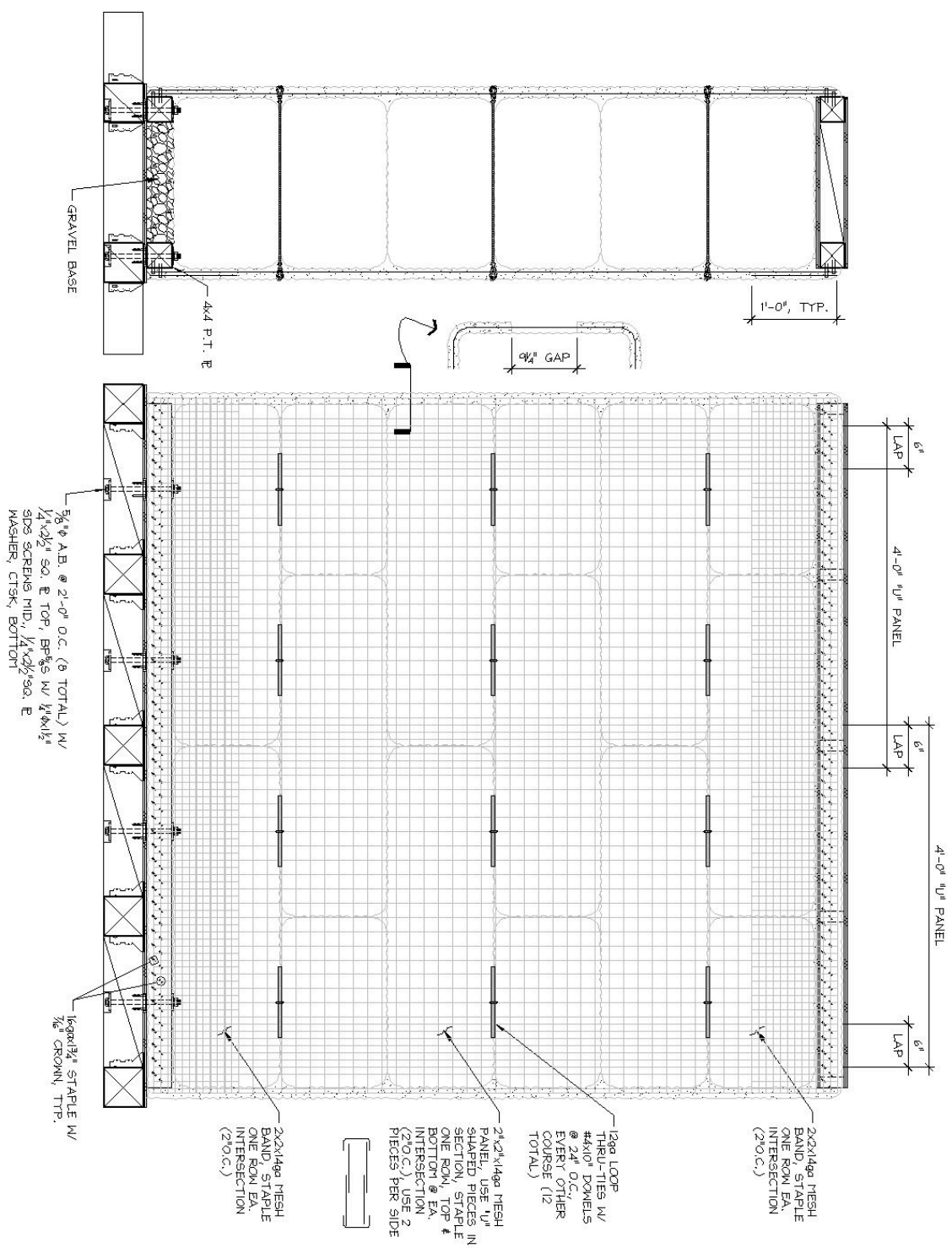


Figure 3: Wall E details; from Ash et al. (2003)

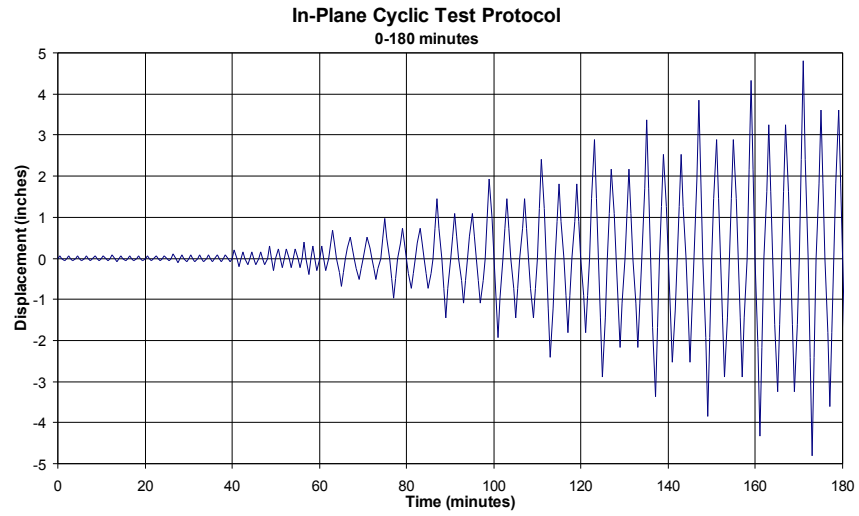
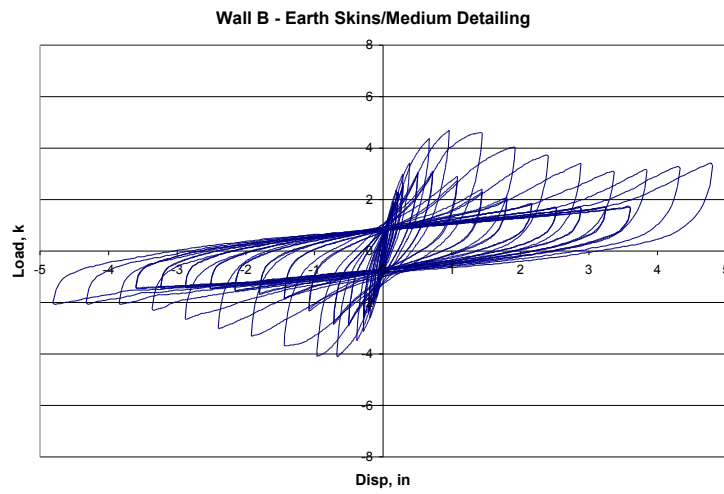


Figure 4: Reversed cyclic loading protocol to 5% drift (4.92 inches).



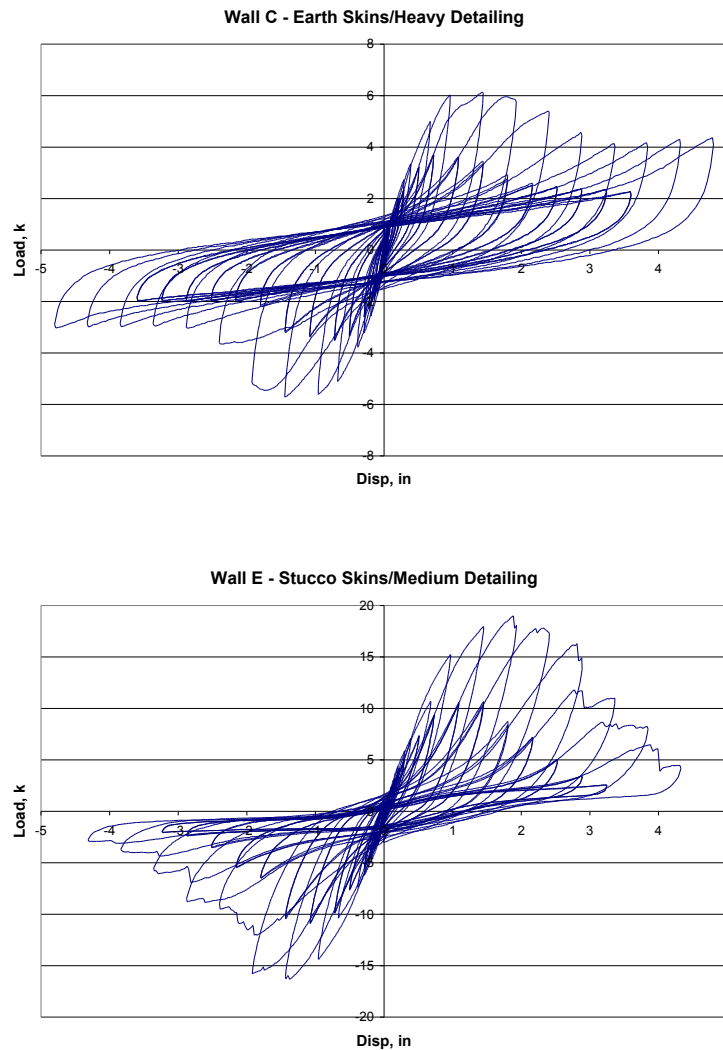


Figure 5: Load-Displacement Plots for Walls B, C, and E

Wall B was designed and built with a plastic reinforcing mesh. During testing, the predominant failure mode observed was compression zone crushing and base sliding, with the base sliding becoming more pronounced at later stages of the test. The peak capacity of 4.7 kips was reached on the 8th load step, at a drift level of 1% (0.96 inches). Looking at the load-displacement plot in Figure 5, the change in the hysteresis loops with increasing displacements suggests that sliding of the wall becomes more significant at higher displacements. Manual measurements taken to assess the sliding behavior indicated 3/4"

amplitude (peak to peak) of slip during load step 14 (4% drift), accounting for 20% of the actuator displacement at this amplitude. The higher amplitude cycles were observed to wear down the earth plaster at the base, which gradually reduced it to sand, clay, and straw components. This wearing and crushing caused a corresponding reduction in the height of the wall, and the soil debris served as a wedge to push the plaster out of plane, away from the bales, in the portion of the cycle in which the plaster was loaded in compression.

Wall C used a heavy 2"×2" 14-gauge wire mesh, with the first course of bales anchored to the base via plywood plates and threaded rods. As shown in Figure 5, these modifications resulted in an increase in the lateral strength of this wall relative to that of Wall B, with a peak load of 6.1 kips occurring at 1.5% drift (1.44 inches). At 1% drift, the 6.0 kip resistance was an increase of nearly 30% over the corresponding resistance of Wall B at this drift level. The overall response of this wall was similar to that of Wall B, with predominant failure modes consisting of crushing of the earth plaster and sliding of the wall at its base. The heavier mesh was observed to reduce the slip at the base of Wall C from a peak-to-peak amplitude of 3/4" in Wall B to 1/2" amplitude in this specimen at a drift of 4%. No flexural tension cracks were observed during testing of Wall C, suggesting the wire mesh created an "over-reinforced" condition in the sense that this word is used in reinforced concrete.

The medium-detailed cement plaster wall also used the heavier 14-gauge 2" × 2" mesh; additional staples were used to attach the plaster to both the sill plate and the header beam. Through-ties running through the thickness of the wall and anchored by dowels in the body of the stucco were installed at every other course, erring on the side of caution that such ties might be important to reduce the likelihood of buckling of the plaster; this is now considered unnecessary as the plaster is well-adhered to the straw, and each piece of straw acting axially provides lateral bracing to the plaster. A 4×4 sill plate was used and was anchored at 2-ft centers. The combination of cement stucco skins and the heavier wire mesh resulted in an increased lateral strength, having a peak value of 19 kips at 2% drift, as shown in Figure 5. Several flexural cracks developed within the bottom third of the wall

height as shown in Figure 6. The ultimate failure mode for Wall E was the loss of tensile capacity of the reinforcing mesh, from both mesh fracture and staple pull out, as shown in Figure 7. The mesh fracture was attributed to a combination of tensile elongation and low-cycle fatigue associated with the load reversals, which appeared to work the vertical wires of the mesh. The failures predominately occurred at the staple locations with some failures also occurring at the intersections of the horizontal and vertical wires, where the wires are spot welded together in the manufacturing of the mesh.



Figure 6: Flexural cracks in Wall E (2.5% drift level) Figure 7: Wall E mesh failure (7.5% drift level)

More generally, for in-plane behavior the plaster provides high initial stiffness that can serve to limit peak displacement response; as inelastic behavior develops in the plaster, a relatively soft core comprising the bales themselves is able to tolerate substantial displacements. During the tests, the walls proved to be very stable for gravity loads, with no gravity load failures occurring. At the conclusion of the prescribed loading (Figure 4), the walls were then tested under manual control for two cycles to drifts of $\pm 7.5\%$, which corresponded to the stroke limit of the actuator. Under manual control, the walls simply rocked, with the bale joints opening up and then closing again. No degradation in the

gravity load support mechanisms was evident, and there seemed little point to applying additional cycles of load. It seems likely that the walls could tolerate simultaneous orthogonal excitation without significantly compromising their ability to maintain support for gravity loads given the relatively generous width of the bales.

2.2. Slender wall tested by Faurot et al. (2004)

Faurot et al. sought to test a more slender version (Figure 8) of the cement plaster wall, Wall E, reported by Ash et al. The Faurot wall was nominally 4 ft long (in plan) and 8 ft high. It used 14-gauge 2" by 2" welded wire mesh, attached with 16-gauge 1-3/4" leg 7/16" crown staples. The nominal 1-1/2" thick cement plaster (stucco) consisted of 12 parts sand, 4 parts Portland cement, 1 part lime, and water.

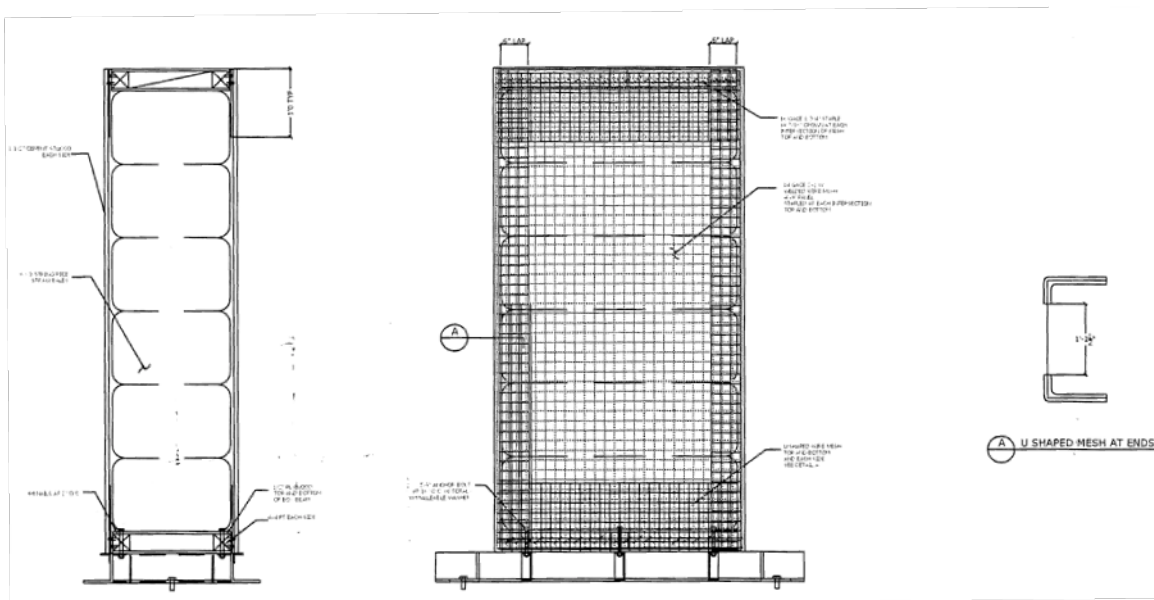


Figure 8: Details of slender wall tested by Faurot et al. (2004).

The lateral loading protocol matched that given in Figure 4. Unlike the Ash et al. tests, no superimposed vertical loads were applied to the Faurot et al. wall. The resulting lateral load-lateral displacement response is given in Figure 9. The peak strength was 7000

pounds.

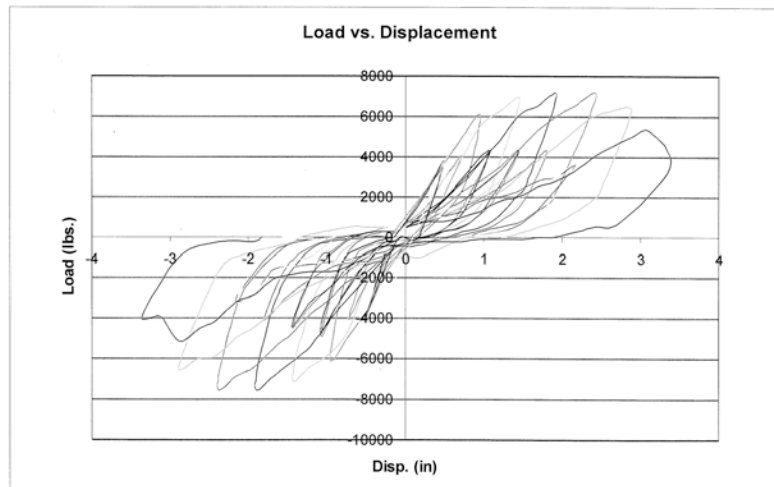


Figure 9: Load-displacement response of slender wall tested by Faurot et al.

2.3. Strawbale infill tests (with post and beam framing) by Ramirez (1999)

Ramirez (1999) reports the results of two full-scale wall tests. Although the details differ from those contained in the proposed code provisions, the tests are of interest because (1) they address the influence of directly confining the plaster within a post and beam frame and (2) Ramirez determines R factors consistent with the methodology described by Uang (1991) and the 1998 NEHRP Provisions.

Test Unit 1 consisted of three-string bales laid flat and plastered with Portland cement plaster (stucco) on one side and gypsum plaster on the other side (Figure 10). Reinforcement on both plaster faces consisted of 17-gauge woven wire stucco netting. The straw bale wall was built as in-fill within a previously constructed timber post and beam frame.

Test Unit 2 consisted of two-string bales laid flat and plastered with Portland cement plaster (stucco) on one side and gypsum plaster on the other side (Figure 11). Because the

two-string bales are narrower, the plaster faces extended to the post and beam framing and thus bore directly on and were confined through direct contact with this framing. Plaster reinforcement was the same as for Test Unit 1.

The cement plaster was composed of approximately 1 part masonry cement, 3 parts sand and enough water for a proper consistency. The gypsum plaster was composed of approximately 1 part gypsum based plaster, 2 parts sand and sufficient water for the correct consistency. Approximately 10g (0.02lbs) of 25.4 mm (1 in) chopped polypropylene fibers was added to both mixtures for crack control. Compressive strengths of 2" cube samples of the cement plaster averaged 2350 psi and 1675 psi for Test Units 1 and 2, respectively, while those of the gypsum plaster averaged 1075 psi and 845 psi, respectively. Average plaster thickness was considered to be 1.4 inches.

Both specimens were subjected to reversed cyclic lateral load applied at the top of the wall. No superimposed gravity loads were applied, not even by a loading beam (Figure 12). Load-displacement response is provided in Figure 13 and Figure 14 for Test Units 1 and 2, respectively. Peak strengths were 9.9 kips (44.4 kN) for Test Unit 1 and 13.6 kips (50.8 kN) for Test Unit 2, illustrating a 37% increase in strength resulting from the direct confinement of the plaster by the post and beam framing.

Test Unit 1 developed its peak strength at $\pm 2\%$ drift (equal to a roof displacement of ± 50.8 mm (2 in)). At $\pm 3\%$ drift, the lateral resistance dropped to less than 80% of the peak strength (a common definition of ultimate displacement capacity) and the test was discontinued to preserve the integrity of the frame for future tests.

Test Unit 2 had a lateral resistance at 2% drift of 53.7kN (12.1kips), 18% higher than unit 1. Unit 2 had a maximum lateral resistance of 60.4kN (13.6kips), at 3% drift. At +3.1% drift, the 101 by 101mm (4 by 4in) Douglas fir member of the built up column cracked in shear, as shown in Figure 15. The crack caused the resistance of Test Unit 2 to drop instantaneously by 20%. The test was discontinued after this crack occurred.

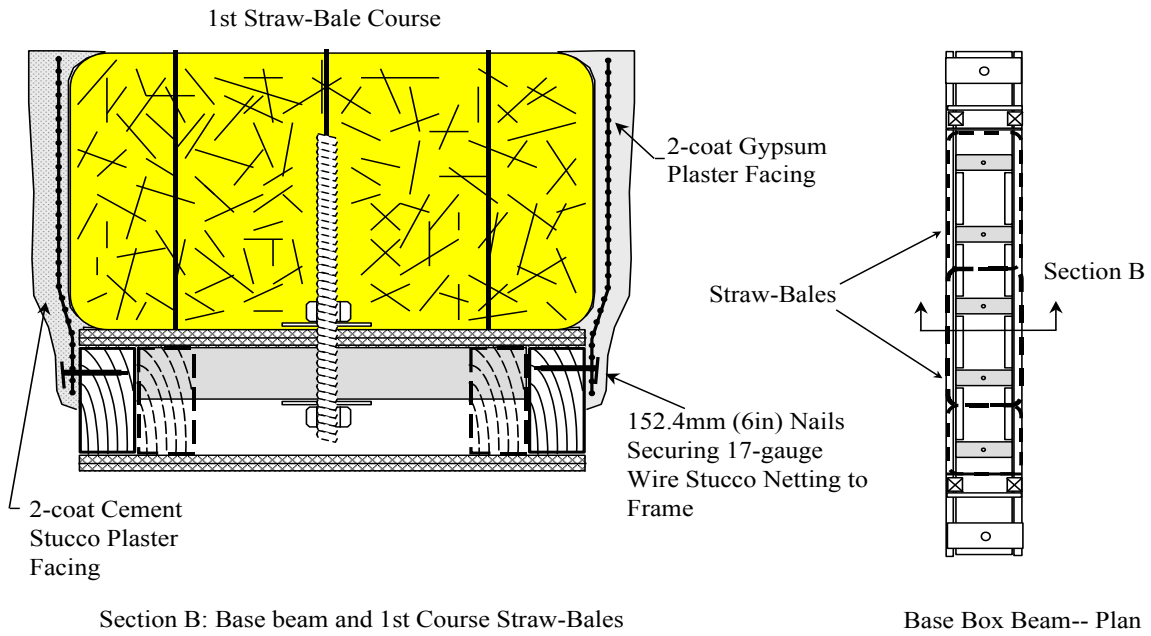


Figure 10: Cross Section of Test Unit 1 (Three-String Straw-Bale Wall), from Ramirez (1999)

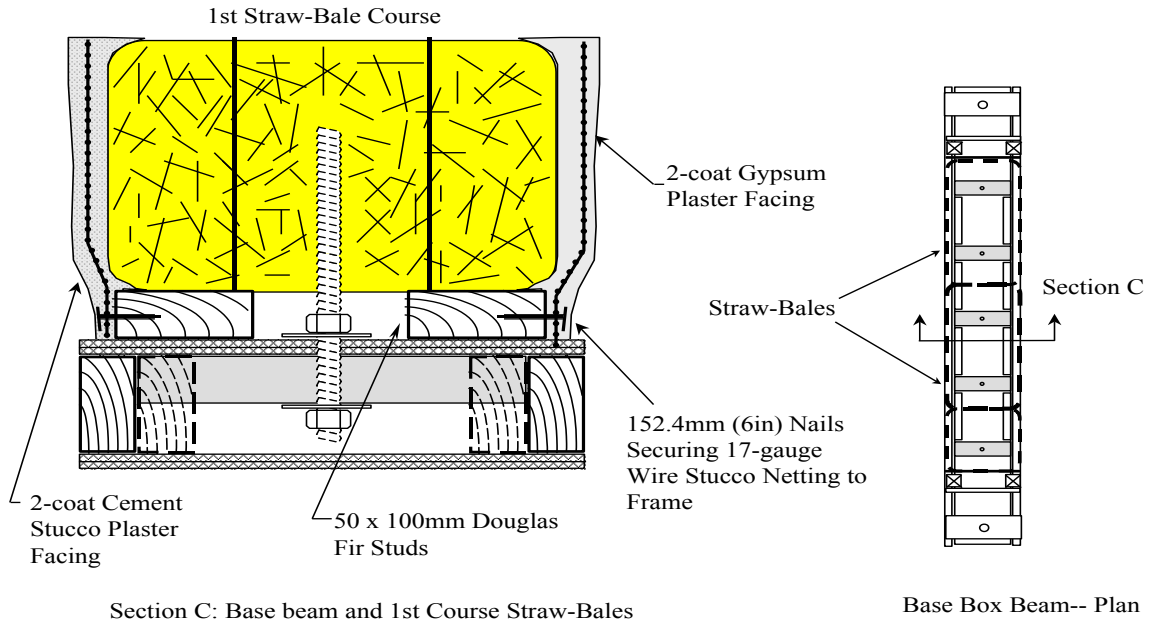


Figure 11: Cross Section of Test Unit 2 (Two-String Straw-Bale Wall), from Ramirez (1999)

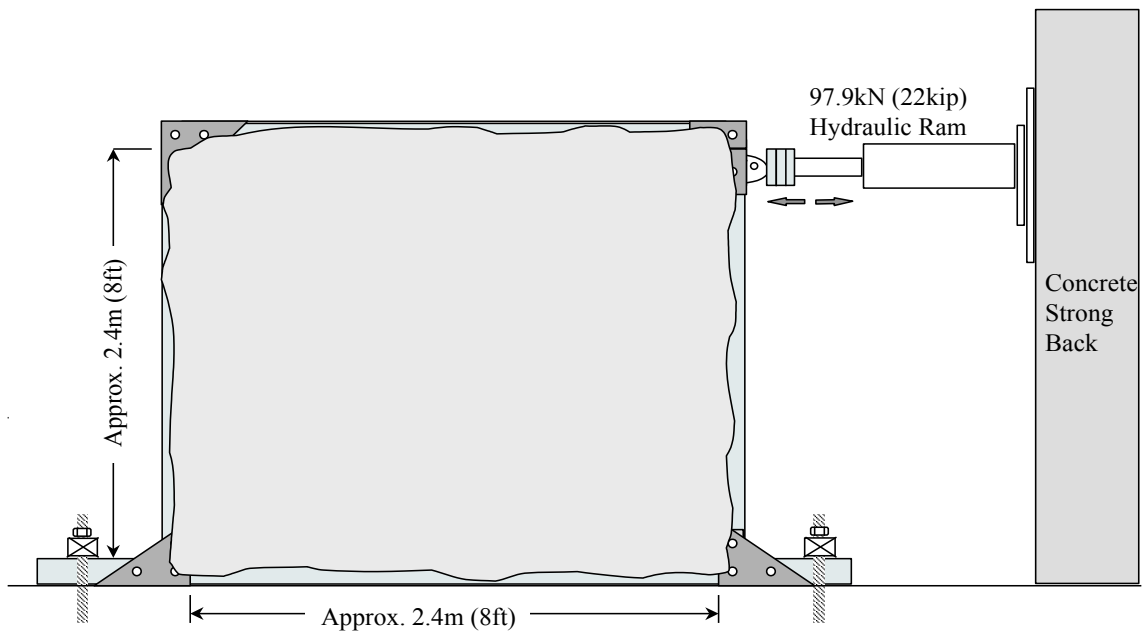


Figure 12: Schematic elevation of wall and test-setup, from Ramirez (1999)

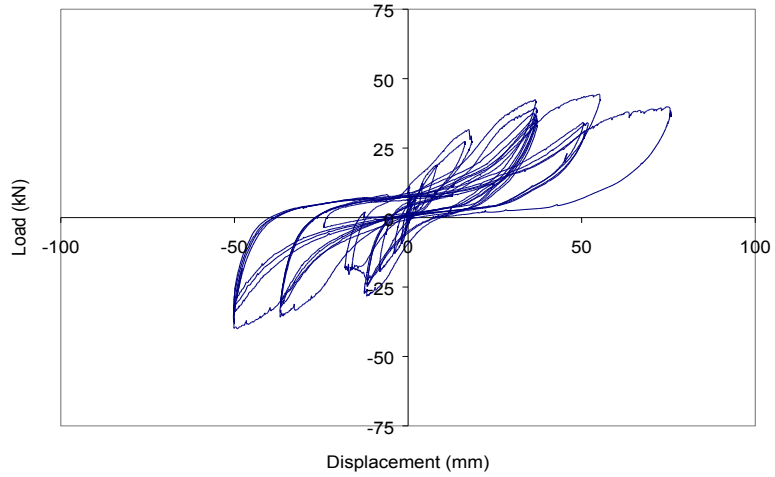


Figure 13: Load-displacement response of Test Unit 1 (from Ramirez (1999))

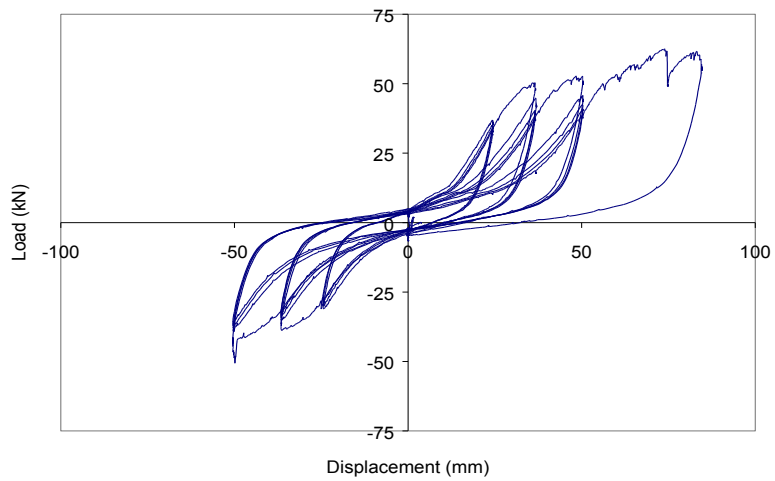


Figure 14: Load-displacement response of Test Unit 2 (from Ramirez (1999))

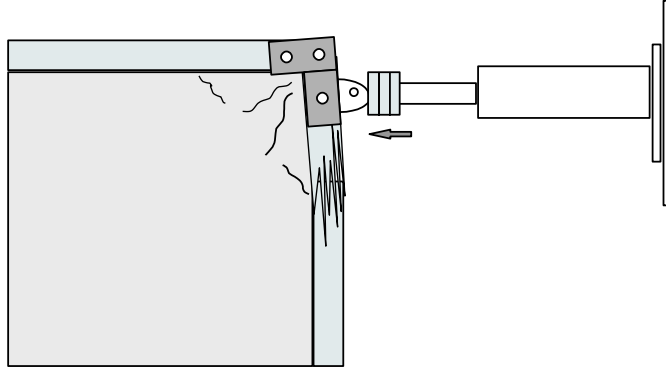


Figure 15: Schematic of Damage to Unit 2 at +3% Drift, from Ramirez (1999)

Figure 16 shows a comparison of the envelope curves obtained for Test Units 1 and 2 as a function of drift.

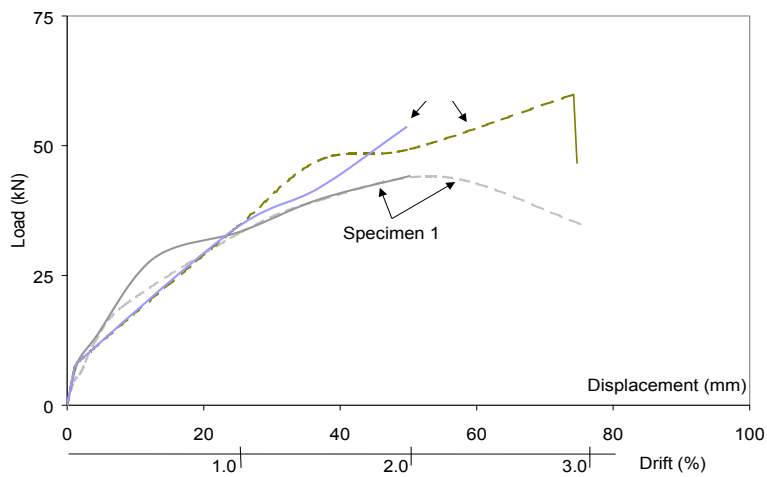


Figure 16: Envelope Curves for Units 1 and 2, from Ramirez (1999)

Using relationship C5.2.1-3 presented in the FEMA 302 provisions and determined by Uang (1991), given as

$$R = R_d \cdot \Omega_0$$

Ramirez determined the response modification factor to be equal to $R = 4 \cdot 1.0 = 4$ (see Figure 17). Based on the elastic response, the elastic seismic force demand, V_E , and elastic seismic

displacement demand, D_E , are respectively interpolated as 144 kN (32.4 kips) and 57 mm (2.2 in). These values are based on the design strength, V_y .

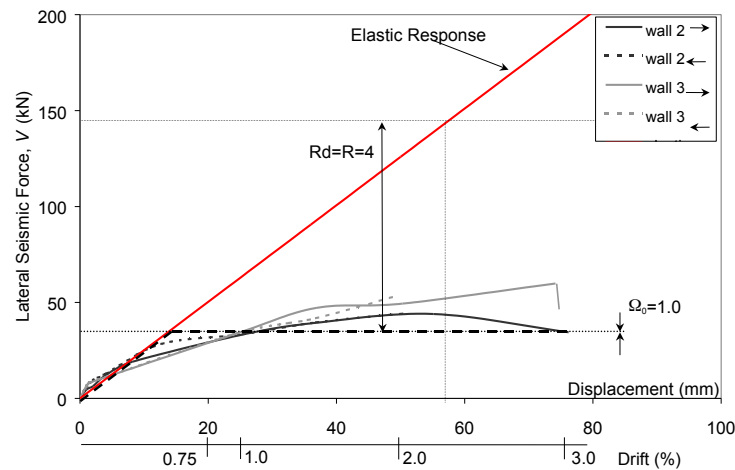


Figure 17: Elastic Response and Envelope Curves for Test Units 1 and 2 versus Drift, from Ramirez (1999)

This framework for determining the response modification factor, R , was applied to Walls B, C, and E in a later section of this report.

2.4. Squat wall tested by Nichols and Raap (2000)

Nichols and Rap (2000) report results for a nominally 8 ft high by 8 ft. long wall subjected to monotonic loading. Cement plaster was applied to both faces of the wall and reinforced with 16 gauge 2 in. by 2 in. welded wire mesh. Each plaster face was approximately 1-1/4 in. thick. Figure 18 illustrates details of the wall, including the use of 5/16 inch diameter lag screws placed at 4 in. around the perimeter of each side of the wall. The lag screws protruded 3/4 inch out from the wood framing in order to engage the plaster so that a very stiff and strong mechanism was available for transfer of shear between the plaster and wood framing. Overturning tension and compression carried by vertical box beam boundary members. The box beams utilized 4 x 6 members at each side, with a pair of Simpson hold-downs at their bases.

The wall was to be tested under monotonic loading until failure. However, due to problems with the test setup, failure was achieved only on the third test. Shortly after cracks appeared on the right face at 31,370 pounds, the wire lath on the left side (which had begun cracking at 21,450 pounds) began to break in tension at the center of the wall (Figure 22). The peak lateral strength was 36,835 pounds.

Figure 18: details of the wall from Nichols and Rap report

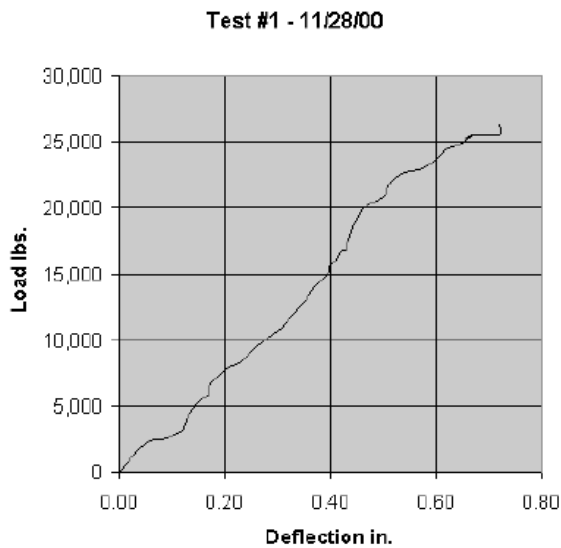


Figure 19: First monotonic loading, until failure of load cell attachment

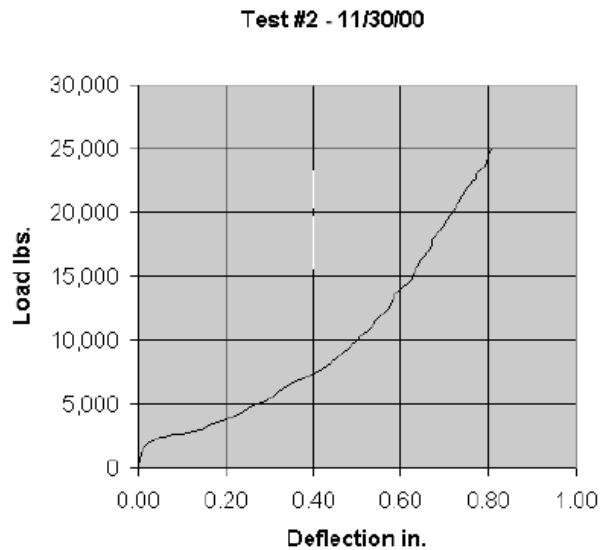


Figure 20: First monotonic loading, until failure of load cell attachment

3. Derivation of Allowable Shears

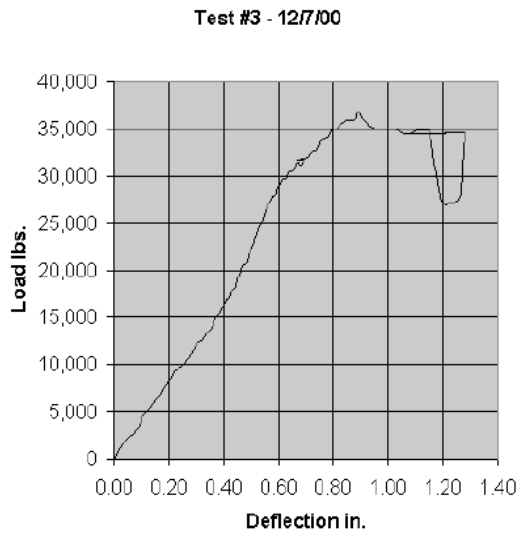


Figure 21: Third monotonic loading, until failure of specimen



Figure 22: Failure of the Raap and Nichols wall in shear

Allowable shears are derived first for the tested walls (B, C, and E) and then extended to consider plasters of different strengths and mesh reinforcement. The tested walls all displayed flexural failures. Therefore, the true shear strengths are higher than the shears required to obtain flexural failures.

All tested walls were nominally 8 ft. high and were tested as cantilevers restrained at the base. The height from the top of the sill to the centerline of the actuator is estimated as 107.5 inches, based on six bales each 16 inches high, a 5-1/2 inch high box beam, and half the height of the 12" high steel tube section used to apply load at the top of the box beam.

The plasters used in the test specimens, having mean cube strengths of 2200 and 290 psi for the cement and clay plasters, respectively, are stronger than the baseline strengths allowed in the proposed IBC provisions. Flexural strengths and associated shears were estimated using a monotonic moment-curvature analysis using the program BIAX (Wallace, 1992). The reinforced plaster was analyzed, without consideration of the relatively small contribution of the bales to flexural strength.

Analyses for Wall E were made using a modulus of elasticity of plaster, E_p , taken as $818 f'_p$, where f'_p is the cube compressive strength of the plaster, and the strain at ultimate strength was taken as 0.0025, based on results presented by Vardy (2009). Parker et al. (2006) reports the mean strength of the mesh wire to be 384.2 pounds (1.709 kN) and this strength was represented in the BIAx model (rather than the lower strengths observed for unplastered meshes anchored by staples). A 5,000-pound vertical load was applied at the top of the wall model, representing the estimated dead load and a superimposed load of 200 plf. Using these assumptions, the flexural strength under monotonic loading was determined to be 2,247 kip-in, and this strength would be reached with an applied force (shear) of 20.90 kips. This result compares well to the flexural strength of 19 kips obtained under reversed cyclic loading, and accommodates the possibility that some degradation in strength and/or stiffness occurred under prior repeated inelastic load reversals.

The average of the strengths observed in each quadrant (I and III) are used to derive allowable shears. For Wall E, the average strength is 17.65 kips; for Walls B and C, the averages are 4.40 kips and 5.93 kips, respectively.

Moment-curvature analyses can readily account for effects such as changes in plaster compressive strengths and plaster thicknesses. Consequently, effects of such changes on flexural strength were evaluated by using moment-curvature analyses to derive factors by which to adjust the empirically determined strengths. For example, so-called “hard” plasters are considered in the proposed IBC provisions, having minimum cube compressive strengths of 600, 1000, and 1400 psi. Minimum plaster thicknesses of 7/8, 1, and 1.5 in. are considered to correspond to average thicknesses of 1, 1-1/8, and 1-5/8 in., respectively. Adjustment factors were derived for these changes on the basis of the peak flexural strengths determined in moment-curvature analyses (Table 1, Columns 7 & 8). The modulus of elasticity used in the analyses of these “hard” plasters was determined as $818 f'_p$.

16-gauge wire is drawn through finer dies and thus the smaller diameter wires tend to display a higher yield strength, due to strain hardening. For example, Parker et al. (2006) report mean strengths of 103.8 ksi (716 MPa) for 16-gauge mesh and 77.2 ksi (532 MPa) for 14-gauge mesh. To be conservative, however, the flexural strength expected for 16-gauge mesh reinforcement was taken at 60% of the strength of that applicable for the 14-gauge mesh, based simply on the reduction in cross-sectional area ($0.003019 \text{ in}^2 / 0.005026 \text{ in}^2 = 0.60$). This is reflected in footnote k of Table 2405.15 of the proposed IBC provisions.

Similarly, 17-gauge woven wire would be expected to have a yield strength greater than that of the tested 14-gauge mesh wires. As with the 16-gauge mesh, this potential increase in yield strength was ignored, and flexural strengths were taken as 72.9% of that obtained for 14-gauge mesh, based on both the reduction in cross sectional area and spacing of the wires ($0.002290 \text{ in}^2 / 0.005026 \text{ in}^2$)*(2 in. / 1.25 in.)= 0.7290 (see Table 1).

The proposed IBC provisions specify a minimum cube compressive strength of 100 psi for clay plasters. The tendency of the moment-curvature analyses to greatly overestimate the lateral strength of Wall C (15.28 kips compared with 6.14 kips) is attributed to the relatively rapid degradation of the compression zone under repeated inelastic cyclic loading. Even so, a reduction in flexural strength would be expected as f'_p changes from 290 to 100 psi. The moment-curvature analyses indicate a flexural strength of 69.22% relative to that obtained with $f'_p = 290$ psi. This reduction was applied to walls made with plaster designations A2 and A3.

Clay plaster designation A1 contains no reinforcing mesh. Its resistance to lateral load is dominated by the resistance to rocking afforded by its self-weight. Self-weight was estimated assuming the average plaster thickness is $\frac{1}{4}$ inch greater than the specified minimum thickness of 1-1/2 inch. To be conservative, possible superimposed load was assumed to be zero. Using the model of Figure 23, a uniform bearing length, L_c , was determined for plaster cube strengths of 290 and 100 psi, in order to generate a vertical

reaction at the base of the wall equal to the self weight of the wall, W . For this free body diagram, the associated lateral force, V , required to cause tipping was determined. The change in cube strength from 290 to 100 psi was determined to result in a tipping strength equal to 93.68% of the lateral strength of 1.36 kips determined in this analysis.

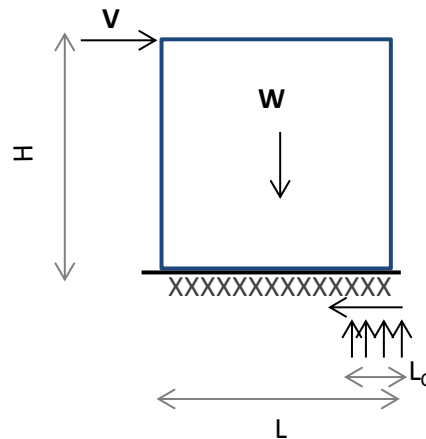


Figure 23: Rocking Model

Factors of safety were applied to develop allowable shears for allowable stress design. The CUREE-Caltech Woodframe project reports that “tabulated ASD values that are currently used for seismic design of woodframe shear walls are not based on the yield strength of the walls, but are instead based on an ultimate strength divided by a safety factor” (p. 158-159, W-30a. 2004). Factors of safety for plywood walls vary from 2.5 to 3.1 and average 2.9. Thus, a factor of safety of 2.9 was applied to the ultimate strength (taken as the average of the ultimate strengths obtained in quadrants I and III) for the hard plaster walls. The clay (soft) plaster walls exhibited greater ductility capacity than the cement plaster walls. For a given load-displacement response, there is a tradeoff between the R value and the Factor of Safety. That is, one can use a lower R value and a higher allowable shear and achieve the same resulting design. The clay plaster walls exhibited greater ductility capacity than the cement plaster walls. Rather than use a higher R value for the clay plaster walls, a lower Factor of Safety, equal to 2.5, was used to establish the allowable shears for the clay plaster walls.

Even though uncertainty related to test data and sample size is addressed in the FEMA P695 methodology, allowable shears to be used with all analysis frameworks were further reduced where some uncertainty was present in expected strengths due to the limited number of full-scale tests. Where full-scale tests reflected the particular plaster types, thicknesses, and reinforcement called for in proposed Table 2405.15, a 10% reduction in allowable shear was applied. Where strain compatibility analyses (e.g. moment curvature analyses using the program BIAx) were used to derive expected strengths accounting for changes in plaster strength, thickness, or reinforcement, a 25% reduction in allowable shear was applied. The one exception to the preceding is the unreinforced clay plaster, given by plaster designation A1. The lateral strength for this plaster is based on self-weight providing resistance to overturning. Because the overturning capacity is based on weight and geometry, for which relatively little uncertainty exists, the allowable shear was reduced by only 10%.

The proposed allowable shears are given to two digits of precision, in tens of pounds per linear foot. Computed values are rounded up to the next increment of ten when ending in 7 or higher, and are rounded down for values ending in 6 or lower. See Table 1.

Walls having larger height to length ratio will also fail in flexure. Thus, the allowable shear for such walls should be determined based on reductions in flexural strength associated with the dimensions of the wall. For walls with reinforced plaster, flexural strength, M , can be taken as approximately proportional to steel area times plan length, L . Since steel area is given by a nominal reinforcing ratio, ρ , times the cross sectional area of the wall, for walls of uniform plaster thickness, $M \propto \rho L^2$. By statics, $V \propto M/h \propto \rho L^2/h$, where h is the height of the wall. The corresponding unit shear, V/L , is proportional to $\rho L/h$. That is, the unit shear should be reduced by multiplying by L/h for walls having L/h less than 1. That this relationship is conservative is confirmed by the wall tested by Faurot et al. That 4 ft. long wall had a lateral strength of 7.37 kips or 1840 pounds/ft. This exceeds the expectation of $2380(4/8) = 1190$ pounds/ft. The higher lateral strength was attributed by Faurot et al. to the additional steel reinforcement present where the mesh was overlapped.

A similar analysis applies to the one unreinforced plaster wall. The rocking moment, M , is proportional to the product of self weight and length. Self weight is also proportional to length. Thus, $M \propto L^2$. Then, $V \propto M/h \propto L^2/h$. Thus, the corresponding unit shear, V/L , is proportional to L/h , just as for the walls with reinforced plasters.

The wall tested by Nichols and Rap at Cal Poly failed in shear at a strength of 36,835 pounds. A simple estimate of the strength approached from the perspective of ACI 318 treatment of reinforced concrete walls considers the nominal shear strength, V_n , to be composed of concrete, V_c , and steel, V_s , components, where, for a squat wall (having aspect ratio of 1:1):

$$V_c = 3 \sqrt{f'_c \cdot b_w \cdot d} = 3 \sqrt{0.8 \cdot 1220 \cdot (2.375)(0.8 \cdot 103)} = 18,341 \text{ pounds}$$

$$V_s = \frac{A_v f_y d}{s} = \frac{(0.9 \cdot 330 \cdot 2)(0.8 \cdot 103)}{2} = 24,473 \text{ pounds}$$

$$V_n = V_c + V_s = 18,341 + 24,473 = 42,815 \text{ pounds}$$

where: b_w = the sum of the plaster thicknesses on each side ($1.125 + 1.25 = 2.375$ in.), d may be taken as 0.8 times the plan length of the wall (8'-7"), f'_c = compressive strength of plaster (taken as 80% of the cube strength of 1220 psi, based on the notion that cube strengths are approximately 1.25 times the cylinder strengths), $A_v f_y$ = yield strength of wire reinforcement (taken equal to 90% of the ultimate strength of 330 pounds for 16 gauge mesh from Parker et al.) and s = horizontal distance between vertical wires of mesh (2 inches). This simple calculation estimates a strength of 42,815 pounds, equal to 116% of the measured shear strength (36,835 pounds).

This approach was used to estimate shear strengths of the various plasters, assuming cube strengths equal to the minimum values in the proposed provision, given in Column 6 of the Table 1. Since $1/1.16=0.86$, 86% of the values calculated by the above approach are provided in Column 13 of Table 1). In no case was there an indication that the changes in plaster thickness, strength, or mesh would result in shear failures at loads less than those required to develop flexural failures. Therefore, the assumption of flexural behavior in

walls having a 1:1 aspect ratio is supported across all wall designations in Table 1.

Walls that are significantly longer in plan are expected to fail in shear rather than flexure. However, as indicated in column 14 of Table 1, the shear strengths are estimated to be 8.2 to 19.9 times the allowable shears (which were based on flexural behavior). In design, allowable shear demands are determined from elastic response spectral values (V_e) divided by R and multiplied by 0.7. Thus, long walls designed by this approach will have shear strength equal to $(0.7)(8.2 \text{ to } 19.8)V_e/R$, or $(5.7 \text{ to } 14)V_e/R$. Thus, sufficient shear strength should be available to resist the design basis earthquake (DBE) if designed using R values of 5.7 to 14, as applicable to the particular reinforced plaster designation (and to resist maximum considered earthquake (MCE) shears elastically using R values of 3.8 to 9.3, where MCE shears are 1.5 times DBE shears). As engineers will proportion walls to have capacity greater than demand, additional conservatism is usually present. This suggests that the chance of shear failure under DBE and MCE events is small for longer walls designed on the basis of flexural response, using R values in the range of 3 to 4. A similar concern has existed for many years with reinforced concrete shear walls, for which it is accepted that the possible reduction in ductility capacity is offset by the strength being significantly higher than required for ductile response. This rationale applies in the present case as well.

Table 1: Development of Allowable Shears for Strawbale Walls

Designation	Plaster Type	Plaster Thickness (min)	Plaster Reinforcement	Unadjusted Shear Strength, kips	Cube strength, min. (psi)	Adjustment Factors		Adjusted Shear Strength, kips	Factor of Safety	Allowable Shear, V_{all} per foot, plf		Shear strength V_n , plf	Factor of Safety for Shear
						Plaster	Mesh			Calculated	Proposed		
(1)	(2)	(3)	(4)	(5)	(6)	(7)	(8)	(9)	(10)	(11)	(12)	(13)	(14)
A1	Clay	1.5"	none	1.36	100	0.9368	1	1.27	$2.5/0.9 = 2.78$	57	60	720	12.0
A2	Clay	1.5"	2 in. by 2 in. high-density polypropylene	4.40	100	0.6922	1	3.05	$2.5/0.9 = 2.78$	137	140	1279	9.1
A3	Clay	1.5"	2"x2"x14ga.	5.93	100	0.6922	1	4.10	$2.5/0.9 = 2.78$	185	180	3573	19.9
B	Soil-cement	1"	2"x2"x14ga.	17.65	1000	0.9215	1	16.26	$2.9/0.75 = 3.87$	526	520	4429	8.5
C1	Lime	7/8"	17ga. woven wire	17.65	600	0.7914	0.7290	10.18	$2.9/0.75 = 3.87$	329	330	3165	9.6
C2	Lime	7/8"	2"x2"x14ga.	17.65	600	0.7914	1	13.97	$2.9/0.75 = 3.87$	452	450	3939	8.8
D1	Cement-lime	7/8"	17ga. woven wire	17.65	1000	0.9103	0.7290	11.71	$2.9/0.75 = 3.87$	379	380	3481	9.2
D2	Cement-lime	7/8"	2"x2"x14ga.	17.65	1000	0.9103	1	16.07	$2.9/0.75 = 3.87$	519	520	4254	8.2
E1	Cement	7/8"	2"x2"x14ga.	17.65	1400	0.9462	1	16.70	$2.9/0.75 = 3.87$	540	540	4511	8.4
E2	Cement	1.5"	2"x2"x14ga.	17.65	1400	0.9885	1	17.45	$2.9/0.9 = 3.22$	677	680	5547	8.2

4. Lateral Stiffness and Compatibility with Light-framed Walls Sheathed with Wood Panels

To evaluate the lateral stiffness of reinforced strawbale walls as well as judge their compatibility with light-framed walls sheathed with wood panels, initial stiffnesses for the tested walls are compared with those of light-framed walls sheathed with wood panels. For simplicity, secant stiffnesses to a design-level shear are compared in Table 2. The design level shear in this evaluation is taken as the ultimate strength in the direction of loading divided by 2.5. Since these values are for nominal 8 ft x 8 ft panels, adjustments for wall length would be indicated in subsequent applications.

Mean stiffnesses for the reinforced straw bale walls ranged from about 11.7 to 19.1 k/in. Interestingly, the stiffnesses obtained in the CUREE-Caltech Woodframe Project were about half those determined in the APA tests, ranging from about 6.9 to 9.5 k/in versus about 19.4 – 19.6 k/in, respectively. It may be observed that the stiffnesses of the strawbale walls are approximately bounded by the range of stiffnesses observed in the light-framed sheathed wall tests.

Mean deflections at the design level shears range from about 0.10 to 0.38 in. for the straw bale wall assemblies, and about 0.21 to 0.49 in. for the light-framed sheathed walls. There is considerable overlap here, suggesting that the allowable shears recommended for strawbale walls will not lead to excessive drifts at service level loads (wind or earthquake) and that strawbale walls may be designed for the same allowable story drifts as other lateral load resisting systems. Because allowable design shears are reached at similar deflections, it is suggested that light-framed sheathed walls and reinforced straw bale walls be considered compatible in those circumstances that might require sheathed light-frame wall panels to be interspersed with reinforced straw bale wall assemblies.

Table 2: Evaluation of Secant Stiffness at the Allowable Design Level

Wall ID	Reference	Left Side			Right Side			Average k, k/in	Average Δ_y , in
		Δ_y , in.	V_{allow} , kips	k, k/in	Δ_y , in.	V_{allow} , kips	k, k/in		
Straw Bale Wall Assemblies—CUREE Loading Protocol									
Wall B (earth plaster reinforced with polypropylene mesh)	Ash	0.074	1.64	22.2	0.13	1.88	14.7	18.4	0.10
Wall C (earth plaster reinforced with 14-gauge wire mesh)	Ash	0.17	2.28	13.4	0.25	2.46	9.9	11.7	0.21
Wall E (cement plaster reinforced with 14-gauge wire mesh)	Ash	0.31	6.52	20.8	0.439	7.6	17.3	19.1	0.38
Cal Poly Test (cement plaster reinforced with 14-gauge wire mesh)	Faurot	0.38	3.01	7.9	0.33	2.88	8.7	8.3	0.36
Light-Frame Sheathed Wall Assemblies—CUREE Loading Protocol									
Test 2 East Wall (15/32" OSB, 8d at 4" centers)	W-13	0.42	3.1	7.4	0.55	3.49	6.3	6.9	0.49
Test 2 West Wall (15/32" OSB, 8d at 4" centers)	W-13	--	--	--	0.38	3.62	9.5	9.5	0.38
Test 6 East Wall (15/32" plywood, 8d at 4" centers)	W-13	0.39	3.28	8.4	0.49	3.91	8.0	8.2	0.44
Test 6 West Wall (15/32" plywood, 8d at 4" centers)	W-13	0.43	3.69	8.6	0.53	4.28	8.1	8.3	0.48
Light-Frame Sheathed Wall Assemblies—Sequential Phased Displacement Loading Protocol									
Test 1A (15/32" plywood, 10d at 4")	Rose	0.19	3.91	20.6	0.23	4.19	18.2	19.4	0.21
Test 6A (3/8" plywood, 8d at 3")	Rose	0.22	4.06	18.5	0.20	4.14	20.7	19.6	0.21

5. Conventional Evaluation of Seismic Design Factors

Uang (1991) discusses the derivation of R , Ω , and C_d factors for use in seismic provisions in building codes on the basis of experimental data. This approach is reflected in the commentary of the 1998 NEHRP Provisions (FEMA-303), where equation (C5.2.1-3) states that the response modification coefficient, R , is the product of two components, one associated with ductility (R_d) and the other associated with overstrength, Ω_o :

$$R = R_d \cdot \Omega_o$$

The definition of these terms is described in Figure 24 (from Uang, 1991), where R_d is

equivalent to R_u and Ω_o may deviate slightly from Ω depending on the degree of overstrength provided. Current seismic provisions are calibrated to a load and resistance factor basis, for which the seismic design coefficient is given by C_s .

With reference to Figure 24, the seismic design coefficient for working stress design, C_w ($= C_{eu}/R_w$), is related to C_s by $C_s = Y \cdot C_w$. Thus,

$$R = \frac{C_{eu}}{C_s} = \left(\frac{C_{eu}}{C_y} \right) \left(\frac{C_y}{C_s} \right) = (R_u) \left(\frac{C_y}{C_w} \frac{C_w}{C_s} \right) = (R_u) \left(\frac{C_y}{C_w} \frac{1}{Y} \right)$$

The use of allowable shears in the design of both strawbale wall assemblies and light-frame construction with wood shear panels implies $Y = 1/0.7 = 1.43$.

The term C_y/C_w is evaluated in Table 3. The proposed allowable shears of Table 1 were obtained by applying a factor of safety to the empirical wall strengths and introducing adjustments to account for the flexural strength expected for plasters having the minimum compressive strengths allowed in the proposed code provisions. A further reduction in strength of 10 or 25% was introduced in Table 1 depending on the plaster type, to provide added conservatism given limited test data. To maintain this conservatism, this reduction is removed in Table 3 (column 7). The allowable shears in Table 3 are also boosted up to the level expected for the plaster strengths used in the tests (column 8). Thus, C_y/C_w (column 11) is obtained as 80% of the unadjusted shear strength (80% of column 5) divided by the adjusted allowable shear (column 10).

The ductility reduction factor, R_μ , is understood to vary with period. In the constant velocity region, R_μ may be taken equal to the ductility capacity, μ_s ($= \Delta_{max}/\Delta_y$). For shorter periods, peak displacements of inelastic systems generally exceed those of elastic systems. Short period displacement amplification, which is generally neglected in the derivation of seismic design parameters for use in building code provisions, can be considered by evaluating R_μ as

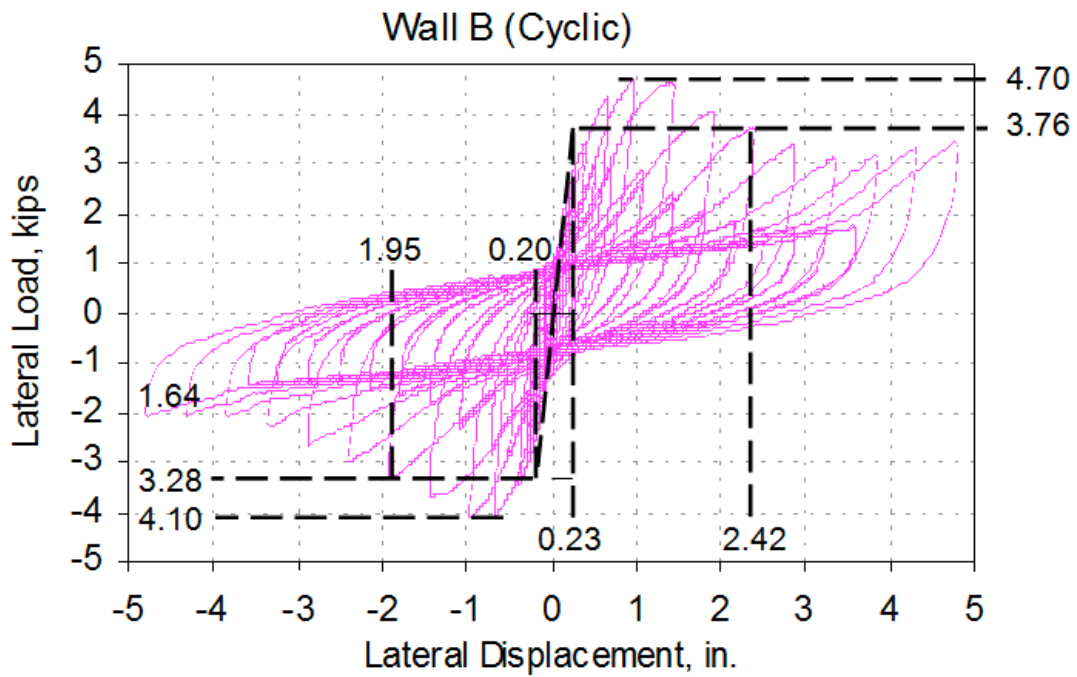


Figure 25: Response of Straw Bale Wall B.

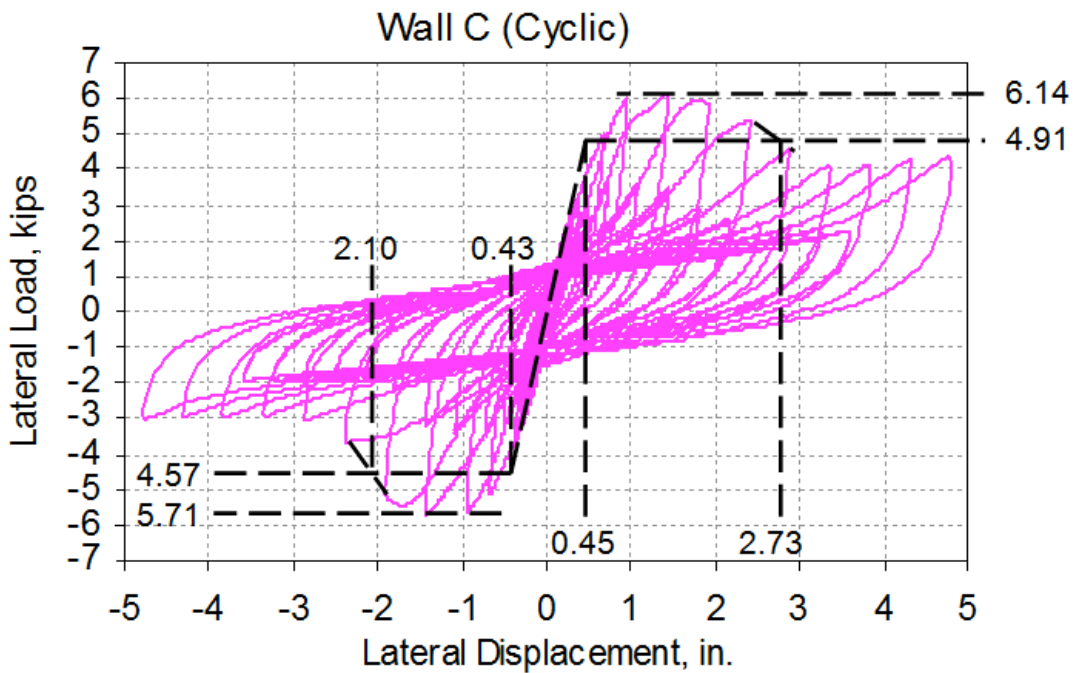


Figure 26: Response of Straw Bale Wall C.

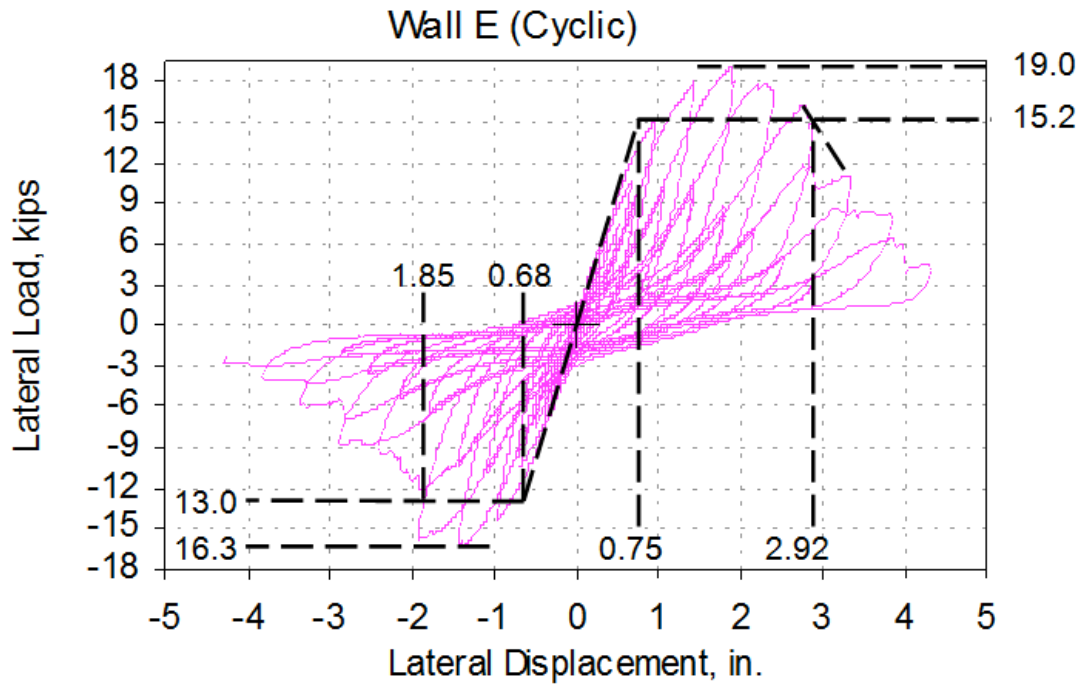


Figure 27: Response of Straw Bale Wall E.

Table 3: Evaluation of component R factors conventional methods.

Wall Specimen	Plaster Type	Plaster Thickness (min)	Plaster Reinforcement	Unadjusted Shear Strength, kips	Proposed Allowable Shear, V_{all} per foot, plf	Expected Allowable Shear, plf	Adjustment Factors		Adjusted Allowable Shear, kips	Component R factors		
							Plaster	Mesh		C_y/C_w	R_{μ} long period	R_{μ} short period
(1)	(2)	(3)	(4)	(5)	(6)	(7)	(8)	(9)	(10)	(11)	(12)	(13)
B	Clay	1.5"	2 in. by 2 in. high-density polypropylene	4.40	140	137/0.9 = 152	0.6922	1	1.76	2.00	10.14	4.39
C	Clay	1.5"	2"x2"x14ga.	5.93	180	185/0.9 = 206	0.6922	1	2.38	1.99	5.48	3.15
E	Cement	1.5"	2"x2"x14ga.	17.65	680	677/0.9 = 752	0.9885	1	6.09	2.32	3.31	2.37

Table 4: Evaluation of ductility capacities.

Wall Specimen	Left Side			Right Side			Average μ_s
	Δ_y , in.	Δ_u , in.	μ_s	Δ_y , in.	Δ_u , in.	μ_s	
Wall B	0.20	1.95	9.75	0.23	2.42	10.52	10.14
Wall C	0.43	2.10	4.88	0.45	2.73	6.07	5.48
Wall E	0.68	1.85	2.72	0.75	2.92	3.89	3.31

Table 5: Evaluation of seismic design coefficients by conventional methods.

Wall Specimen	Response Modification Coefficient, R		Overstrength Factor, Ω_o	Displacement Amplification Factor, C_d
	long period	short period		
(1)	(2)	(3)	(4)	(5)
B	14	6.2	2.75	14.2
C	7.6	4.4	2.88	7.64
E	5.4	3.9	2.27	5.37

6. Seismic Design Parameters Determined by Adjustment Based on Empirical Ductility Capacities

A comparison between the experimentally determined response of strawbale wall and light-framed wood panel sheathed walls is made to establish R , Ω_o , and C_d factors for design.

The response modification coefficient, or R -factor, is intended to account for the elongation of period with the development of inelastic response, energy dissipation, ductility, and overstrength present in the structural system.

The CUREE-Caltech Woodframe Project tested light-framed wood sheathed walls using the CUREE Protocol. This protocol has gradually increasing displacement amplitudes that are separated by trailing cycles; the trailing cycle amplitudes are smaller than those of previous cycles. One conclusion of the Woodframe Project is that the failure modes obtained with the CUREE protocol are most consistent with observed seismic behavior and that this protocol is recommended to be used as a standard for future testing of woodframe structures. This protocol was also used in the testing of the strawbale wall assemblies. The Woodframe Project also used the Sequential Phased Displacement protocol, and determined that this protocol caused fastener fatigue failures that did not seem to be representative of the behavior observed in seismic events. Consequently, this protocol was not recommended for cyclic evaluation of woodframe shearwalls. (pp. 204-205, W-13) Thus, in the following analyses, only results obtained using the CUREE protocol are used.

Quantitative and qualitative comparisons of performance are made. To provide a quantitative basis for comparison, a number that could be termed a “design-level ductility” was calculated from measured test results as follows. With reference to Figure 28, a nominal design value is determined as the ultimate strength divided by 2.5. The “design-level displacement” is determined as the intersection of the nominal design strength (an

allowable stress level set equal to the ultimate strength divided by 2.5) with the load-displacement envelope. The ultimate displacement capacity is where the degrading portion of the design envelope is at 80% of the ultimate strength. Thus, the “design-level” ductility (μ) is determined as the ratio of the ultimate and design-level displacements, given by Δ_u/Δ_y in Figure 28. By this procedure it is possible to compare the ductility available from straw bale walls with that available from light-framed walls sheathed with wood panels.

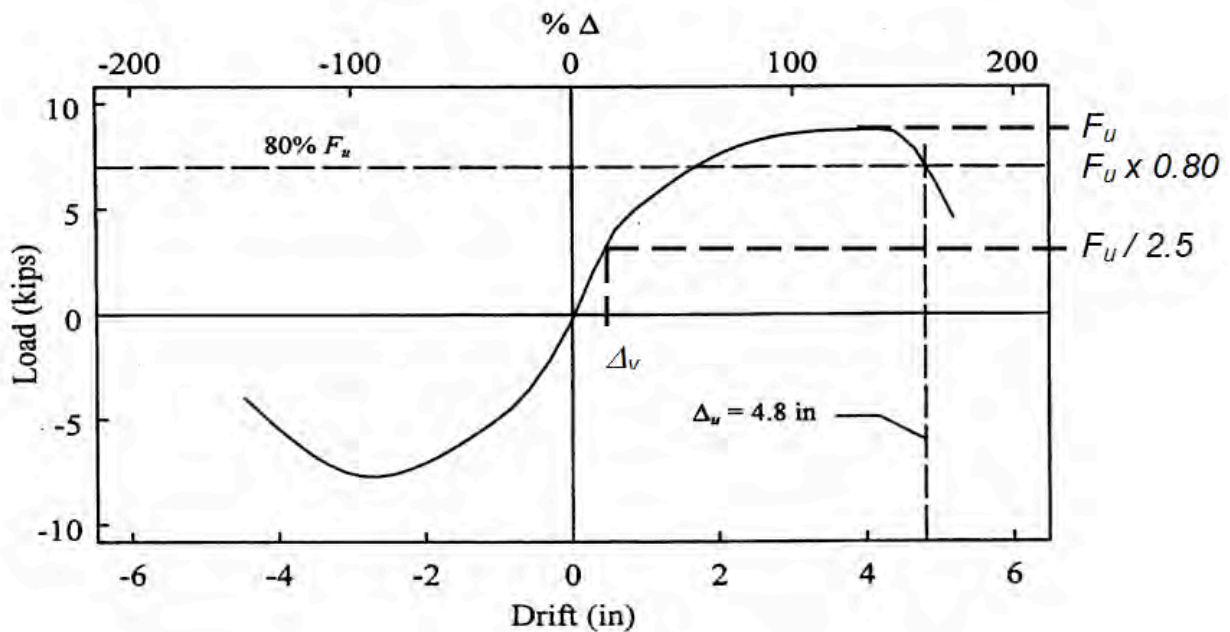


Figure 28: Evaluation of Displacement Quantities (adapted from W-13 for evaluation of Δ_y)

Table 6 shows mean values of “design-level” ductilities for straw bale wall assemblies and light-framed walls sheathed with plywood and OSB obtained from CUREE-Caltech Woodframe Project reports. Additional data is presented for light-framed walls sheathed with plywood and OSB tested under the Sequential Phased Displacement protocol in a project supported by APA—The Engineered Wood Association (Rose, 1998). All walls reported in Table 6 have nominal dimensions of 8’ by 8’. Detailed load displacement plots used to generate the data of Table 6 are provided in Appendix B

Mean design-level ductility values are similar for the light-framed walls sheathed with plywood and OSB, and collectively average 11.2 and 11.0, respectively. The average for both types of sheathing rounds to 11.2. The R , Ω_o , and C_d values for such walls are $6\frac{1}{2}$, 3, and 4 when used in Bearing Wall Systems and 7, $2\frac{1}{2}$, and $4\frac{1}{2}$ when used in Building Frame Systems.

In comparison, Wall B is seen to be substantially more ductile, while Wall E is much less ductile. Walls B and C experienced flexural compression failures, associated with failure of the clay plaster in compression. The ductility of Wall E appeared to be limited by the ductility of the wire mesh reinforcement, not the compressive strength of the cement plaster wall. The shorter companion to Wall E, tested by Faurot et al., displayed a ductility capacity greater than that of Wall E. While these walls experienced flexural failures, walls with smaller height-to-length ratios are more likely to fail in shear. The accepted wisdom regarding the behavior of reinforced concrete walls is that walls with smaller height to length ratios will be stronger and thus, their enhanced strength can be relied upon to compensate for any loss of ductility (as discussed in detail in the section on allowable shears). Applied to cement plaster walls, the corresponding R factor would be $6\frac{1}{2}(6.3/11.2) = 3.7$ for Bearing Wall systems. Similarly, an R factor of $7(6.3/11.2) = 3.9$ would apply to a Building Frame system. These values can be rounded to 3.5 for Bearing Wall systems and 4 for Building Frame systems.

The substantially larger ductility of clay plaster walls (22.6 and 11.7 for Walls B and C, respectively) merits recognition. Using the smaller of these two values, the corresponding R factor would be $6\frac{1}{2}(11.7/11.2) = 6.8$ for Bearing Wall Systems, and $7(11.7/11.2) = 7.3$ for Building Frame Systems. These values can be rounded down to $6\frac{1}{2}$ and 7, respectively. However, the current code proposal does not identify larger R factors for clay plaster walls. Instead, allowable shears are increased slightly and an R factor common to all strawbale plasters is used.

An adjustment based on a qualitative comparison of the load-displacement response is now considered. Both straw bale walls assemblies and light-framed walls sheathed with wood panels appear to have a similar degree of pinching and loss of stiffness upon reloading. Consequently, the R -factors as determined above are recommended without further adjustment for pinching and loss of stiffness.

Table 6: Evaluation of “Design-Level” Ductility Capacities

Wall ID	Reference	Left Side			Right Side			Average μ
		Δ_y , in.	Δ_u , in.	μ	Δ_y , in.	Δ_u , in.	μ	
Straw Bale Wall Assemblies—CUREE Loading Protocol								
Wall B	Ash	0.074	1.95	26.4	0.128	2.42	18.9	22.6
Wall C	Ash	0.17	2.1	12.4	0.248	2.73	11.0	11.7
Wall E	Ash	0.313	1.85	5.9	0.439	2.92	6.7	6.3
Cal Poly Test	Faurot	0.38	2.98	7.8	0.33	3.02	9.2	8.5
Light-Frame Sheathed Wall Assemblies—CUREE Loading Protocol								
Test 2 East Wall (15/32" OSB, 8d at 4" centers)	W-13	0.42	3.61	8.6	0.55	4.78	8.7	8.6
Test 2 West Wall (15/32" OSB, 8d at 4" centers)	W-13	--	--	--	0.38	5.09	13.4	13.4
Test 6 East Wall (15/32" plywood, 8d at 4" centers)	W-13	0.39	4.89	12.5	0.49	6.03	12.3	12.4
Test 6 West Wall (15/32" plywood, 8d at 4" centers)	W-13	0.43	4.41	10.3	0.53	5.79	10.9	10.6
Light-Frame Sheathed Wall Assemblies—Sequential Phased Displacement Loading Protocol								
Test 1A (15/32" plywood, 10d at 4")	Rose	0.19	2.38	12.5	0.23	2.43	10.6	11.5
Test 6A (3/8" plywood, 8d at 3")	Rose	0.22	2.21	10.0	0.2	2.17	10.9	10.4

The similarity in hysteretic characteristics suggest that C_d values should be proportional to the R values. Using values for cement plaster walls, $C_d = 4(3.7/6.5) = 2.3$ for Bearing Wall systems and $C_d = 4.5(3.9/7) = 2.5$ for Building Frame systems. Thus, $C_d = 2.5$ is recommended in both cases.

For light-framed walls with sheathed wood panels, overstrength factors of 3 and $2\frac{1}{2}$ are used for Bearing Wall Systems and Building Frame Systems, respectively. Since allowable shears for strawbale walls were established using a factor of safety of 2.5, while a factor of safety of approximately 3 can be used to estimate the allowable values for light-framed walls with sheathed wood panels, it is conservative to simply use an overstrength factor of 3.0 for both types of strawbale walls systems.

7. FEMA P695 Overview

The methodology of FEMA P695 [4] provides seismic performance factors (SFCs), including the response modification coefficient (R factor), the system over strength factor (Ω_o) and deflection amplification factor (C_d) for new seismic force resisting system. The purpose of the methodology as expressed by FEMA P695 is “to provide a rational basis for determining building seismic performance factors that, when properly implemented in the seismic design process, will result in equivalent safety against collapse in an earthquake, comparable to the inherent safety against collapse intended by current seismic codes, for buildings with different seismic-force-resisting systems.”

The Methodology consists of a framework for determining seismic performance factors (SPFs). Four key elements form this framework:

- (1) Design Information requirements,
- (2) Test Data requirement,
- (3) System analysis methods, and
- (4) Ground motions.

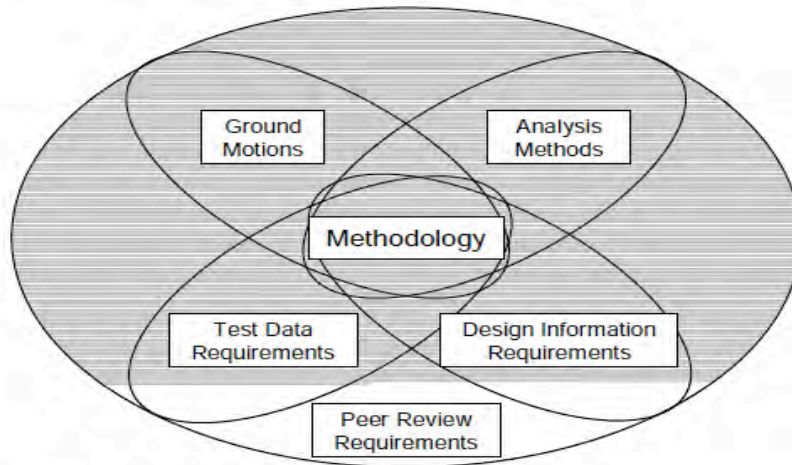


Figure 29: Key elements of the Methodology. [adapted from FEMA P695]

FEMA P695 provides detailed nonlinear analysis of representative building models, termed archetypes and performance groups. Structural archetypes covering the range of building configurations and characteristics that may be used for the relevant seismic force-resisting system should be developed based on the design requirements and test data, for new buildings. Structural system archetypes are assembled to form performance groups that have similar behavior within the archetype design space. The required configurations and characteristics to be considered when establishing archetypes and performance groups are more thoroughly explained within FEMA P695. Nonlinear dynamic analyses using earthquake ground motions with increasing intensity are used to simulate collapse and establish the intensity of ground motion that causes collapse. FEMA P695 evaluates collapse under Maximum considered Earthquake (MCE) ground motion, which corresponds to 2% probability of exceedance in 50 years. The nonlinear analysis results are used to establish the collapse capacities of each archetype and the value of adjusted collapse margin ratio, ACMR, is compared to acceptance criteria.

The period-based ductility (μ_T) and overstrength (Ω) parameters are determined using the capacity curve obtained by nonlinear static pushover analysis. In order to quantify these parameters, the lateral load is applied in a displacement-controlled analysis; the lateral

displacement is increased monotonically until the base shear strength decreases 20% from the peak strength. Figure 30 shows an idealized capacity curve obtained from nonlinear static pushover analysis.

Based on the obtained nonlinear static pushover curve for each index archetype model, the overstrength, Ω , and ductility, μ_T , can be determined as follows.

The overstrength factor, Ω , is defined as the ratio of the maximum base shear strength, V_{max} , to the design base shear, V .

$$\Omega = \frac{V_{Max}}{V} \quad \text{Equation 1}$$

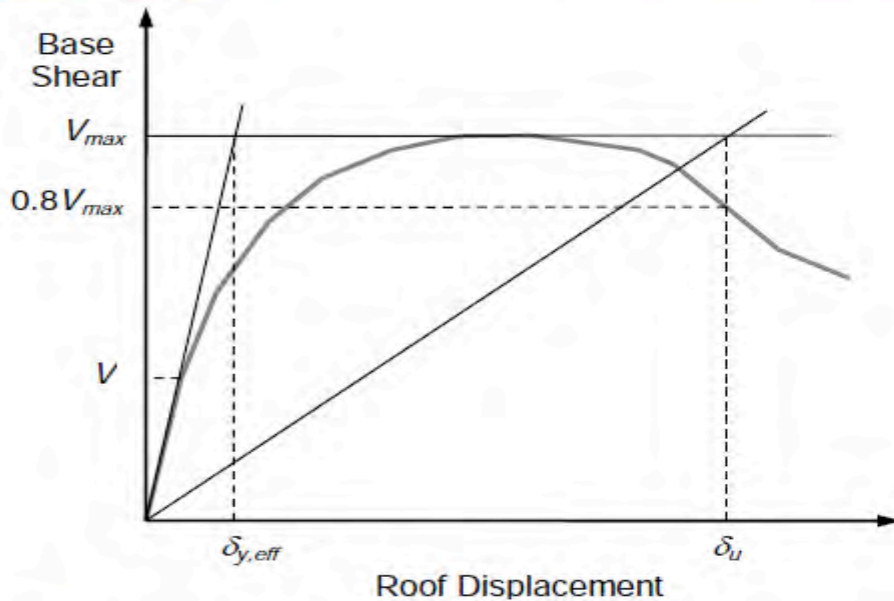


Figure 30: Idealized nonlinear static pushover curve. [adapted from FEMA P695]

The period-based ductility for a given index archetype model, μ_T is defined as the ratio of ultimate roof drift displacement, δ_u to the effective yield roof drift displacement $\delta_{y,eff}$.

$$\mu_T = \frac{\delta_u}{\delta_{y,eff}} \quad \text{Equation 2}$$

The effective yield roof drift displacement $\delta_{y,eff}$ is given in Equation 3 is related to period, maximum base shear strength, the total weight of the building and C_0 .

$$\delta_{y,eff} = C_0 \frac{V_{Max}}{W} \left[\frac{g}{4\pi^2} \right] (\max(T, T_1))^2 \quad \text{Equation 3}$$

where V_{max} is the maximum shear strength of the base shear, W is the total weight of the building, T is the fundamental period ($T=C_u T_a$) with a lower bound limit of 0.25 sec, and T_1 is the fundamental period of the archetype model computed by eigenvalue analysis.

C_0 is the ratio of MDOF displacement to SDOF displacement, also given equivalently as the first mode participation factor when computed with the mode shape normalized to unit value at the roof. C_0 is defined, equivalently, in Equation 4 based on ASCE/SEI 41-06, as:

$$C_0 = \phi_{1,r} \frac{\sum_1^N m_x \phi_{1,x}}{\sum_1^N m_x \phi_{1,x}^2} \quad \text{Equation 4}$$

Where $\phi_{1,x}$ is the ordinate of the fundamental mode at level x (roof), m_x is the mass at level x ; and N is the number of levels.

Nonlinear dynamic analysis is conducted using many ground motion records, each successively scaled in amplitude and the associated peak response quantities recorded. The intensity of the ground motion records is indexed by the spectral acceleration of the scaled record for an oscillator having period equal to (T) and viscous damping equal to 5% of critical damping. A Far-Field record set is identified that can be used in the incremental dynamic analysis. This set includes twenty-two record pairs (44 individual ground motions) that are applied in each archetype to assess collapse. The median collapse

spectral acceleration (\hat{S}_{CT}) is spectral acceleration of the scaled records at which half the ground motion records cause the structure to collapse. Collapse is defined as peak interstory drift of a specified amount (e.g. 7% based on test results) or where the IDA curve is flat.

Once the median collapse spectral acceleration (\hat{S}_{CT}) has been determined, the collapse margin ratio (CMR) and adjusted CMR (ACMR) for each of the index archetype models can be evaluated.

The value of CMR for each archetype is calculated as the ratio of the median collapse spectral acceleration at 5% damping, S_{CT} , and the maximum considered earthquake (MCE) spectral response acceleration at the fundamental period, T , for 5% damping, denoted S_{MT} .

$$CMR = S_{CT} / S_{MT} \quad \text{Equation 5}$$

The Adjusted Collapse Margin Ratio, ACMR is determined as the product of Collapse Margin Ratio, CMR, and the Spectral Shape Factor, SSF.

$$ACMR = CMR \times SSF \quad \text{Equation 6}$$

The value of the spectral shape Factor, SSF is a function of the Fundamental period and the period-based ductility, μ_T , determined from pushover analysis. Table 7-1a and Table 7-1b of FEMA P695 has provides the values of SSF.

In order to evaluate whether the response modification coefficient, R , used in the design is acceptable, an acceptable ACMR is established. The acceptable value of ACMR is a function of the total system uncertainty. The total system uncertainty is based on uncertainty components associated with ground motion variability, design requirements, test data, and modeling uncertainty. Where greater uncertainty exists, a larger ACMR will be required, and this can be obtained using a smaller value of the response modification coefficient in design.

The total system collapse uncertainty β_{TOT} is calculated using the following relationship:

$$\beta_{TOT} = \sqrt{\beta_{RTR}^2 + \beta_{DR}^2 + \beta_{TD}^2 + \beta_{MDL}^2} \quad \text{Equation 7}$$

As mentioned previously, the total system collapse uncertainty β_{TOT} is a function of record-to-record (RTR) uncertainty, design requirement-related (DR) uncertainty, test data-related (TD) uncertainty, and modeling (MDL) uncertainty. β_{RTR} is set to a fixed value and is taken equal to 0.4 for systems with period-based ductility larger than 3.0. The β_{DR} and β_{TD} values are specified based on descriptive characteristics provided in Chapter 3 of the FEMA P695, while β_{MDL} can be determined by the method described in Chapter 5 of the document.

After defining the total uncertainty system, β_{TOT} the last step for evaluation of the response modification coefficient, R, is ensuring that the resulting adjusted collapse margin ratio satisfies two requirements:

1. The value of ACMR obtained for each individual archetype must exceed the ACMR corresponding to 20% of the individual archetype buildings collapsing termed $ACMR_{20\%}$.

$$ACMR_i > ACMR_{20\%}$$

2. The average of the ACMR values obtained in each performance group should exceed the ACMR corresponding to 10% of the archetypes within each performance group collapsing, termed $ACMR_{10\%}$.

$$\text{Average } ACMR_i > ACMR_{10\%}$$

Table 7-3 in FEMA P695 provides the values of $ACMR_{20\%}$ and $ACMR_{10\%}$ associated with different values of total system uncertainty, β_{TOT} .

8. Application of FEMA P695 methodology to the quantification of seismic performance factors to one and two-story strawbale wall buildings

Seismic performance factors for two strawbale wall assemblies made using two different plaster finish materials are determined in this section. All archetypes are designed for seismic demands based on the ground motion intensities of Seismic Design Category D (SDC D). The load deformation relationships are based on test data reported by Ash et al (2003).

The initial R value used for the cement plaster system (represented by Wall E) is 2.5 and the initial R value used for the clay plaster system (represented by Wall B) is 3.5. Wall C, (clay plaster with 2"x2"x14" gauge reinforcement) is not explicitly considered in these analyses because, as compared to Wall B, it has greater strength and ductility capacity. Therefore, Wall B is the more critical of the two clay plaster wall assemblies.

The Archetypes that were used in this research are one-story and two-story buildings in the short period range ($T < 0.5$). As mentioned in FEMA P695, short-period buildings generally do not meet collapse performance objectives of the Methodology unless a lower R value is used. In other words, the FEMA P695 methodology is acknowledged as having some limitations in properly addressing variations in collapse performance associated with differences in building period. For resolving this problem ATC-84 (*March 2012*) provides some recommendations to develop more realistic archetypes of short-period systems that better represent observed collapse performance. As stated in the ATC-84 report: "incorporation of diaphragm flexibility, base flexibility including foundation effects, and other sources of flexibility typical of real buildings would lengthen the calculated period of models with very short periods, decrease inelastic demand on initially stiff elements, and better represent collapse performance of the system of interest." However, in pilot studies conducted as part of this research, incorporation of diaphragm flexibility had a very minor effect on the ACMR value. Inclusion of soil structure interaction was not investigated due to model complexity and a lack of definitive guidance on model parameter evaluation.

8.1. System Design Requirements

System design requirements are considered to be established by ASCE 7-10 with respect to fundamental period of the building, determination of base shear, and distribution of seismic force according to the Equivalent Lateral Force method. The strength capacity of the shear walls is in accordance with currently proposed IBC Table 1 (Allowable Shear (pounds per foot) for Plastered Strawbale walls), which is excerpted in Table 7.

Table 7: Proposed allowable shears for plastered strawbale wall assemblies

Reference Wall	Plaster			Allowable Shear (plf)
	Type	Minimum Thickness (each side)	Reinforcement	
B	Clay	1.5"	polypropylene mesh	140
E	Cement	1.5"	14-gauge wire mesh	680

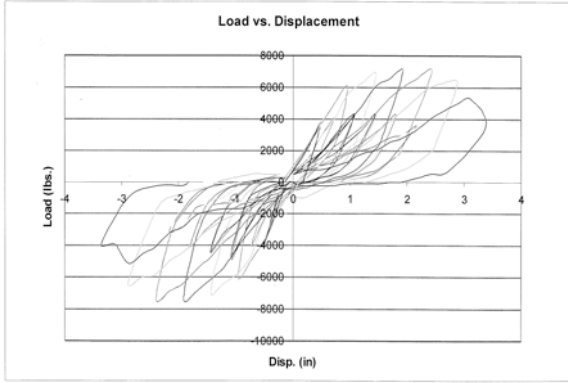
8.2. Test Data Requirement

Full-scale experimental studies reported by Ash et al. (2003) and Faurot et al. (2004) are used to establish the expected behavior of the walls used in the archetype designs. Ash established the behaviors of full-scale straw bale wall assemblies under quasi-static reversed cyclic loading on to characterize the inelastic response of these walls to earthquake ground shaking. The tests were used to establish the details required in the proposed IBC provisions. Data from two walls are of primary importance: the “medium-detailed” Wall B, made using clay plaster reinforced with a polypropylene mesh, and the “medium-detailed” Wall E, made using with cement plaster reinforced with welded wire

mesh. Reverse cyclic loading progressed until the capacity of the test equipment was reached, which corresponded to an interstory drift of $\pm 7.5\%$ of the wall height. Even under such large drifts, there was no loss of support of gravity loads. Cracks opened between the bale courses but the cracks would close on reversal and the relatively wide surface of the bales at these cracks provide ample bearing surface so that failure due to misalignment of the bales would be nearly inconceivable. The test reported by Faurot et al [7] is a full-scale test of a wall that resembled Wall E except that it was nominally 4 ft in plan rather than 8 ft. Figure 31 shows the experimentally determined load-displacement response of the different length walls made using cement plaster.

Figure 32 presents the idealized back bone curve of the two walls, after minor reductions to account for the flexural strength expected for plasters having the proposed minimum cube compressive strength of 1400 psi, recognizing that the experimental specimens had plaster strengths of approximately 2200 psi (as explained in more detail in the experimental behavior section earlier). As it is seen in the graph, the yield displacement of the two walls, having the same plaster materials and reinforcement, can be considered to be the same. Both walls yield at approximately 1-inch displacement. The maximum average shear strength is 17.65 kips and 7.5 kips for the 8x8 and 4x8 walls, respectively (Figure 32).

Where designs require walls less than 8 ft in length, the allowable shears are adjusted as described in the proposed IBC provisions, where the unit shear is multiplied by the aspect ratio (length/height) of the wall. As noted in Section 3. the test reported by Faurot et al. (2004) shows that this is a very conservative assessment of shear strength. Models of the load-displacement behavior of the wall can be based on a backbone curve that is interpolated between those shown for 4-ft and 8-ft walls in Figure 32. In the case of the archetype designs herein, the models of the walls were based on the simplified backbone curve for the 8-ft. walls.



(a)

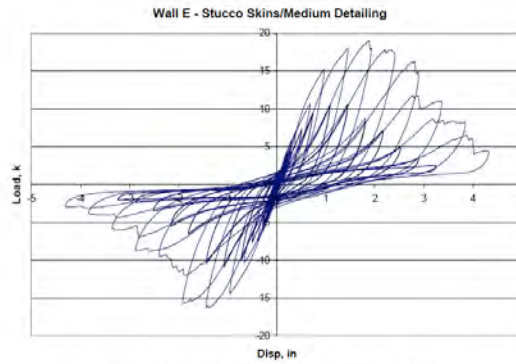


Figure 6.7 – Wall E load-displacement plot

(b)

Figure 31: Test data for cement plaster walls reinforced with 2 x 2 by 14 gauge mesh (a) 4 feet long by 8 feet high (Faurot et al. 2004) (b) 8 feet long by 8 feet high (Ash et al. 2003)

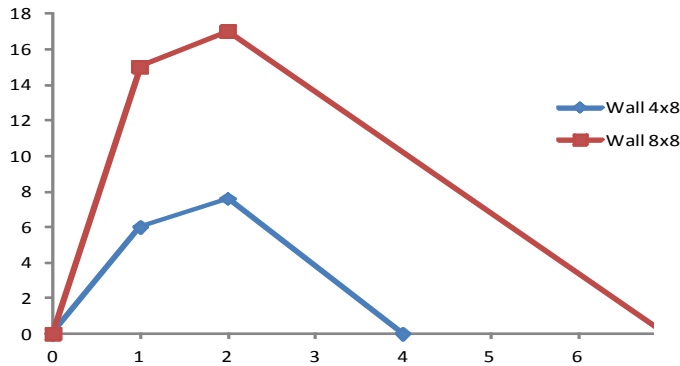


Figure 32: The simplified backbone curves derived from test data of full-scale reinforced cement plaster walls having lengths of 4 and 8 ft, nominally 8 ft high.

8.3. Adjustments for Allowable Shears and Seismic Mass

In the early part of this research we were still becoming accustomed to the analysis perspective of the FEMA P695 approach and in particular the modeling of inelastic components and the treatment of uncertainty. Different assumptions were made in establishing the shear strengths of the hysteretic models and the seismic mass.

Table 1 identified factors of safety used to derive allowable shears. Shear strengths were adjusted to account for the influence of material strengths less than those used in the test specimens (but satisfying minimum values prescribed in the proposed provisions). Common to all analyses is the adjustment of strength data to reflect strengths expected for materials that just satisfy the minimum threshold strengths prescribed in the proposed code provisions.

It is convenient to distinguish the assumptions made for those analyses done using the SAWS model from those done using the Pinching4 model.

8.3.1. Adjustments made in the analyses using the SAWS model

After adjusting the allowable shears for the code-prescribed minimum materials strengths, allowable shears were obtained by applying factors of safety (typically 2.9) and were further reduced by 10 to 25% in recognition of the limited number of specimens tested having the prescribed plaster and reinforcement.

To be “consistent” with these adjustments, the strengths used in the hysteretic models were taken as the allowable shear multiplied by a factor of safety of 2.9 for the cement plaster walls and 2.5 for the earth plaster walls. Corresponding displacements were not adjusted. Details of this calculation are provided below for Walls E and B, along with the reduction of experimental data to this strength level for the purpose of fitting of hysteretic models used in the dynamic analyses.

Wall E. Figure 33 shows how allowable design value has adjusted in test data of Wall E. The test result shows the maximum average shear strength is 17.65 kips for Wall E (Figure 27). The allowable shear design according to Table 7 is 680 plf. The length of the wall is 8 ft, and the safety factor considered for this wall based on previous discussion (Section 3.) is 2.9. Therefore, as shown in the following calculations, each shear force value in test data was multiplied by 0.89 while the displacement value was left unchanged.

$$680 \text{ plf} * 2.9 = 1972 \text{ plf}$$

$$1972 \text{ plf} * 8 \text{ ft} = 15776 \text{ lbs}$$

$$15776 \text{ lbs} / 1000 = 15.78 \text{ kips}$$

$$\text{Allowable shear design} / \text{Test data} = 15.78 / 17.65 = 0.89$$

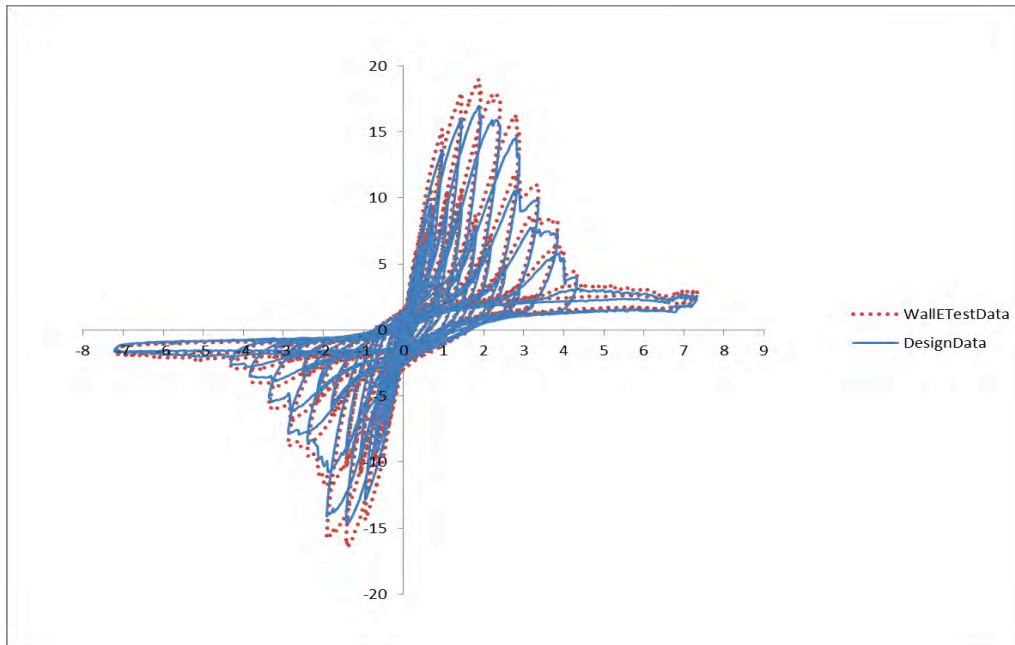


Figure 33: Adjusted experimental data for Wall E, reported by Ash et al (2003)

Wall B. The same procedure was applied to Wall B (with clay plaster). The allowable shear design value of Wall B according to Table 7 is 140 plf. The maximum average shear strength is 4.7 kips (Figure 25). The safety factor considered for The Wall is 2.5. The force reduction factor used is 0.59 (Figure 34).

$$140 \text{ plf} * 2.5 = 350 \text{ plf}$$

$$350 \text{ plf} * 8 \text{ ft} = 2800 \text{ lbs}$$

$$2800 \text{ lbs} / 1000 = 2.8 \text{ kips}$$

Force Reduction Factor $2.8/4.7 = 0.59$

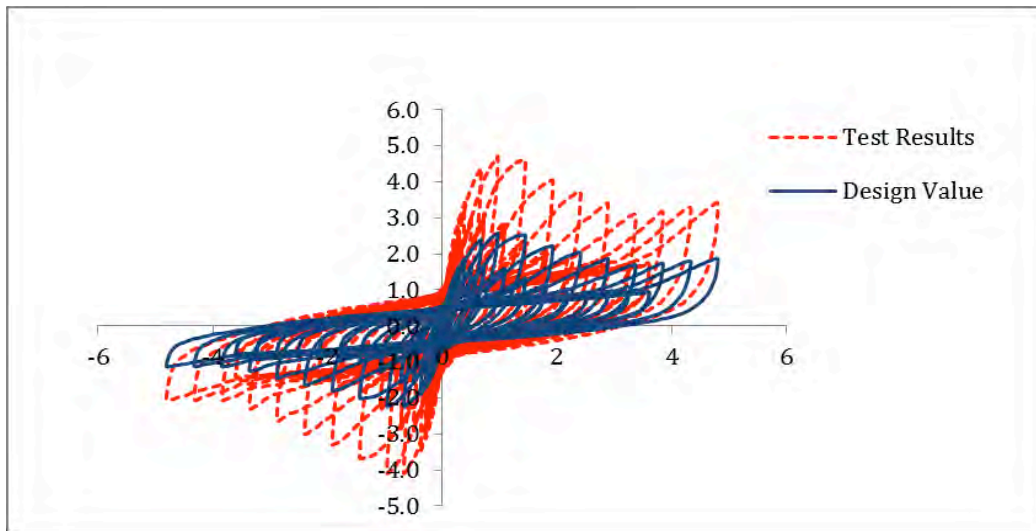


Figure 34: Adjusted experimental data for Wall B, reported by Ash et al (2003)

Note that early in this research, adjustments for materials strengths being less than those used in the test specimens were based on the square root of the plaster compressive strength rather than the effect of this reduction on the flexural strength. At that time, allowable shears were determined to be 607 and 129 plf for Walls E and B, respectively. Results obtained for these archetype models are reported herein using the proposed allowable shears (Table 1), with wall length slightly reduced from 8 ft increments following the proposed L/h reduction. Thus, for all archetypes modeled with the SAWS hysteresis model, wall lengths were adjusted, to 7.7 ft and 7.56 ft for Wall B and Wall E, respectively (Appendix F).

As a new user to FEMA P695 methodology, when using the SAWS model, a conservative approach to calculating seismic mass was taken, in which an extra $\frac{1}{4}$ " thickness of plaster was assumed present on each plaster face. Therefore, the weight of the archetype in the nonlinear dynamic analysis was greater than in the determination of design forces (Appendix D, Table 31).

8.3.2. Adjustments made in the analyses using the Pinching4 model

Recognizing fully the treatment of uncertainty embodied in the P695 approach, there should be no need to discount allowable shears to account for the limited amount of test data. The only considerations in establishing strengths should be the expected materials strengths relative to the strengths of the materials used in the test specimens. Here, being somewhat conservative, estimated shear strengths for materials strengths just satisfying the minimum strengths of the proposed code provisions are used. That is to say, experimental data was modified based on material strengths alone to establish adjusted empirical curves that were used to fit the Pinching4 hysteretic model.

Wall E: The strength of the wall: In SAWS model the allowable shear design had been considered 607 plf, but the newly proposed IBC provisions increased the allowable shear for wall E to 680 plf. Then for fitting the Wall E with pinching4, an extra 10% strength was added to the Wall (755.5 plf).

Wall B: At this writing, Pinching4 has been used only with Wall E.

Seismic masses were calculated based on the specified plaster thickness. The conservative approach of adding ¼” thickness of the wall to calculate seismic mass was not followed. As a result the weight of the all archetypes in Pinching4 model is lower than in the SAWS model.

8.4. Identification of Archetype Configurations

The archetypes are established according to the requirements of FEMA P695. Table 8 lists the range of design parameters considered for the development of the two-dimensional archetype wall models. Residential buildings with only one and two stories are represented. A total of four performance groups were established, each characterized by eight-foot tall shear walls in Seismic Design Category D. Clay plaster and cement plaster wall finishes reinforced as per Walls B and E, respectively, are modeled. Table 8 presents

the range of variables considered for Wall E (cement plaster) and Table 9 shows the range of variables considered for Wall B (clay plaster).

Table 8: Range of Variables Considered for the Definition of Strawbale Frame Archetype Buildings for Wall E (cement plaster)

Variable	Range
Number of stories	1 & 2
Seismic Design Categories (SDC)	D_{max} and D_{min}
Story height	8 ft
structural wall finishes	Cement plaster
aspect ratio of wall	≤ 1 (plan length) : 1 (height)

Table 9: Range of Variables Considered for the Definition of Strawbale Frame Archetype Buildings for Wall B (clay plaster)

Variable	Range
Number of stories	1 & 2
Seismic Design Categories (SDC)	D_{max} and D_{min}
Story height	8 ft
structural wall finishes	Clay plaster
aspect ratio of wall	≤ 1 (plan length) : 1 (height)

Table 10 shows the performance groups (PG) in accordance with the requirements of FEMA P695. To represent these ranges of design parameters, two performance groups are

used for Wall E and Wall B to evaluate the systems as presented in Table 10 and Table 11, respectively.

Table 10: Performance group for Wall E

Performance Group Summary for Wall E					
Group No.	Grouping Criteria				Number of Archetypes
	Basic Configuration	Design Load Level		Period Domain	
		Gravity	Seismic		
PG-1	Low Wall	Light (200 plf)	SDC D _{max}	Short	3
PG-2	Aspect ratio		SDC D _{min}		3

Table 11: Performance group for Wall B

Performance Group Summary for Wall B					
Group No.	Grouping Criteria				Number of Archetypes
	Basic Configuration	Design Load Level		Period Domain	
		Gravity	Seismic		
PG-1	Low Wall	Light (200 plf)	SDC D _{max}	Short	2 ¹
PG-2	Aspect ratio		SDC D _{min}		3

¹Only two index archetypes are used for Wall B because the length of clay plaster walls required for the two-story building design loads exceeded the building dimensions. Thus a two-story Wall B index building was not considered in SDC D_{max}.

The performance group for Wall E consists of: 1) three Low aspect ratio wall short-period archetypes designed for SDC D_{max} (PG-1), and 2) three SDC D_{min} - Low aspect ratio wall short-period archetypes (PG-2). The performance group for Wall B consists of: 1) two Low aspect ratio wall short-period archetypes designed for SDC D_{max} (PG-1), and 2) three SDC D_{min} - Low aspect ratio wall short-period archetypes (PG-2).

Table 12 provides the detailed descriptions of the archetype models developed for strawbale frame buildings for clay plaster and cement stucco material. Strawbale walls generally will be used in one- and two-story buildings that have very similar characteristics to conventional light-framed construction with regard to occupancy and building size, roof and floor framing, openings in walls, and interior partitions. Therefore, the one and two-story archetypes for strawbale systems were selected to match those used for light-framed construction with wood shear panels in the P-695 study reported by NAHB (2011). The selected index building archetypes are: 1) small-single family with 1200 square feet, 2) large-single family house with 2100 square feet, and 3) two story single family with 3000 square feet.

Appendix C and Appendix D display the index building of the archetype and unit area load in the three archetypes in accordance with NAHB report. Appendix E shows the building archetype loading for Wall B and Wall E. The thickness of plaster finishes is in accordance with the proposed provisions for a minimum thickness of 1-1/2 in. Where the SAWS hysteretic model is used, the seismic weight (and resulting base shear demand) is established assuming the average plaster thickness is 1/4 inch greater (1-3/4 in.). This seismic weight is also represented in the structural model used in nonlinear static and nonlinear dynamic analysis (Table 12).

Table 12: Index Archetype Configurations for Straw bale wall Shear

Model No	No. of Stories	Seismic Design Coef. (SDS)	Wall E, Cement Stucco		Wall B, Earth Plaster	
			Tributary Width for Seismic Weight (ft)	Tributary Seismic Weight (kips)	Tributary Width for Seismic Weight (ft)	Tributary Seismic Weight (kips)
1	1	1	15	22.59	15	20.55
2	1	0.5	15	22.59	15	20.55
3	1	1	17.5	34.09	17.5	31.32
4	1	0.5	17.5	34.09	17.5	31.32
5 ¹	1	1	15	46.15	-	-
	2		15	27.68	-	-
6	1	0.5	15	46.15	15	41.48
	2		15	27.685	15	25.35

¹The design required shear wall lengths greater than the building dimensions for Wall B in Model Number 5

The number of shear walls in each Archetype, their lengths, and the demand to capacity ratio are provided in Appendix F. Table 13 and Table 14 report the properties of each of these 6 archetypes for Wall B and Wall E, respectively. Design spectra for SDC D are used, as specified in FEMA P695: $S_{DS} = 1.0$ g and $S_{D1} = 0.6$ g for SDC D_{max} , and $S_{DS} = 0.50$ g and $S_{D1} = 0.20$ g for SDC D_{min} . The fundamental periods of the archetypes are reported in the tables, and were determined based on FEMA P695 and ASCE/SEI 7-10. T_a is the approximate period and $T (=C_u T_a)$ has a lower bound limit of 0.25 sec). T_1 is the fundamental period of the building as determined by eigenvalue analysis of the structural model. V/W (equivalent to the LRFD seismic coefficient, C_s) is defined as the ratio of design spectral response acceleration, S_{DS} and the response modification coefficient, R . (Equation 8)

$$C_s = S_{DS}/R \quad \text{Equation 8}$$

The C_s values of Wall B, designed with $R=3.5$, for SDC D_{max} and SDC D_{min} are 0.29 and 0.14, respectively. The seismic coefficient values for Wall E, designed with $R=2.5$, for SDC D_{max}

and SDC D_{min} are 0.4 and 0.2, respectively. As seen in Figure 35, the corresponding MCE ground motion spectral response accelerations, S_{MT} , are 1.5 g for D_{max} and 0.75 g for D_{min} for short period $T=0.25$ Sec.

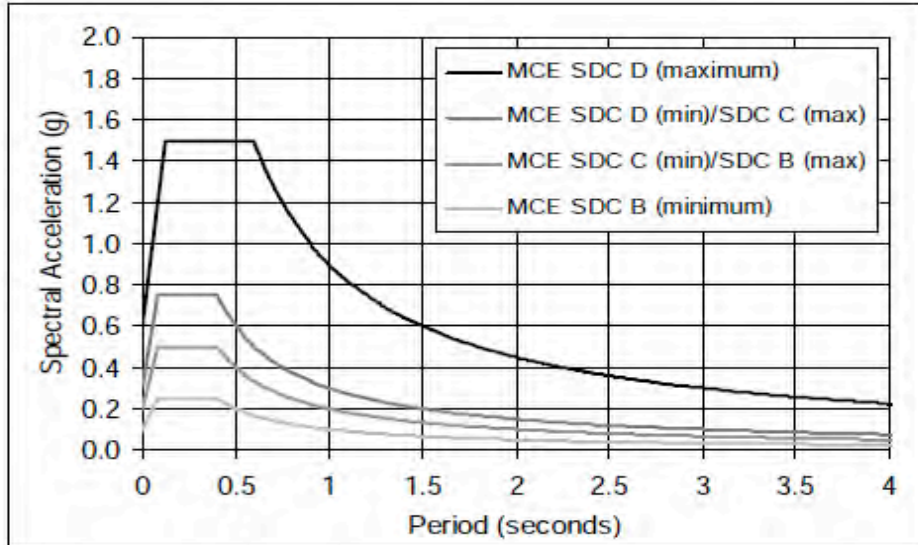


Figure 35: MCE response spectra required for collapse evaluation of index archetypes designed for Seismic Design Category (SDC) D, FEMA P695

Table 13: Structural Properties for Wall B Archetype Designs

Arch. ID	Design Configuration				Pushover and IDA Results			
	No. of Stories	Building Configuration	Wall Aspect	SDC	T [sec]	T_1 [sec]	V/W [g]	$S_{MT}(T)$ [g]
Performance Group No. PG- (Short Period, Low Aspect Ratio, SDC D_{max})								
1	1	Small Family	Low	D_{Max}	0.25	0.23	0.29	1.5
3	1	Large Family	Low	D_{Max}	0.25	0.23	0.29	1.5
Performance Group No. PG- (Short Period, Low Aspect Ratio, SDC D_{min})								
2	1	Small Family	Low	D_{Min}	0.25	0.33	0.14	0.75
4	1	Large Family	Low	D_{Min}	0.25	0.32	0.14	0.75
6	2	TownHouse	Low	D_{Min}	0.25	0.65	0.14	0.75

Table 14: Structural properties for Wall E Archetype Designs, using the SAWS model

Arch. ID	Design Configuration				Pushover and IDA Results			
	No. of Stories	Building Configuration	Wall Aspect	SDC	T [sec]	T_1 [sec]	V/W [g]	$S_{MT}(T)$ [g]
Performance Group No. PG- (Short Period, Low Aspect Ratio, SDC D_{max})								
1	1	SmallFamily	LOW	D_{Max}	0.25	0.19	0.40	1.5
3	1	Large Family	LOW	D_{Max}	0.25	0.24	0.40	1.5
5	2	Townhouse	low	D_{Min}	0.25	0.39	0.40	1.5
Performance Group No. PG- (Short Period, Low Aspect Ratio, SDC D_{min})								
2	1	Small Family	LOW	D_{Min}	0.25	0.28	0.20	0.75
4	1	Large Family	LOW	D_{Min}	0.25	0.34	0.20	0.75
6	2	Townhouse	low	D_{Min}	0.25	0.39	0.20	0.75

8.5. Nonlinear Model Development

Structural modeling of the strawbale frame archetypes follows the use of a “pancake” model in the analysis of wood light frame systems, as done in the FEMA P695 and NAHB reports (2011). The pancake model is described in detail in the report by Isoda, Folz, and Filiatrault (2001) entitled “*Seismic Modeling of Index Wood frame Buildings*”. The pancake model is a two-dimensional model in the horizontal plane in which each wall panel’s hysteretic behavior is represented by an equivalent nonlinear shear spring. As such, the model captures plan torsion effects in rigid diaphragm systems, but does not represent the effects of variable axial forces (due to overturning) on the stiffness and strength of the lateral force-resisting elements. The pancake model also cannot explicitly represent P- Δ effects (e.g. using a leaning column model), although it is possible to alter the hysteretic relationship of the equivalent nonlinear shear springs used to represent the lateral force-resisting elements to include P- Δ effects for the story.

8.5.1. Hysteretic Models

Two hysteretic models, known as SAWS and Pinching4, which are implemented in OpenSees, were used to represent the lateral resistance of the strawbale walls within the

pancake model. The SAWS model was used to represent the load-displacement response of strawbale Walls B and E for all individual Archetype IDs. The Pinching4 hysteretic model was used for each individual Wall E Archetype ID.

Figure 36 illustrates the hysteretic behavior of SAWS hysteretic model, which includes pinching, stiffness degradation, and strength degradation.

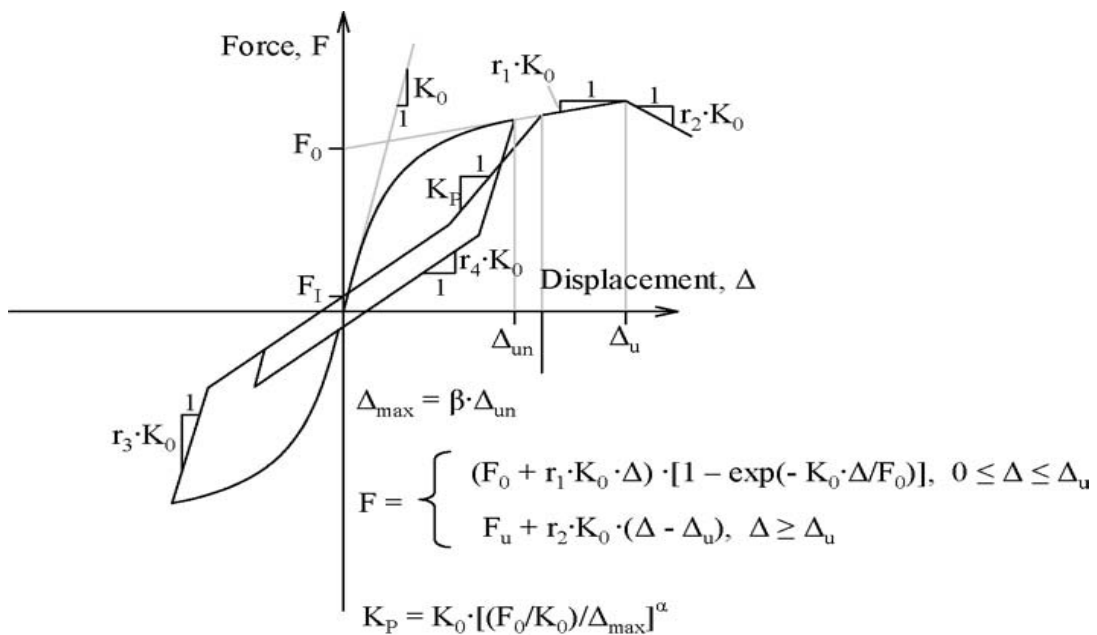


Figure 36: Hysteretic model of shear spring element included in SAWS program (Folz and Filiatrault, 2004a, b).

In the SAWS model, there are 10 different parameters, of which five relate to stiffness, two to force, one to displacement, and two to cyclic degradation. The definition of each parameter is explained in Table 15.

Table 15: SAWS Model Hysteretic Parameters Definitions

Notation	Definition
F0	Intercept strength of the shear wall spring element for the asymptotic line to the envelope curve $F0 > FI > 0$
FI	Intercept strength of the spring element for the pinching branch of the hysteretic curve. ($FI > 0$).
DU	Spring element displacement at ultimate load. ($DU > 0$).
S0	Initial stiffness of the shear wall spring element ($S0 > 0$).
R1	Stiffness ratio of the asymptotic line to the spring element envelope curve. The slope of this line is $R1 S0$. ($0 < R1 < 1.0$).
R2	Stiffness ratio of the descending branch of the spring element envelope curve. The slope of this line is $R2 S0$. ($R2 < 0$).
R3	Stiffness ratio of the unloading branch off the spring element envelope curve. The slope of this line is $R3 S0$. ($R3 < 0$).
R4	Stiffness ratio of the pinching branch for the spring element. The slope of this line is $R4 S0$. ($R4 > 0$).
alpha	Stiffness degradation parameter for the shear wall spring element. ($ALPHA > 0$).
beta	Stiffness degradation parameter for the spring element. ($BETA > 0$).

(Adapted from <http://opensees.berkeley.edu/OpenSees>)

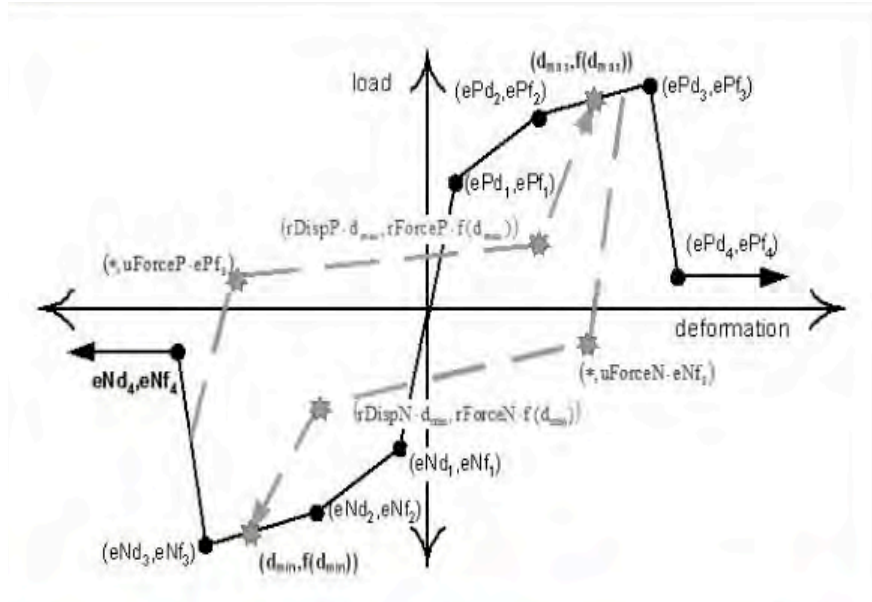


Figure 37: Pinching4 Hysteretic Model

(Adapted from <http://opensees.berkeley.edu/OpenSees>)

The Pinching4 hysteretic model enables pinched load-deformation response and exhibits degradation under cyclic loading. Cyclic degradation of strength and stiffness occurs in three ways: unloading stiffness degradation, reloading stiffness degradation and strength degradation (Figure 37). This model includes 37 different parameters; the definition of each parameter has been described in (Table 16).

Table 16:: Pinching4 model hysteretic parameter definitions

Notation	Definition
ePf1 ePf2 ePf3 ePf4	floating point values defining force points on the positive response envelope
ePd1 ePd2 ePd3 ePd4	floating point values defining deformation points on the positive response envelope
eNf1 eNf2 eNf3 eNf4	floating point values defining force points on the negative response envelope
eNd1 eNd2 eNd3 eNd4	floating point values defining deformations points on the negative response envelope
rDispP rDispN	floating point value defining the ratio of the deformation at which reloading occurs to the maximum/minimum historic deformation demand
rForceP rForceN	floating point value defining the ratio of the force at which reloading begins to force corresponding to the maximum/minimum historic deformation demand
uForceN	floating point value defining the ratio of the strength developed upon unloading from a positive load to the minimum strength developed under monotonic loading
gK1gK2 gK3 gK4 gKLim	floating point values controlling cyclic degradation model for unloading stiffness degradation
gD1gD2 gD3 gD4 gDLim	floating point values controlling cyclic degradation model for reloading stiffness degradation
gF1 gF2 gF3 gF4 gFLim	floating point values controlling cyclic degradation model for strength degradation
gE	floating point value used to define maximum energy dissipation under cyclic loading. Total energy dissipation capacity is defined as this factor multiplied by the energy dissipated under monotonic loading
dmgType	string to indicate type of damage (option: "cycle", "energy")

(Adapted from <http://opensees.berkeley.edu/OpenSees>)

8.5.2. Modeling Procedure

The nonlinear dynamic analysis software SAPWood [14] was utilized for determining the SAWS model response and fitting parameters to the experimental test data. The hysteretic behavior of the adjusted response (Section 8.3.1), which accounts for allowable shear design of the Wall B and E, was modeled in SAWS program (Appendix G). Figure 38 and Figure 39

Figure 39: Wall E, Hysteretic response for test results and SAWS model compare the fitted the SAWS Model and adjusted response for Wall B and Wall E.

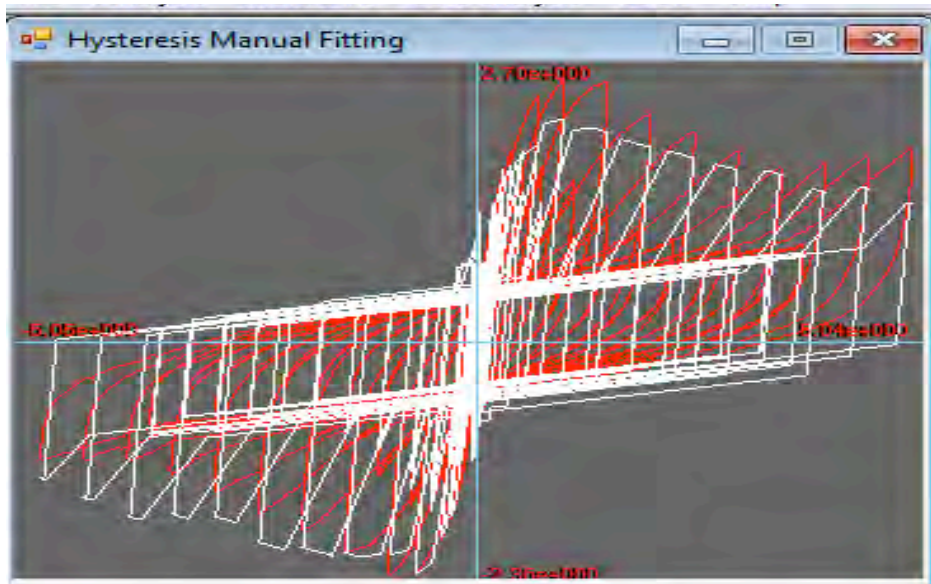


Figure 38: Wall B, Hysteretic response for test results and SAWS model

The 10 parameters derived using the SAWS program is provided in Table 17 for both Wall B and Wall E. It should be noted that while the overall responses in Figure 38

Figure 38: Wall B, Hysteretic response for test results and SAWS model and most of Figure 39

Figure 39: Wall E, Hysteretic response for test results and SAWS model

may appear to match well, the goodness of the match may be conditioned on the particular displacement cycles used in the testing. Of particular significance is the negative tangent stiffness required for the SAWS model to match the overall degrading behavior of the test specimens. In the experimental tests, the specimens nearly always display positive stiffness up to the instant that unloading begins. If unloading had been delayed to a larger displacement, the load being resisted would have increased further, while the negative stiffness in the SAWS model would lead to a reduction in load resisted. (Figure 41 and Figure 42)

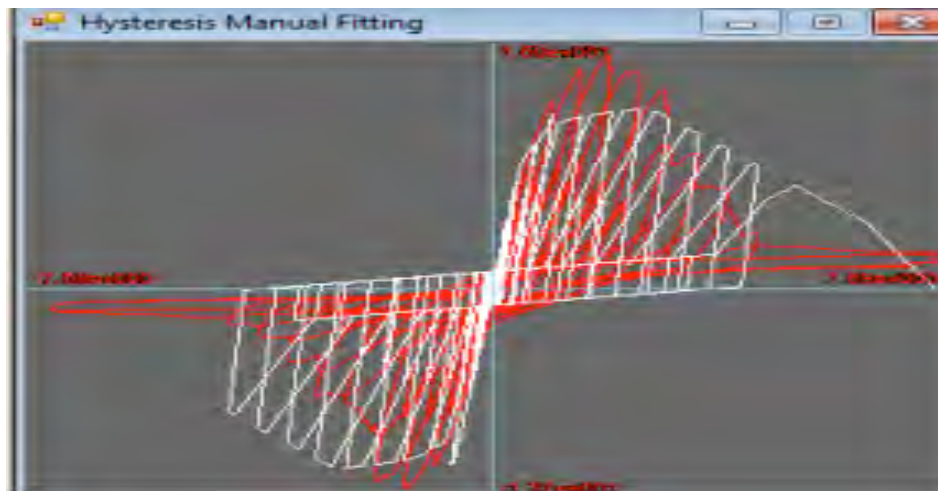


Figure 39: Wall E, Hysteretic response for test results and SAWS model

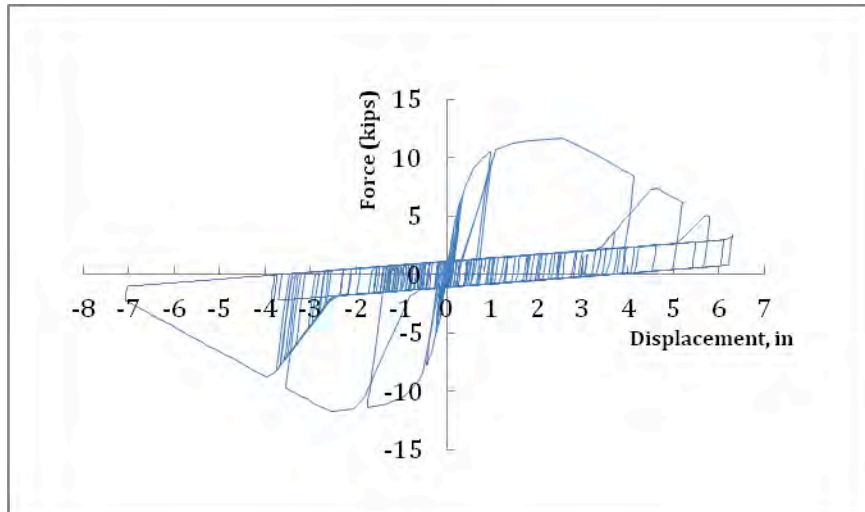


Figure 40: The behavior of model Wall E under earthquake using SAWS model in OpenSees (Archetype ID1, small-single family house, Imperial Valley 1979 earthquake)

Table 17: SAWS model parameters for Wall B and Wall E (8'x8')

Saws Parameters	K_0	F_0	F_1	r_1	r_2	r_3	r_4	D_U	alpha	beta
Wall B Clay plaster finish	9.869	1.924	0.384	0.01	-0.024	1.0	0.010	1.26	0.75	1.10
Wall E Cement plaster finish	30.314	10.966	1.100	0.010	-0.070	1.000	0.010	2.580	0.750	1.100

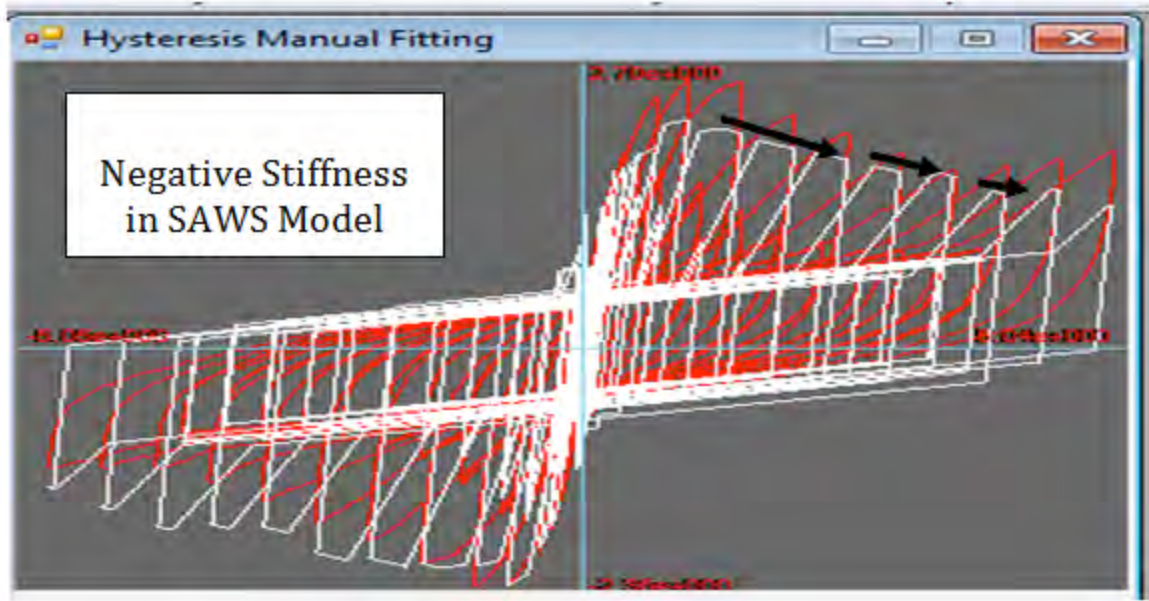


Figure 41: Illustration of negative stiffness in SAWS Model, Wall B

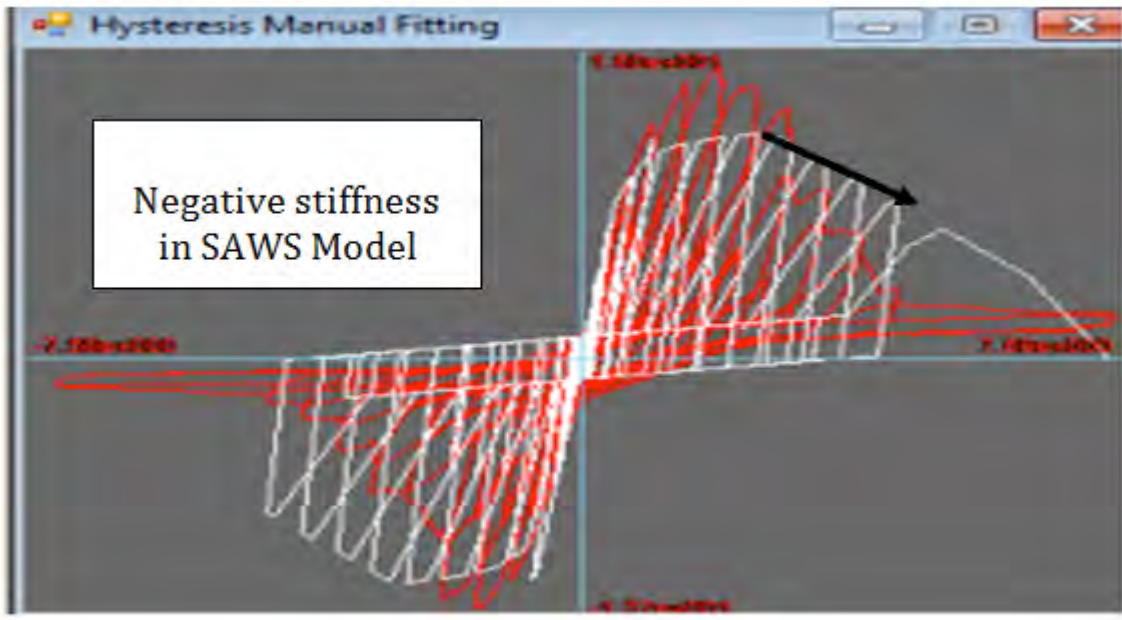


Figure 42: Illustration of negative stiffness in SAWS Model, Wall E

The importance of strength deterioration modeling was investigated by Haselton (2006). Haselton shows that incorrect calibration with negative stiffness while the test data has positive stiffness will change the collapse simulation results. Haselton explains that the negative stiffness calibration causes the negative failure slope to be reached a lower drift level and leads to a steeper post-failure slope than in positive stiffness calibration. Haselton identifies as “correct” the calibration with positive stiffness as shown in Figure 43 (Haselton, 2006).

The SAWS model does not provide a parametric formulation that allows for properly representing the degrading stiffness of the strawbale walls. While results are reported herein for the SAWS model, these do not reflect proper modeling of the degrading stiffness. Henceforth, some results were obtained using a more capable hysteretic model, termed Pinching4 in OpenSees. Using the OpenSees modeling platform, the adjusted response of Wall E was modeled and fitted with Pinching4 hysteretic model. As seen in Figure 44, this hysteretic model shows positive stiffness up to the instant that unloading begins, similar to the test results.

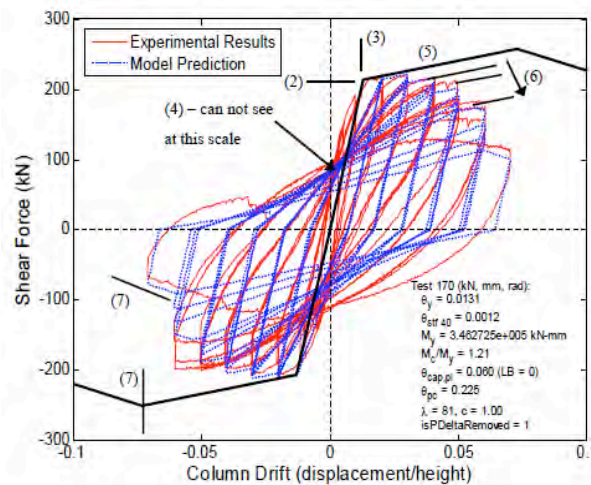


Figure 43: Example of correct calibration procedure (Haselton, 2006)

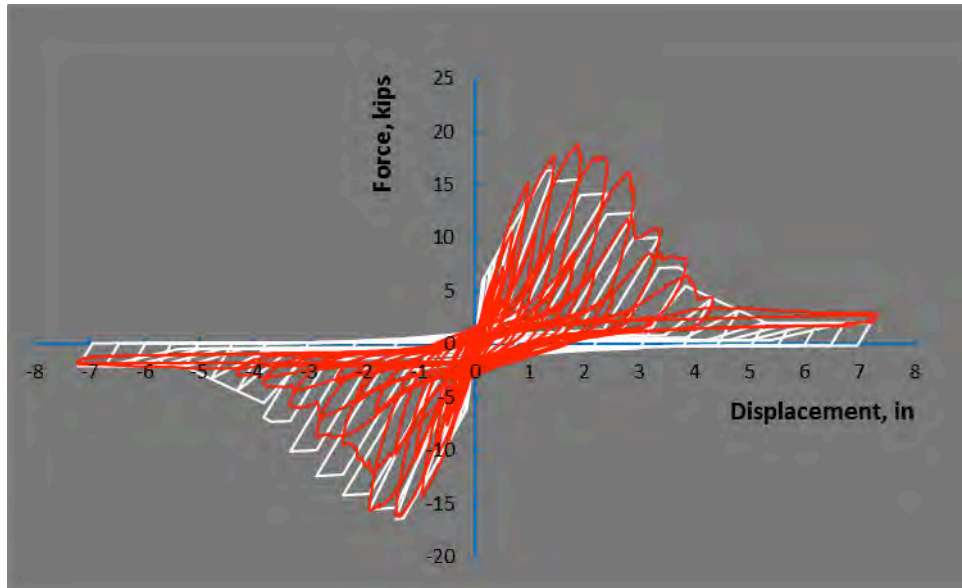


Figure 44: Wall E, Hysteretic response for test results and Pinching4 model

Figure 45 presents the behavior of Wall E modeled with Pinching4 for Archetype ID 5 (Two-story Family building) under Loma Prieta 1989 ground motion. Table 18 provides the parameters derived for this model. The Envelope point values, epf1, epf2, epf3, epf4, enf1, enf2, enf3 and enf4 are chosen based on the monotonic load-displacement behavior assumption.

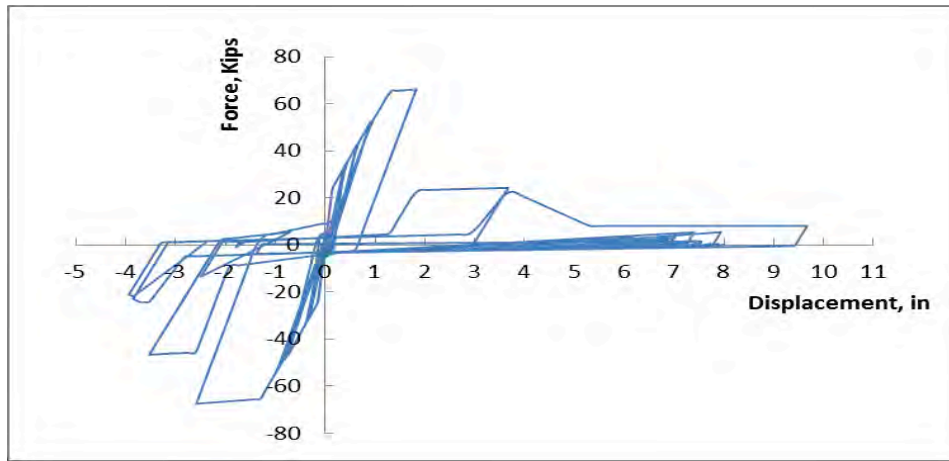


Figure 45: The behavior of model Wall E under earthquake using Pinching4 model in OpenSees (Archetype ID5, Two Story Building, Loma Prieta, Capitola 1989 earthquake)

Table 18: Pinching4 hysteretic model parameters for Wall E (8'x8')

Notation	Point1	Point2	Point3	Point4	Limit
pEnvelopeStress	6	17.2	18.2	6.35	-
nEnvelopeStress	-6	-17.2	-18.2	-6.35	-
pEnvelopeStrain	0.14	1.3	3.7	5.3	-
nEnvelopeStrain	-0.14	-1.3	-3.7	-5.3	-
rDisp	0.8	0.8	-	-	-
rForce	0.2	0.2	-	-	-
uForce	0.05	0.05	-	-	-
gammaK	0.8	0.15	0.05	0	0.8
gammaD	0.5	0	2	0	0
gammaF	1.5	0	2	0	0.68
gammaE	10				

Figure 46 illustrates the rocking model used to determine the residual strength in pinching4 model for Wall E. Recognizing that resistance provided by reinforcing mesh is not represented in the rocking model, for simplicity, the bearing length, L_c , was ignored and the residual strength values, epf_4 and enf_4 , are computed based on equilibrium of the free body rocking about the corner of the wall, as shown in Figure 23.

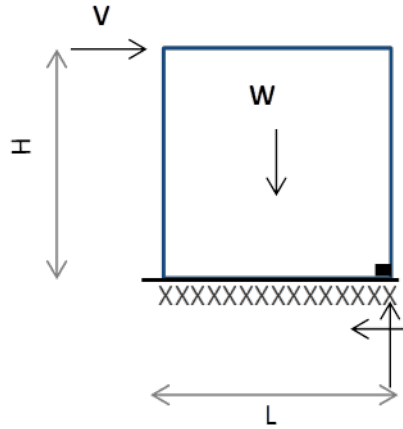


Figure 46: The illustration of Rocking in Pinching4 model for Wall E

For an 8 foot by 8 foot wall, $V_{\text{Rocking}} = WL/2H = W/2$. In particular, the gravity load on the system is represented by the weight of the strawbale, plaster, and the superimposed load. For the test specimen, the weight of the strawbales¹ are assumed to be 13.42² psf , the weight of each plaster surface is assumed to be 35³ psf, and the weight of the superimposed load is 200 plf. Consequently, V_{Rocking} is computed to be 2.35 kips, based on the following:

Superimposed Load	200 plf x 8 inches=	1600 lbs
Weight of the Strawbale and plaster (Wall E)	48.42 psf x (8x8) =	3099 lbs
Total Weight	1600 + 3099 =	4699 lbs

Thus, $V_{\text{Rocking}} = WL/2H = W/2 = 4699/2 = 2349 \text{ lb}$

¹ The thickness of the wall E in Pinching4 model is considered to be 1.5 inches

² 7 pcf* 23"/12= 13.42 psf

³ 140 pcf * 1.5" * 2/12= 35 psf

In order to obtain this rocking resistance in the Pinching 4 model, which also implements strength degradation, 6.35 kips strength was used for epf4 and enf4 so that with cyclic degradation the value degrades to 2.35 kips (Figure 44).

9. Modeling of Archetypes

The archetypes were designed so that each shear wall in the system has the same length and capacity. The models display symmetry and thus no plan torsional response develops. Two-dimensional structural models were prepared for each archetype based on the “pancake” model. These models used zero-length springs defined by the SAWS model. Because plan torsional response cannot develop, the rotational degree-of-freedom was restrained in the OpenSees model to reduce computational time. Each spring as seen in Figure 47 represents one straw bale shear wall. This approach to design and modeling follows that used for light frame walls with wood shear panels, as described in “Seismic analysis of woodframe structures” [Folz and Filiatrault (2004a, b)]. The OpenSees input modeling scripts for representative archetypes of Walls B and E are provided in Appendix G.

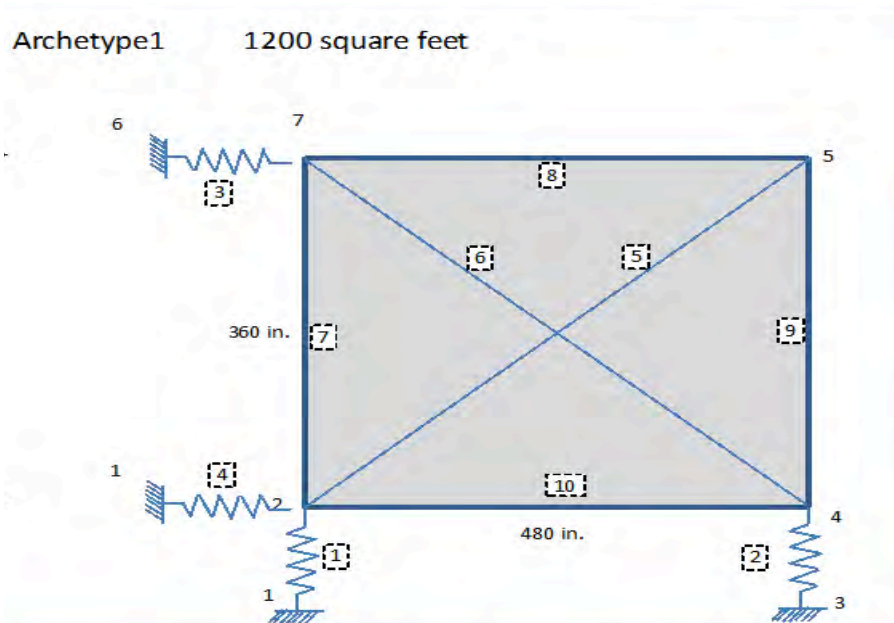


Figure 47: Modeling Straw bale shear wall in SAWS model

10. Nonlinear Static (Pushover) Analysis

A nonlinear static pushover analysis was done for each archetype. The capacity curve resulting from the pushover analysis is used to determine the values of the overstrength factor, Ω and period-based ductility, μ_T based on FEMA P695. , determined using the SAWS model.

The period-based ductility, μ_T , of 8.81 is calculated as the ratio of the ultimate roof displacement, δ_u , (which is defined as the displacement at the 20% reduction of capping strength ($0.8 V/W$)) to the equivalent yield roof displacement, δ_{yeff} :

Figure 48 shows a monotonic static pushover curve for a one-story Large single family building (Archetype ID 3) with Cement plaster wall material finishes. The lateral force (ordinate) is normalized with respect to the seismic weight to obtain a capacity curve in terms of the seismic coefficient, C_s . The ordinate plots the roof drift ratio, defined as displacement at the roof level divided by the height of the roof, relative to the base of the structure.

The design seismic coefficient (for strength design) for this archetype model, V/W is calculated as follows:

$$C_s = \frac{V}{W}$$
$$C_s = \frac{S_{DS}}{R} = \frac{1}{2.5} = 0.40$$

The maximum normalized base shear resistance value, V_{max}/W obtained by monotonic static pushover analysis is equal to 0.687. Therefore the overstrength factor value, Ω , is calculated to be equal to 1.7 for this archetype model:

$$\Omega = \frac{0.4}{0.687} = 1.7$$

Based on Equation 3, the larger of the fundamental period ($T=C_uT_a$) with lower bound limit of 0.25 sec and the value of T_1 (fundamental period of the archetype model computed by eigenvalue analysis) should be used in the equation. In Table 14 the $T= 0.25$ sec and $T_1= 0.24$ sec. Therefore 0.25 was selected for determining the effective yield displacement. Thus, the effective yield displacement obtained from Equation 3 is equal to 0.42 in.

$$\delta_{y,eff} = 1 * \frac{46.85}{68.2} \left[\frac{386}{4\pi^2} \right] (0.25)^2 = 0.42in.$$

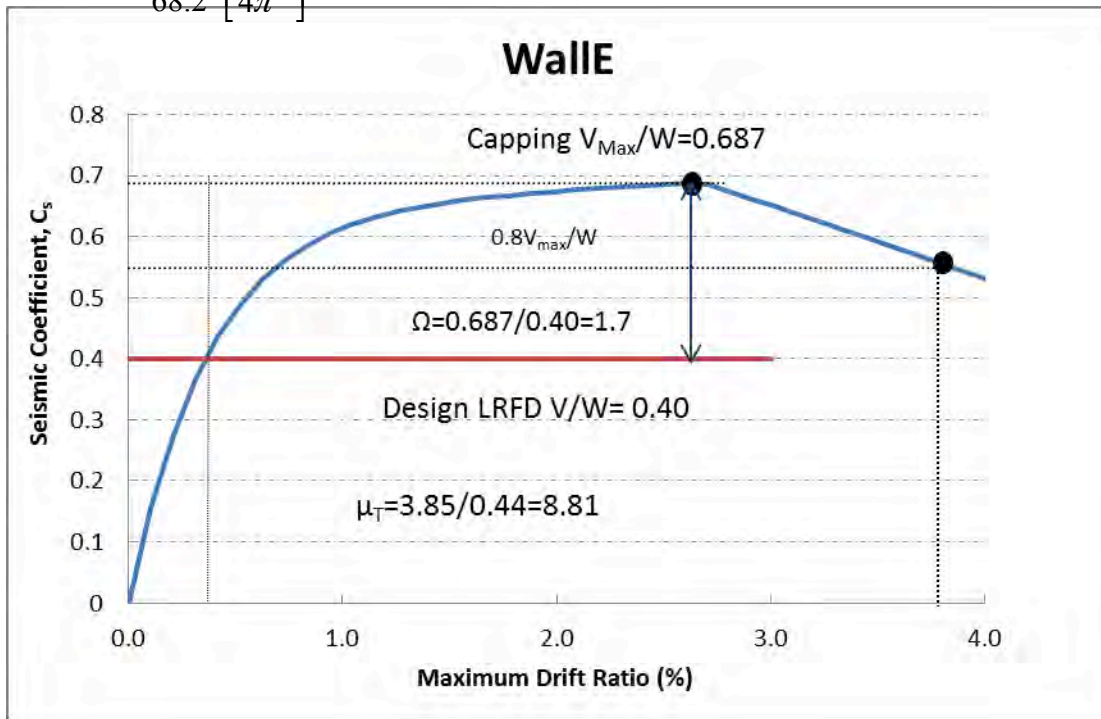


Figure 48: Monotonic Static Pushover curve on one story single family with Cement plaster wall material finishes (Wall E Archetype ID 3), determined using the SAWS model.

The period-based ductility, μ_T , of 8.81 is calculated as the ratio of the ultimate roof displacement, δ_u , (which is defined as the displacement at the 20% reduction of capping strength ($0.8 V/W$)) to the equivalent yield roof displacement, $\delta_{y,eff}$:

$$\mu_T = \frac{\delta_u}{\delta_{yeff}} = \frac{3.7}{0.42} = 8.81$$

The overstrength and period-based ductility values for all archetypes are summarized in Table 25 and **Error! Reference source not found.**

for Wall B (clay plaster) and Wall E (cement plaster), respectively.

11. Nonlinear Dynamic Analyses

Nonlinear dynamic analysis was done to determine the median collapse capacity, S_{CT} , and collapse margin ratio, CMR, for each of the archetype model.

As prescribed in FEMA P695, the Far-Field record set was used in the incremental dynamic analyses of each archetype for collapse assessment. The Far field record set includes 22 ground motion component pairs recorded at sites greater than or equal to 10 km from fault rupture. The prescribed Far-Field records are identified in Table A-4A of FEMA P695 Report (Table 19). The acceleration time history record for each ground motion can be obtained from the PEER NGA Database (http://peer.berkeley.edu/peer_ground_motion_database) further information describing the records can be found in Appendix A of FEMA P695.

The ground motions obtained from the PEER NGA database were scaled based on FEMA P695 requirement. Based on FEMA P695 Methodology, normalization and scaling of the records was performed for all 44 ground motion components. The procedure is briefly explained in the next section.

11.1. Normalization of the Records

Normalization was done with respect to the value of peak ground velocity, PGV_{PEER} to "remove unwarranted variability between records due to inherent differences in event magnitude, distance to source, source type and site conditions, while still maintaining the

inherent aleatory (i.e., record-to-record) variability necessary for accuracy predicting collapse fragility.” (FEMA P695 page A-10)

Table 19: Summary of Earthquake Event and Recording Station Data [FEMA P695]

for the Far-Field Record Set

ID No.	Earthquake			Recording Station	
	M	Year	Name	Name	Owner
1	6.7	1994	Northridge	Beverly Hills - Mulhol	USC
2	6.7	1994	Northridge	Canyon Country-WLC	USC
3	7.1	1999	Duzce, Turkey	Bolu	ERD
4	7.1	1999	Hector Mine	Hector	SCSN
5	6.5	1979	Imperial Valley	Delta	UNAMUCSD
6	6.5	1979	Imperial Valley	El Centro Array #11	USGS
7	6.9	1995	Kobe, Japan	Nishi-Akashi	CUE
8	6.9	1995	Kobe, Japan	Shin-Osaka	CUE
9	7.5	1999	Kocaeli, Turkey	Duzce	ERD
10	7.5	1999	Kocaeli, Turkey	Arcelik	KOERI
11	7.3	1992	Landers	Yermo Fire Station	CDMG
12	7.3	1992	Landers	Coolwater	SCE
13	6.9	1989	Loma Prieta	Capitola	CDMG
14	6.9	1989	Loma Prieta	Gilroy Array #3	CDMG
15	7.4	1990	Manjil, Iran	Abbar	BHRC
16	6.5	1987	Superstition Hills	El Centro Imp. Co.	CDMG
17	6.5	1987	Superstition Hills	Poe Road (temp)	USGS
18	7.0	1992	Cape Mendocino	Rio Dell Overpass	CDMG
19	7.6	1999	Chi-Chi, Taiwan	CHY101	CWB
20	7.6	1999	Chi-Chi, Taiwan	TCU045	CWB
21	6.6	1971	San Fernando	LA - Hollywood Stor	CDMG
22	6.5	1976	Friuli, Italy	Tolmezzo	--

The following equations⁴ were used for this purpose:

$$NM_i = \frac{\text{Median}(PGV_{PEER})}{PGV_{PEER,i}} \quad \text{Equation 9}$$

$$\begin{aligned} NTH_{1,i} &= NM_i \times TH_{1,i} \\ NTH_{2,i} &= NM_i \times TH_{2,i} \end{aligned} \quad \text{Equation 10}$$

where:

NM_i = Normalization factor of both horizontal components of the Ith record

$PGV_{PEER,i}$ = Peak ground velocity of the ith record (PEER NGA database)

$\text{Median}(PGV_{PEER,i})$ = Median of $PGV_{PEER,i}$ values of records in the set,

$NTH_{1,i}$ = Normalized ith record, horizontal component 1,

$NTH_{2,i}$ = Normalized ith record, horizontal component 2,

$TH_{1,i}$ =Record I, horizontal component 1 (PEER NGA database), and

$TH_{2,i}$ = Record I, horizontal component 2 (PEER NGA database).

Column 5 of Table 20 shows peak ground velocity, PGV_{PEER} , reported in the Peer NGA database. PGV_{PEER} values vary from 17.8 cm/s to 90.7 cm/s with a median of 37.2 cm/s.

⁴ From FEMA P695 page A-10

Based on the Equation 10, Normalization factor was calculated and summarized in column 6 of Table 20. For example the Normalization factor for fifth ground motion of (ID number 5) of the table (Imperial Valley, Delta) would be 1.31, which is determined as $NM_5 = 37.2 / 28.4 = 1.31$, where 37.2 cm/s is the median of the $PGV_{PEER,i}$ values of records in the set and 28.4 cm/s is the $PGV_{PEER,i}$ value.

11.2. Scaling of Record Sets

For scaling the records, the entire record set was systematically scaled up until collapse was observed for each record. Collapse was taken equal to the smaller of 7% drift and the point at which the IDA curve flatlines.

The acceleration time history record of 44 ground motion components at the fundamental period of the building, T , was provided in Table 21. The fundamental period of the building is 0.25 sec for all archetypes.

$$T = C_u T_a \quad \text{Equation 11}$$

$$T_a = c_t h_n^x \quad \text{Equation 12}$$

where:

T = fundamental period of the building (with lower bound limit of 0.25 sec)

C_u =Upper-limit period coefficient as determined in Table 12.8-1 of ASCE/SEI 7-10

T_a =the approximate fundamental period of the building, in seconds, as determined in section 12.8.2.1 of ASCE/SEI 7-10

C_t =Approximate period coefficient as determined in Table 12.8-2 of ASCE/SEI 7-10, taken equal to 0.02 for strawbale buildings

h_n = building height, in ft.

x =parameter of equation given in Table 12.8-2 of ASCE/SEI 7-10, taken equal to 0.75 for strawbale buildings

For modeling of the one- and two-story archetypes, the slope of the roof was ignored and the total height of the wall was defined as the height of the building in Equation 12. Considering the massive walls and relatively light wood roof trusses, the center of mass will be approximately at the top of the wall. Therefore, for determining T_a , the height of the buildings in one-story archetype was defined to be 8 ft (the same as height of shear walls) and in two-story building archetypes the height was defined to be 18 ft. The fundamental period of the building, $T=C_uT_a$, based on ASCE/SEI 7-10 (Equation 11) is 0.18 sec for the one-story buildings and 0.24 sec for two-story buildings. As lower bound limit of the T in ASCE/SEI 7-10 is 0.25 sec, the value of 0.25 sec was selected for all archetype cases.

The software packages used for nonlinear dynamic analysis were OpenSees (Open System for Earthquake Engineering Simulation), and C# (pronounced "c-sharp"). OpenSees was used to run the nonlinear dynamic analyses for twenty-two records (44 individual components). Due to the volume of the analyses 44 ground motion components at different scaling factors, the C# program was used for creating the input files and post processing the output results. For each ground motion, C# software was programmed to produce input files with different ground motion intensities. In the C# program, the ground motion records were systematically scaled up until collapse was detected or the drift reached 7% of the story height. The C# program script is provided in Appendix I.

Figure 49 illustrates the IDA curves obtained for the 44 components for one archetype (Archetype ID 3), which is a one-story large single family building with cement plaster wall finish, using the SAWS model. In accordance with FEMA P695 and ASCE/SEI 7-10 the

values of S_{CT} and S_{MT} are computed based on Fundamental Period the archetypes ($T = C_u T_a$ with lower bound limit 0.25 Sec). Collapse is defined when the drift of IDA curve reaches an interstory drift of 7% of the story height.

As illustrated in the figure, the spectral acceleration causing collapse in 50% of the analysis, S_{CT} , is 3.18 g. S_{MT} , the MCE spectral acceleration, value at $T=0.25$ is 1.5 g. Based on Equation 5, the CMR (Collapse Margin Ratio) was determined as $3.18/1.5=2.12$.

Table 20: Summary of PEER NGA database information and Normalization Factors

Record ID	ID Number	Earthquake	Station	PGV _{max} cm/s	Normalization Factor
1a 1b	1	Northridge	Beverly Hills- Mulhol	57.2	0.65
2a 2b	2	Northridge	Canyon Country-WLC	44.8	0.83
3a 3b	3	Duzce, Turkey	Bolu	59.2	0.63
4a 4b	4	Hector Mine	Hector	34.1	1.09
5a 5b	5	Imperial Valley	Delta	28.4	1.31
6a 6b	6	Imperial Valley	El Centro Array #11	36.7	1.01
7a 7b	7	Kobe, Japan	Nishi-Akashi	36	1.03
8a 8b	8	Kobe, Japan	Shin-Osaka	33.9	1.10
9a 9b	9	Kocaeli, Turkey	Duzce	54.1	0.69
10a 10b	10	Kocaeli, Turkey	Arcelik	27.4	1.36
11a 11b	11	Landers	YermoFire Station	37.7	0.99
12a 12b	12	Landers	Coolwater	32.4	1.15
13a 13b	13	Loma Prieta	Capitola	34.2	1.09
14a 14b	14	Loma Prieta	Gilroy Array #3	42.3	0.88
15a 15b	15	Manjil, Iran	Abbar	47.3	0.79
16a 16b	16	Superstition Hills	El Centro Imp. Co.	42.8	0.87
17a 17b	17	Superstition Hills	PoeRoad (temp)	31.7	1.17
18a 18b	18	Cape Mendocino	Rio Dell Overpass	45.4	0.82
19a 19b	19	Chi-Chi, Taiwan	CHY101	90.7	0.41
20a 20b	20	Chi-Chi, Taiwan	TCU045	38.8	0.96
21a 21b	21	San Fernando	LA- Hollywood	17.8	2.09
22a 22b	22	Friuli, Italy	Tolmezzo	25.9	1.44

Table 21: Characteristics of the acceleration records at T=0.25 sec

Record ID	ID Number	Earthquake	Station	Duration time (sec)	Peer Sa (g) T=0.25 sec
1a	1	Northridge	Beverly Hills- Mulhol	0.01	0.84
1b				0.01	0.9822
2a	2	Northridge	Canyon Country-WLC	0.01	0.9947
2b				0.01	1.0726
3a	3	Duzce, Turkey	Bolu	0.01	1.9342
3b				0.01	0.9792
4a	4	Hector Mine	Hector	0.01	0.6533
4b				0.01	0.6722
5a	5	Imperial Valley	Delta	0.01	0.539
5b				0.01	0.6264
6a	6	Imperial Valley	El Centro Array #11	0.005	1.4151
6b				0.005	1.9073
7a	7	Kobe, Japan	Nishi-Akashi	0.01	1.4773
7b				0.01	1.1834
8a	8	Kobe, Japan	Shin-Osaka	0.01	0.3735
8b				0.01	0.5611
9a	9	Kocaeli, Turkey	Duzce	0.005	0.6615
9b				0.005	1.0024
10a	10	Kocaeli, Turkey	Arcelik	0.005	0.2765
10b				0.005	0.3637
11a	11	Landers	YermoFire Station	0.02	0.3978
11b				0.02	0.6071
12a	12	Landers	Coolwater	0.0025	1.09
12b				0.0025	0.84
13a	13	Loma Prieta	Capitola	0.005	1.1124
13b				0.005	1.4395
14a	14	Loma Prieta	Gilroy Array #3	0.005	1.1231
14b				0.005	1.3946
15a	15	Manjil, Iran	Abbar	0.02	1
15b				0.02	1
16a	16	Superstition Hills	El Centro Imp. Co.	0.005	0.672
16b				0.005	0.6595
17a	17	Superstition Hills	PoeRoad (temp)	0.01	0.768
17b				0.01	0.5872
18a	18	Cape Mendocino	Rio Dell Overpass	0.02	0.9798
18b				0.02	1.3559
19a	19	Chi-Chi, Taiwan	CHY101	0.005	0.5278
19b				0.005	0.5929
20a	20	Chi-Chi, Taiwan	TCU045	0.005	0.97
20b				0.005	1.03
21a	21	San Fernando	LA- Hollywood	0.01	0.3712
21b				0.01	0.792
22a	22	Friuli, Italy	Tolmezzo	0.005	1.1292
22b				0.005	0.7464

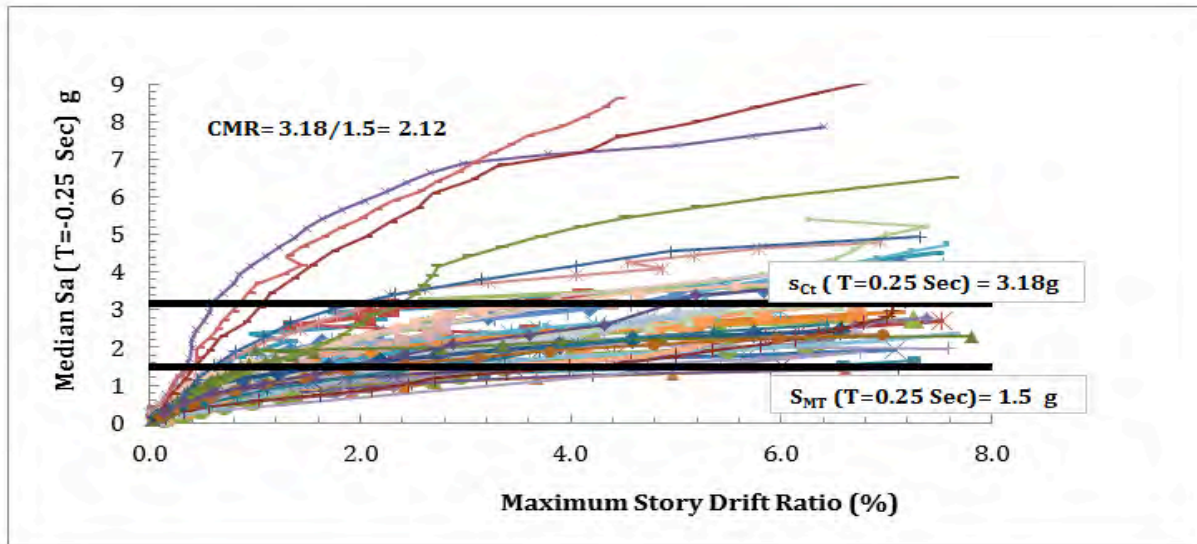


Figure 49: Results of incremental dynamic analysis to collapse for the one-story large family building with Cement plaster wall material finishes (Archetype ID 3)

Figure 50 displays a collapse fragility collapse curve for the one story large family building, archetype ID 3 of Wall E. This plot shows that median collapse capacity, which corresponds to the median ground motion intensity associated with collapse (i.e. 22 records causing collapse have higher intensity and 22 records causing collapse have lower intensity), expressed in terms of S_a at $T=0.25$ sec, is 3.18 g.

Based on Equation 6, the Adjusted Collapse Margin Ratio, ACMR was computed as the product of Collapse Margin Ratio, CMR, and the Spectral Shape Factor, SSF.

Table 22 Table 22 Shows the SSF value for the ductility of 8.81 obtained from Monotonic static pushover (Figure 48) is 1.33. As CMR value from nonlinear dynamic analysis is 2.12. The value of ACMR, Adjusted Collapse Margin Ratio, for this archetype was computed ($1.33 \times 2.12 = 2.82$).

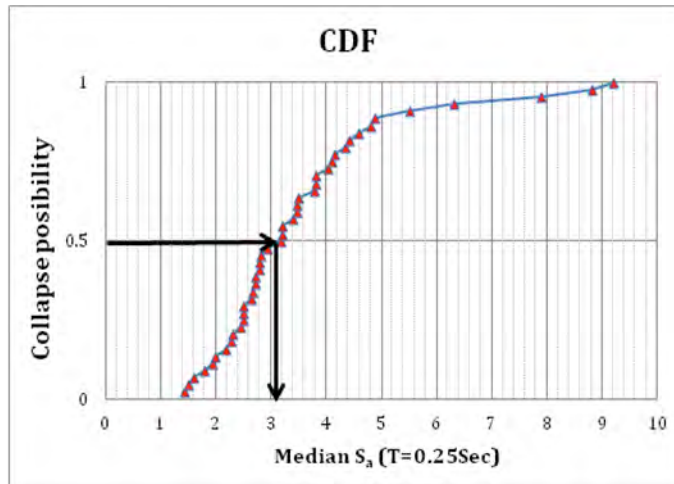


Figure 50: Collapse fragility collapse curve for archetype 3 of Wall E

Table 22: Spectral Shape Factor (SSF) for Archetypes Designed using SDC D_{max} (Taken from Table 7-1b FEMA P695)

T (sec.)	Period-Based Ductility, μ_T							
	1.0	1.1	1.5	2	3	4	6	≥ 8
≤ 0.5	1.00	1.05	1.1	1.13	1.18	1.22	1.28	1.33
0.6	1.00	1.05	1.11	1.14	1.2	1.24	1.3	1.36
0.7	1.00	1.06	1.11	1.15	1.21	1.25	1.32	1.38
0.8	1.00	1.06	1.12	1.16	1.22	1.27	1.35	1.41
0.9	1.00	1.06	1.13	1.17	1.24	1.29	1.37	1.44
1.0	1.00	1.07	1.13	1.18	1.25	1.31	1.39	1.46
1.1	1.00	1.07	1.14	1.19	1.27	1.32	1.41	1.49
1.2	1.00	1.07	1.15	1.2	1.28	1.34	1.44	1.52
1.3	1.00	1.08	1.16	1.21	1.29	1.36	1.46	1.55
1.4	1.00	1.08	1.16	1.22	1.31	1.38	1.49	1.58
≥ 1.5	1.00	1.08	1.17	1.23	1.32	1.4	1.51	1.61

After completing the analyses of archetypes and determining μ_T , CMR, and ACMR, the response modification coefficient, R, was evaluated based on FEMA P695 methodology. In this approach the individual values of ACMR obtained for each archetype and the average of the ACMR values obtained for the archetypes within each performance group were compared to the acceptable values of ACMR, consisting of ACMR_{20%} for each individual archetype and ACMR_{10%} for each performance group. The acceptable ACMR values are based on a characterization of uncertainty, as described below.

12. Uncertainty Evaluation

Acceptable values of ACMR_{20%} and ACMR_{10%} are a function of the total system uncertainty. The uncertainty components as defined within FEMA P695 (associated with design requirements, test data, modeling, and ground motions) were evaluated according to the FEMA P695 methodology.

Table 23 summarizes the quality ratings associated with design requirement uncertainty, β_{DR} , test data from an experimental investigation uncertainty, β_{TD} , index archetype model uncertainty, β_{MDL} , and record-to-record uncertainty β_{RTR} . The various β terms represent estimates of the standard deviations of natural logarithm of the relevant random variable; numerical values are tabulated where specified by the methodology.

FEMA P695 assigns a fixed value of $\beta_{RTR} = 0.4$ in performance evaluation. Based on careful review of the quality ratings provided for design requirements, test data, and archetype model uncertainty, quality ratings of “medium” were assigned for determining the values of β_{DR} , β_{TD} and β_{MDL} resulting in each being assigned a value of 0.35. (Chapters 3 and 5 of FEMA P695 explain the way these uncertainties should be evaluated and Table 3-1, Table 3-2 and Table 5-3 of FEMA P695 present the quality rating value.) Consequently, using Equation 7, a total uncertainty of 0.726 was determined.

$$\beta_{TOT} = \sqrt{0.4^2 + 0.35^2 + 0.35^2 + 0.35^2} = 0.726$$

For a total uncertainty of 0.726, the limits on adjusted collapse margin ratio (ACMR) can be determined from tabulated data, as given in Table 24

. Values of ACMR for each individual archetype cannot be less than $ACMR_{20\%}$ (= 1.85). Average values of ACMR for each of the strawbale performance groups cannot be less than $ACMR_{10\%} = 2.54$ (Table 7-3 FEMA P695).

Table 23: Quality rating of test design, modeling and design uncertainties

	β_{RTR}	β_{DR}	β_{TD}	β_{MDL}	β_{TOT}
Plasters detailed for strength (cube compression strengths demonstrated)	0.40	FAIR	FAIR	FAIR	0.726

Table 24: Acceptable values of adjusted collapse margin values $ACMR_{10\%}$ and $ACMR_{20\%}$

Total system Collapse uncertainty, β_{TOT}	$ACMR_{20\%}$	$ACMR_{10\%}$
0.726	1.85	2.54

13. Performance Evaluation

The pushover and dynamic analysis results are summarized in the tables below for Wall B and Wall E respectively, based on analysis using the SAWS hysteretic model. The results displayed in Table 25 and Table 26

show that all individual archetypes pass the $ACMR_{20\%}$ criteria and the average of each performance group pass the $ACMR_{10\%}$ criteria. This indicates that strawbale Wall B with

R=3.5 and strawbale Wall E with R=2.5 meet the collapse performance objective of the FEMA P695 methodology and would be suitable to be approved as a new system.

Table 25: The Summary of collapse results and adjusted collapse margin ratio for Wall B (clay plaster), using the SAWS hysteretic model

Arch. ID	Design Configuration				Pushover and IDA Results				Acceptance Check			Accept ACMR	Pass/Fail
	No. of Stories	Building Configuration	Wall Aspect Ratio	Wall Finishes	Static Ω	S_{MT} (g)	S_{CT} (g)	CMR	μ_r	SSF	ACMR		
Performance Group No. PG- (Short Period, Low Aspect Ratio, SDC D_{max})													
1	1	Small Family	LOW	Clay Plaster	1.39	1.5	2.88	1.92	12.27	1.33	2.55	1.85	Pass
3	1	Large Family	LOW	Clay Plaster	1.37	1.5	2.84	1.89	12.47	1.33	2.52	1.85	Pass
Mean of Performance Group:					1.38						2.54	2.54	Pass
Performance Group No. PG- (Short Period, Low Aspect Ratio, SDC D_{min})													
2	1	Small Family	LOW	Clay Plaster	1.39	0.75	2.14	2.85	14	1.14	3.25	1.85	pass
4	1	Large Family	LOW	Clay Plaster	1.37	0.75	1.96	2.61	13.86	1.14	2.98	1.85	pass
6	2	Town House	LOW	Clay Plaster	1.3	0.75	1.78	2.37	4.1	1.090	2.59	1.85	pass
Mean of Performance Group:					1.35						2.94	2.54	pass

Table 26: The Summary of collapse results and adjusted collapse margin ratio for Wall E (cement plaster), using the SAWS hysteretic model

Arch. ID	Design Configuration				Pushover and IDA Results				Acceptance Check			Accept ACMR	Pass/Fail
	No. of Stories	Building Configuration	Wall Aspect Ratio	Wall Finishes	Static Ω	S_{MT} (g)	S_{CT} (g)	CMR	μ_r	SSF	ACMR		
Performance Group No. PG- (Short Period, Low Aspect Ratio, SDC D_{max})													
1	1	Small Single Family	LOW	Cement	2.6	1.5	3.72	2.48	5.91	1.28	3.17	1.85	Pass
3	1	Large Single Family	LOW	Cement	1.7	1.5	3.18	2.12	8.81	1.33	2.82	1.85	Pass
5	2	Townhouse	LOW	Cement	1.5	1.5	2.48	1.65	4.92	1.25	2.07	1.85	Pass
Mean of Performance Group:					1.93						2.69	2.54	Pass
Performance Group No. PG- (Short Period, Low Aspect Ratio, SDC D_{min})													
2	1	Small Single Family	LOW	Cement	2.6	0.75	2.65	3.53	9.4	1.14	4.03	1.85	pass
4	1	Large Single Family	LOW	Cement	1.7	0.75	2.18	2.91	9.4	1.14	3.31	1.85	pass
6	2	Townhouse	LOW	Cement	1.6	0.75	1.896	2.53	7.93	1.14	2.88	1.85	pass
Mean of Performance Group:					1.97						3.41	2.54	pass

Results for cement plaster (Wall E) and modeled with the pinching4 model are given in Table 27. Data in this table show that each individual archetype passes the $ACMR_{20\%}$ criteria and the average of each performance group passes the $ACMR_{10\%}$ criteria.

Table 27: The Summary of collapse results and adjusted collapse margin ratio for Wall E (cement plaster) using the Pinching4 model

Arch. ID	Design Configuration				Pushover and IDA Results				Acceptance Check			Accept ACMR	Pass/ Fail
	No. of Stories	Building Configuration	Wall Aspect Ratio	Wall Finishes	Static Ω	S_{MT} (g)	S_{CT} (g)	CMR	μ_r	SSF	ACMR		
Performance Group No. PG- (Short Period, Low Aspect Ratio, SDC D_{max})													
1	1	Small Single Family	LOW	Cement	4.3	1.5	4.15	2.77	3.96	1.22	3.38	1.85	Pass
3	1	Large Single Family	LOW	Cement	2.9	1.5	3.19	2.13	6.0	1.28	2.72	1.85	Pass
5	2	Townhouse	LOW	Cement	2.5	1.5	2.71	1.81	4.80	1.24	2.25	1.85	Pass
Mean of Performance Group:					3.23						2.78	2.54	Pass
Performance Group No. PG- (Short Period, Low Aspect Ratio, SDC D_{min})													
2	1	Small Single Family	LOW	Cement	4.3	0.75	2.74	3.65	7.91	1.14	4.16	1.85	Pass
4	1	Large Single Family	LOW	Cement	2.9	0.75	2.07	2.76	9.89	1.14	3.15	1.85	Pass
6	2	Townhouse	LOW	Cement	2.7	0.75	2.05	2.73	8.75	1.14	3.12	1.85	Pass
Mean of Performance Group:					3.30						3.48	2.54	pass

An alternative grouping of archetypes into performance groups would separate the one- and two-story archetypes of Table 27. Table 28 presents a complete performance group of one-story archetypes. Table 29 presents a partial performance group consisting of a single two-story archetype. With this definition of performance groups, the mean ACMR values become 3.05 and 2.25 for the one-story archetypes and two-story archetypes, respectively. As there are two archetypes in Table 28, the mean value of ACMR (3.05) is to be compared with $ACMR_{10\%}$ (2.54) while for the single two-story archetype in Table 29, the ACMR value (2.25) is to be compared with $ACMR_{20\%}$ (1.85).

Table 28: Results for Performance Group comprising one-story archetypes, Wall E (cement plaster), modeled with the Pinching4 hysteretic model.

Arch. ID	Design Configuration				Pushover and IDA Results				Acceptance Check			Accept ACMR	Pass/Fail
	No. of Stories	Building Configuration	Wall Aspect Ratio	Wall Finishes	Static Ω	S_{MT} (g)	S_{CT} (g)	CMR	μ_T	SSF	ACMR		
Performance Group of One-story archetypes													
1	1	Small Single Family	LOW	Cement	4.3	1.5	4.15	2.77	3.96	1.22	3.38	1.85	Pass
3	1	Large Single Family	LOW	Cement	2.9	1.5	3.19	2.13	6.0	1.28	2.72	1.85	Pass
Mean of Performance Group:					3.60						3.05	2.54	Pass

Table 29: Results for Partial Performance Group comprising a single two-story archetype, Wall E (cement plaster), modeled with Pinching4 hysteretic model.

Arch. ID	Design Configuration				Pushover and IDA Results				Acceptance Check			Accept ACMR	Pass/Fail
	No. of Stories	Building Configuration	Wall Aspect Ratio	Wall Finishes	Static Ω	S_{MT} (g)	S_{CT} (g)	CMR	μ_T	SSF	ACMR		
Performance Group of Two-story archetype													
5	2	Townhouse	LOW	Cement	2.5	1.5	2.71	1.81	4.80	1.24	2.25	1.85	Pass

Based on this classification of the archetypes into performance groups, it is apparent that there is significant reserve capacity. An estimate of the R factor for which the ACMR values would match the minimum acceptable ACMR values can be obtained using a relationship presented in ATC-84 (2011). This relationship is:

$$R_{UR10\%} = \left(\frac{S_{MT} / 1.5}{V / W} \right) \left(\frac{ACMR}{ACMR_{10\%}} \right) \quad \text{Equation 13}$$

where:

$R_{UR10\%}$ = Value of the R factor of the archetype model of interest that corresponds approximately to a 10 percent probability of collapse,

S_{MT} = MCE response spectral acceleration at archetype period, T,

V/W = normalized base shear (C_s coefficient) used for archetype design,

ACMR = adjusted collapse margin ratio of archetype model of interest, and

ACMR_{10%} = acceptable value of ACMR (based on total uncertainty of collapse fragility).

Application to the one-story performance group results in

$$R = \left(\frac{1.5/1.5}{0.4} \right) \left(\frac{3.05}{2.54} \right) = 3.00 \quad \text{one-story archetypes with cement plaster}$$

Since for the two-story structure, there is only one archetype in its partial performance group (Table 29), ACMR_{20%} value is used, resulting in

$$R = \left(\frac{1.5/1.5}{0.4} \right) \left(\frac{2.25}{1.85} \right) = 3.04 \quad \text{two-story archetype with cement plaster}$$

Since the clay plaster walls were designed with $R=3.5$ and were shown to have acceptable performance using the SAWS model, their performance is not expected to control the determination of the R-factor.

14. Effect of different hysteretic model

Based on the results provided in Table 26 and **Error! Reference source not found.**, the effect of the use of different hysteretic models and assumptions related to plaster thickness on the resulting ACMR is illustrated in Table 30. (The choice of hysteretic model affects the determination of yield displacement and hence ductility demand and the value of the spectral shape factor, SSF. The plaster thickness as assumed to be $\frac{1}{4}$ inch greater than specified for purposes of calculating nodal masses in the case of the SAWS model.) In this table, it is apparent that the choice of hysteretic model and associated assumptions taken together had a relatively minor effect on the ACMR values. Despite decreasing the seismic mass by 7.6% and increasing the strength of the hysteretic model by 11.1%, the switch to

the Pinching4 model is seen to increase the individual archetype ACMR values by an average of only 3.9%.

Table 30: Influence of hysteretic model and related assumptions on resulting ACMR for each archetype, for Wall E (cement plaster), for Seismic Design Category D_{max} .

Archetype ID (1)	ACMR obtained with Pinching4 Model (2)	ACMR obtained with SAWS Model (3)	Ratio = (2)/(3) (4)
1	3.38	3.17	1.066
3	2.72	2.82	0.965
5	2.25	2.07	1.087
		Mean	1.039

15. Evaluation of overstrength Factor, Ω_0

FEMA P695 (Section 7.6) specifies the requirement for evaluation the system overstrength factor, Ω_0 . It states that “the value of the system overstrength factor, for use in design should not be taken as less than the largest average value of calculated archetype overstrength from any performance group. The system overstrength factor, Ω_0 , should be conservatively increased to account for variation in overstrength results of individual index archetypes, and judgmentally rounded to half unit intervals (e.g., 1.5, 2.0, 2.5, and 3.0).” Table 25 shows the average values of each performance group for Wall B are 1.38 and 1.35. The average values of each performance group for Wall E, determined using the SAWS model, are 1.93 and 1.97 for each performance group (**Error! Reference source not found.**). When using the Pinching4 model, the average values for each performance group are 3.23 and 3.30 (Table 27). However, a monotonic pushover analysis with the Pinching4 model may be misleading, as the backbone curve was made artificially high so that the incorporation of strength degradation would provide results consistent with experimental tests when subjected to reversed cyclic loading (Figure 44). Therefore, on the basis of the

SAWS model results, the overstrength factor value, Ω_0 , for Wall B would be 1.5, while that for Wall E would be 2.0.

16. Evaluation of the Deflection Amplification Factor, C_d

FEMA P695 prescribes the evaluation of the deflection amplification factor, C_d , according to the following:

$$C_d = \frac{R}{B_1} \quad \text{Equation 14}$$

where R = the system response modification Factor, and B_1 = component of effective damping of the structure due to the inherent dissipation of energy by element of the structure.

Based on FEMA P695 and in accordance with Table 18.6-1 ASCE/SEI 7-10, the B_1 value can be assumed to be 1.0. Therefore, the value of the C_d is numerically equal to the R value.

17. Summary and Recommendations

Allowable shears for strawbale wall assemblies for in-plane loading, for different plaster and reinforcement combinations were developed on the basis of available test data. Recommended values are given in Table 1.

Lateral displacements of strawbale wall assemblies under service-level in-plane lateral forces were comparable to those of light-framed walls with wood sheathing. Thus, strawbale wall assemblies may be used interchangeably with light-framed walls with wood sheathing. Code requirements for use of multiple lateral force resisting systems along the same framing lines already exist. As well, it appears that strawbale wall assemblies should be designed for seismic loading using the usual allowable story drift limits (2.5% of the story height for buildings with 4 or fewer stories).

Values of seismic design parameters were determined using three distinct frameworks. The most computationally intensive approach, described by FEMA P695, required a large number of inelastic dynamic response history analyses of multiple building “archetype” building models subjected to a suite of 44 ground motion components that were incrementally scaled until a simulated collapse occurred. We first used the SAWS hysteretic model and found R values of 3.5 for Wall B (clay plaster) and 2.5 for Wall E would satisfy the collapse performance objective given a total collapse uncertainty, β_{TOT} , equal to 0.726 (with corresponding values of $ACMR_{20\%} = 1.85$ and $ACMR_{10\%} = 2.54$). Analyses with a more realistic hysteretic model (the Pinching4 model) have been completed for the cement plaster wall in Seismic Design Categories D_{max} and D_{min} . For the archetypes in SDC D_{max} , $ACMR$ values increased by an average of only 3.9% (Table 30). If the performance groups are re-organized to focus separately on the one- and two-story archetypes, sufficient reserve margin is present to allow the R value for the cement plaster walls to increase to an estimated value of 3.0.

As noted in the draft ATC-84 report (2011), the P695 methodology is known to predict higher probabilities of collapse for short period systems, as illustrated in Figure 51.

The statement within the draft ATC-84 document that the “lack of clear evidence that short-period systems are problematic outside of the computational/theoretical arena” suggests that the R values determined for strawbale systems according to the current P695 approach are needlessly conservative. The possibility of revising the P695 methodology to address this issue is discussed in the ATC-84 report. Since the straw bale archetypes comprise only short-period buildings ($C_u T_a \leq 0.25$ sec), reliance solely on the current P695 methodology to establish strawbale R factors would needlessly penalize this seismic force resisting system. For this reason, we also consider other, more established approaches to determine appropriate seismic design factors.

A conventional analysis, described by Uang (1991) and referred to in the commentary of the 1998 Seismic Provisions (FEMA-303), established $R = 5.4$ where the equal

displacement rule applies and $R = 3.85$ for shorter period structures subject to displacement amplification.

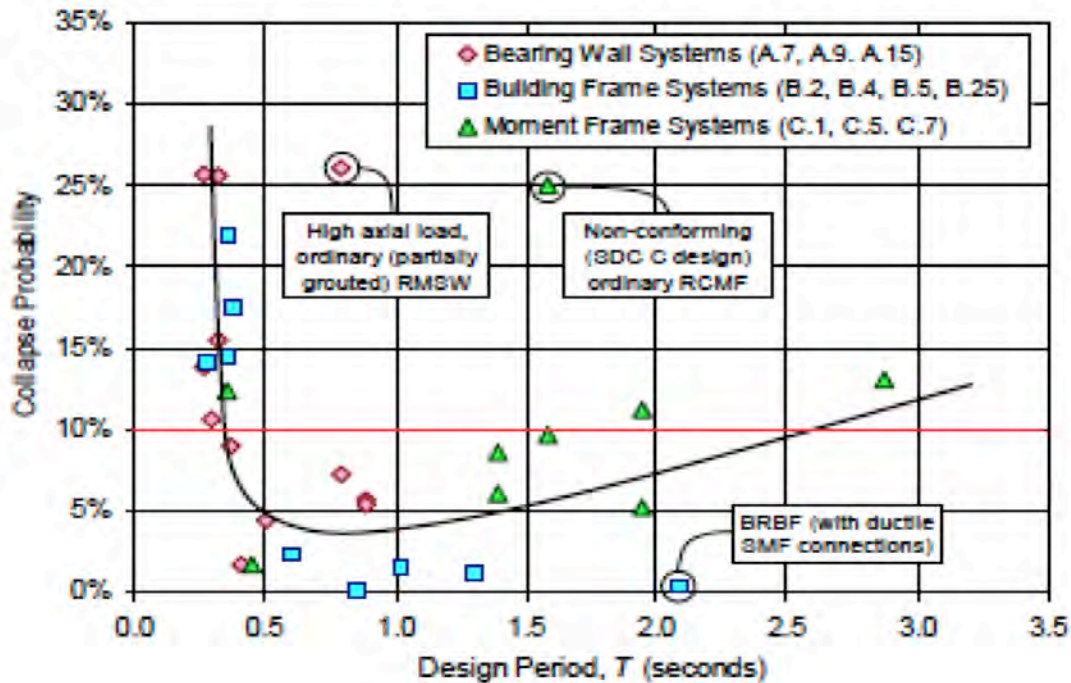


Figure 51: Plot showing the trend (and three circled outliers) in the probability of collapse of selected bearing wall systems, building frame systems and moment-resisting frame systems as a function of design period. Representative collapse probability and design period data shown in this figure are based on results of prior studies of FEMA P-695 (FEMA 2009) and NIST GCR 10-917-8 (NIST, 2010). From ATC-84 (2011).

An analysis in which existing R factors (in this case, for light-framed walls with wood shear panels) are modified on the basis of experimentally determined ductility capacities established $R = 3.7$ for Bearing Wall systems and $R = 3.9$ for Building Frame systems.

Considering the foregoing, R values of 3.5 and 4.0 are tentatively recommended for strawbale walls used in Bearing Wall and Building Frame systems, respectively.

The preceding analyses established overstrength factors ranging from 1.5 to 3. A value of $\Omega_o = 3$ is conservative and is recommended for use with strawbale wall systems.

Finally, the preceding analyses suggest displacement amplification factors in the range of 2.3 to 5.4. Values of 3 and 3.5 are recommended for Bearing Wall and Building Frame systems, respectively, and would be considered to be conservative in light of current code requirements.

References

1. ASCE, 2010, Minimum Design Loads for Buildings and Other Structures, ASCE 7-10, American Society of Civil Engineers, Reston, Virginia.
2. Ash, C, Aschheim, M., and Mar, D. (2003). In-Plane Cyclic Tests of Plastered Straw Bale Wall Assemblies, Ecological Building Network, Sausalito, CA, June 30, 31 pages. Also available from <http://www.ecobuildnetwork.org>.
3. ATC-84 (2011) NIST GCR 11-917-16 Tentative Framework for Development of Advanced Seismic Design Criteria for New Buildings, National Institute of Standards and Technology, 90% Draft, Report No. GCR 10-917-16, Gaithersburg, MD, Nov.
4. FEMA 303 (1998) - Edition NEHRP Recommended Provisions for Seismic Regulations for New Buildings and Other Structures - Part 2: Commentary;
5. FEMA P695 (2009) - Quantification of Building Seismic Performance Factors, prepared by the Applied Technology Council for the Federal Emergency Management Agency, Washington, D.C.
6. Folz, B., and Filiatrault, A., 2004a, "Seismic analysis of woodframe structures I: model formulation," ASCE Journal of Structural Engineering, Vol. 130, No. 8, pp. 1353-1360.
7. Folz, B., and Filiatrault, A., 2004b, "Seismic analysis of wood frame structures II: model implementation and verification," ASCE Journal of Structural Engineering, Vol. 130, No. 8, pp. 1361-1370.
8. Faurot, S., Kelly, K., and Kim, H. (2004). In-Plane Cyclic Straw Bale Shear Wall Testing, Senior Project Report, California Polytechnic University, San Luis Obispo.
9. Haselton, C. 2006, Assessing Seismic Collapse Safety of Modern Reinforced Concrete Moment Frame Buildings, Ph.D. Dissertation, Department of Civil and Environmental Engineering, Stanford University, Stanford, California.
10. Isoda, H., Folz, B., and Filiatrault, A., 2001, Seismic Modeling of Index Woodframe Buildings, CUREE Report No. W-12, Consortium of Universities for Research in Earthquake Engineering, Richmond, California, 144 pp.
11. NAHB ,Application of FEMA P695 (ATC-63) to Analysis and Design of Light-Frame Wood Residential Buildings, March 2011
12. Nichols, J., and Raap, S. (2000). Straw Bale Shear Wall Lateral Load Test, Senior Project Report, Department of Architectural Engineering, California Polytechnic University, San Luis Obispo.
13. Parker, A., Aschheim, M., Mar, D., Hammer, M., and King, B. (2006). "Recommended

- Mesh Anchorage Details for Straw Bale Walls,” *Journal of Green Building*, 1(4):141-151.
14. Ramírez, J. C. (1999). *Cyclic In-Plane Testing of Post and Beam Walls with Straw-bale In-fill and Stucco/Plaster*, M.S. Thesis, University of Washington.
 15. Rose, J. D. 1998. *Preliminary Testing of Wood Structural Panel Shear Walls Under Cyclic (Reversed) Loading*, Report 158, APA The Engineered Wood Association, 38 pages.
 16. SAPWOOOP, *Seismic Analysis Package for Woodframe Structures*, Developed by John Willem van de Lindt, Shiling Pei . Version 2.0 (<http://nees.org/resources/sapwood>)
 17. Vardy, S. P. (2009). *Structural Behaviour of Plastered Straw Bale Assemblies Under Concentric and Eccentric Loading*, Doctoral Thesis, Queen’s University Kingston, Ontario, Canada.
 18. W-13, 2002. Gatto, K., and Uang, C.-M., *Cyclic Response of Woodframe Shearwalls: Loading Protocol and Rate of Loading Effects*, CUREE Publication W-13, Consortium of Universities for Research in Earthquake Engineering, Richmond, California.
 19. W-30a, 2004. Cobeen, K., Russell, J., and Dolan, J. D., *Recommendations for Earthquake Resistance in the Design and Construction of Woodframe Buildings*, CUREE Publication W-30a, Consortium of Universities for Research in Earthquake Engineering, Richmond, California.
 20. Wallace, J. W. (1992). *BIAX : revision 1, a computer program for the analysis of reinforced concrete sections*, Report CU/CEE-92/4, Clarkson University, Dept. of Civil Engineering Potsdam, N.Y. 52 pages

Appendix A

Draft Provisions (as proposed for the *Oregon Structural Specialty Code* on December 17, 2012)

STRAWBALE CONSTRUCTION

The provisions contained in this appendix are not mandatory unless specifically referenced in the adopting ordinance.

SECTION 101 GENERAL

101.1 Scope. This appendix provides prescriptive and performance-based requirements for the use of baled straw as a building material. Other methods of strawbale construction shall be subject to approval in accordance with Section 104.11

SECTION 102 DEFINITIONS

102.1 Definitions. The following words and terms shall, for the purposes of this appendix, have the meanings shown herein. Refer to Chapter 2 of the *International Building Code* for general definitions.

BALE. Equivalent to straw bale.

CLAY. Inorganic soil with particle sizes less than 0.00008 in. (0.002 mm) having the characteristics of high to very high dry strength and medium to high plasticity.

CLAY SLIP. A suspension of clay particles in water.

FINISH. Completed compilation of materials on the interior or exterior faces of stacked bales.

FLAKE. An intact section of compressed straw removed from an untied bale.

LAID FLAT. The orientation of a bale with its largest faces horizontal, its longest dimension parallel with the wall plane, its ties concealed in the unfinished wall and its straw lengths oriented across the thickness of the wall.

LOAD-BEARING WALL. For the purposes of this appendix, any strawbale wall that supports more than 100 lb/linear ft (1,459 N/m) of vertical load in addition to its own weight.

MESH. An openwork fabric of linked strands of metal, plastic, or natural or synthetic fiber, embedded in plaster.

NONLOAD-BEARING WALL. For the purpose of this appendix, any wall that is not a load-bearing wall.

NONSTRUCTURAL WALL. All walls other than load-bearing walls or shear walls.

ON-EDGE. The orientation of a bale with its largest faces vertical, its longest dimension parallel with the wall plane, its ties on the face of the wall, and its straw lengths oriented vertically.

PIN. A vertical metal rod, wood dowel, or bamboo, driven into the center of stacked bales, or placed on opposite surfaces of stacked bales and through-tied.

PLASTER. Gypsum, lime, cement-lime, or cement plasters, as defined in Chapter 25 and in Section 104, or clay plaster as defined in Section 104.4.3, or soil-cement plaster as defined in Section 104.4.4.

PRE-COMPRESSION. Vertical compression of stacked bales before the application of finish.

REINFORCED PLASTER. A plaster containing mesh reinforcement.

RUNNING BOND. For the purposes of this appendix, the placement of straw bales such that the head joints in successive courses are offset at least one quarter the bale length.

SHEAR WALL. A strawbale wall designed to resist lateral forces parallel to the plane of the wall in accordance with Section 106.16.

SKIN. The compilation of plaster and reinforcing, if any, applied to the surface of stacked bales.

STRUCTURAL WALL. A wall that meets the definition for a load-bearing wall or shear wall.

STACK BOND. For the purposes of this appendix, the placement of straw bales such that head joints in successive courses are vertically aligned.

STRAW. The dry stems of cereal grains after the seed heads have been removed.

STRAW BALE. A rectangular compressed block of straw, bound by ties.

STRAWBALE. The adjective form of straw bale.

STRAW-CLAY. Loose straw mixed and coated with clay slip.

TIE. A synthetic fiber, natural fiber, or metal wire used to confine a straw bale.

TRUTH WINDOW. An area of a strawbale wall left without its finish, to allow view of the straw otherwise concealed by its finish.

SECTION 103 BALES

103.1 Shape. Bales shall be rectangular in shape.

103.2 Size. Bales shall have a minimum height and thickness of 12 inches (305 mm), except as otherwise permitted or required in this appendix. Bales used within a continuous wall shall be of consistent height and thickness to ensure even distribution of loads within the wall system.

103.3 Ties. Bales shall be confined by synthetic fiber, natural fiber, or metal ties sufficient to maintain required bale density. Ties shall be at least 3 inches (76 mm) and not more than 6 inches (152 mm) from

bale faces and shall be spaced not more than 12 (305 mm) inches apart. Bales with broken ties shall be retied with sufficient tension to maintain required bale density.

103.4 Moisture content. The moisture content of bales at the time of application of the first coat of plaster or the installation of another finish shall not exceed 20 percent of the weight of the bale. The moisture content of bales shall be determined by use of a moisture meter designed for use with baled straw or hay, equipped with a probe of sufficient length to reach the center of the bale. At least 5 percent and not less than ten bales used shall be randomly selected and tested.

103.5 Density. Bales shall have a minimum dry density of 6.5 pounds per cubic foot (92 kg/cubic meter). The dry density shall be calculated by subtracting the weight of the moisture in pounds (kg) from the actual bale weight and dividing by the volume of the bale in cubic feet (cubic meters). At least 2 percent and not less than five bales to be used shall be randomly selected and tested on site.

103.6 Partial bales. Partial bales made after original fabrication shall be retied with ties complying with 103.3.

103.7 Types of straw. Bales shall be composed of straw from wheat, rice, rye, barley, or oat.

103.8 Other baled material. The dry stems of other cereal grains or grasses shall be acceptable when approved by the *building official*.

SECTION 104 FINISHES

104.1 General. Finishes applied to strawbale walls shall be any type permitted by the *International Building Code*, and shall comply with this section and with Chapters 14 and 25 of the *International Building Code* unless stated otherwise in this section.

104.2 Purpose, and where required. Strawbale walls shall be finished so as to provide mechanical protection, fire resistance, protection from weather, and to restrict the passage of air through the bales, in accordance with this appendix and the *International Building Code*.

Exception: Truth windows shall be permitted where a fire-resistive rating is not required. Weather-exposed truth windows shall be fitted with a weather-tight cover.

104.3 Vapor retarders. Class I and Class II vapor retarders shall not be used on a strawbale wall, nor shall any other material be used that has a vapor permeance rating of less than 5 perms, except as permitted or required elsewhere in this appendix.

104.4 Plaster. Plaster applied to bales shall be any type described in this section, and as required or limited in this appendix.

104.4.1 Plaster and membranes. Plaster shall be applied directly to strawbale walls to facilitate transpiration of moisture from the bales, and to secure a mechanical bond between the skin and the bales, except where a membrane is allowed or required elsewhere in this appendix.

104.4.2 Lath and mesh for plaster. The surface of the straw bales functions as lath, and no other lath or mesh shall be required, except as required for out-of-plane resistance by Table 105.4, or for structural walls by Table 106.14 and Table 106.16.

104.4.3 Clay plaster. Clay plaster shall comply with 104.4.3.1 through 104.4.3.6.

104.4.3.1 General. Clay plaster shall be any plaster having a clay or clay-soil binder. Such plaster shall contain sufficient clay to fully bind the plaster, sand or other inert granular material, and shall be permitted to contain reinforcing fibers. Acceptable reinforcing fibers include, chopped straw, sisal, and animal hair.

104.4.3.2 Lath and mesh. Clay plaster shall not be required to contain reinforcing lath or mesh except as required in Table 105.4 and Table 106.15. Where provided, mesh shall be natural fiber, corrosion-resistant metal, nylon, high-density polypropylene, or other *approved* material.

104.4.3.3 Thickness and coats. Clay plaster shall be a minimum 1 inch (25 mm) thick, unless required to be thicker for structure, as described elsewhere in this appendix, and shall be applied in not less than two coats.

104.4.3.4 Rain-exposed. Clay plaster, where exposed to rain, shall be finished with lime wash, linseed oil, or other *approved* erosion-resistant finish.

104.4.3.5 Prohibited finish coat. Cement plaster shall not be permitted as a finish coat over clay plasters.

104.4.3.6 Plaster additives. Additives shall be permitted to increase plaster workability, durability, strength, or water resistance.

104.4.4 Soil-cement plaster. Soil-cement plaster shall comply with 104.4.4.1 through 104.4.4.3.

104.4.4.1 General. Soil-cement plaster shall be comprised of soil (free of organic matter), sand, and not less than 10% Portland cement by volume, and shall be permitted to contain reinforcing fibers.

104.4.4.2 Lath and mesh. Soil-cement plaster shall use any corrosion-resistant lath or mesh permitted by the *International Building Code*, or as required in Section 105 where used on a structural wall.

104.4.4.3 Thickness. Soil-cement plaster shall be not less than 1 inch (25 mm) thick.

104.4.5 Gypsum plaster. Gypsum plaster shall comply with Section 2511 of the *International Building Code*. Gypsum plaster shall be limited to use on interior surfaces of non-structural walls, and as an interior finish coat over a structural plaster that complies with this appendix.

104.4.6 Lime plaster. Lime plaster shall comply with 104.4.6.1 and 104.4.6.2.

104.4.6.1 General. Lime plaster is any plaster whose binder is comprised of calcium hydroxide (CaOH) including Type N or Type S hydrated lime, hydraulic lime, natural hydraulic lime, or quicklime. Hydrated lime plasters shall comply with ASTM C 206. Quicklime plasters shall comply with ASTM C 5.

104.4.6.2 Structural walls. Lime plaster on structural strawbale walls in accordance with Table 105.14 or Table 105.15 shall use a binder comprised of hydraulic or natural hydraulic lime.

104.4.7 Cement-lime plaster. Cement-lime plaster shall be plaster mixes CL, F, or FL as described in ASTM C 926.

104.4.8 Cement plaster. Cement plaster shall comply with Section 2512 of the *International Building Code*, except that the amount of lime in all plaster coats shall be not less than 1 part lime to 6 parts cement to allow a minimum acceptable vapor permeability. The combined thickness of all plaster coats shall be not more than 1 1/2 inch (38 mm) thick.

104.4.9 Prohibited plasters and finishes. Any plaster or finish with a singular or cumulative perm rating less than 5 perms shall be prohibited on straw bale walls, when required elsewhere in this appendix.

104.4.10 Separation of wood and plaster. Where wood framing or wood sheathing occurs in strawbale walls, such wood surfaces shall be separated from exterior plaster with No.15 asphalt felt, grade D paper, or other *approved* material in accordance with Section 1404.2 of the *International Building Code*, except where the wood is *preservative-treated* or *naturally durable*.

Exception: Exterior clay plasters shall not be required to be separated from wood.

SECTION 105 STRAWBALE WALLS – GENERAL

105.1 General. Strawbale walls shall be designed and constructed in accordance with this section.

105.2 Finishes. Finishes shall be in accordance with Section 104.

105.3 Sill plates. Sill plates shall support and be flush with each face of the straw bales above and shall be of *naturally durable* or *preservative-treated wood* where required by the *International Building Code*. Sill plates shall be a minimum of nominal 2 inches by 4 inches with attachment complying with the Section 2308.6 of the *International Building Code*, except with additional requirements as stipulated in Tables 105.4, 106.16.

105.4 Out-of-plane resistance and unrestrained wall dimensions. Strawbale walls shall employ a method of out-of-plane resistance described in Table 105.4, and comply with its associated limits and requirements, except where an *approved* engineered design otherwise demonstrates the wall will resist buckling from superimposed vertical loads and out-of-plane design loads.

R105.4.1 Determination of out-of-plane loading. Out-of-plane loading shall be determined in accordance with Chapter 16 of the *International Building Code* in accordance with *allowable stress design*.

Exception: Out-of-plane loading shall be considered to be no greater than 25 pounds per square foot when all of the following conditions are met.

1. Occupancy category - I or II.
2. Seismic design category – A, B, C, or D, as determined by Section 1613.5.6 of the *International Building Code* or Section 301.2.2.1 of the *International Residential Code*.
3. Design wind speed – not exceeding 90 miles per hour
4. Stories – not exceeding 2
5. Building height – not exceeding 25 feet

6. Plaster thickness for plastered strawbale walls – not exceeding 2 inches (51mm) each side
 Strawbale walls in such structures shall be permitted to use any type of out-of-plane resistance described in Table 105.4 with its associated limits and requirements.

TABLE 105.4: OUT-OF-PLANE RESISTANCE AND UNRESTRAINED WALL DIMENSIONS

Method of resistance ^a	Maximum allowable out-of-plane loading (pounds per square foot)	Unrestrained Wall Dimensions, H ^b		Mesh Staple Spacing at Boundary Restraints
		Absolute limit in feet	Limit based on bale thickness in feet (mm)	
Non-plaster finish or unreinforced plaster	25	H ≤ 10	H ≤ 5T	none
Pins per 105.4.2	25	H ≤ 12	H ≤ 8T	none
Pins per 105.4.2	30	H ≤ 10	H ≤ 7T	none
Reinforced ^c clay plaster	30	H ≤ 10	$H \leq 8T^{0.5}$ ($H \leq 140T^{0.5}$)	≤ 6 inches
Reinforced ^c clay plaster	30	10 < H ≤ 12	$H \leq 8T^{0.5}$ ($H \leq 140T^{0.5}$)	≤ 4 inches ^d
Reinforced ^c cement, cement-lime, lime, or soil-cement plaster	30	H ≤ 10	$H \leq 9T^{0.5}$ ($H \leq 157T^{0.5}$)	≤ 6 inches
Reinforced ^c cement, cement-lime, lime, or soil-cement plaster	40	H ≤ 13	$H \leq 9T^{0.5}$ ($H \leq 157T^{0.5}$)	≤ 4 inches ^d

For SI: 1 foot = 304.8 mm, 1 pound per square foot = 47.8803 N/m²

^a Finishes applied to both sides of stacked bales. Where different finishes are used on opposite sides of a wall, the more restrictive requirements shall apply.

^b H = stacked bale height in feet (mm), or the horizontal distance in feet (mm) between vertical restraints. For load-bearing walls, H refers to vertical height only. T = bale thickness in feet (mm).

^c Plaster reinforcement shall be any mesh allowed in Table 106.16 for the matching plaster type, but with staple spacing per this table. Mesh shall be installed in accordance with Section 106.10

^d Sill plate attachment shall be with 5/8 inch anchor bolts or *approved* equivalent at a maximum of 48 inches on center where staple spacing is required to be ≤ 4 inches.

105.4.2 Pins. Pins used for out-of-plane resistance shall comply with the items below or shall be in accordance with an *approved* engineered design. Pins may be external, internal or a combination of the two.

105.4.2.1 Pins shall be 3/8 inch (10 mm) diameter steel, 3/4 inch (19 mm) diameter wood, or 1/2 inch (13 mm) diameter bamboo.

105.4.2.2 External pins shall be installed vertically on both sides of the wall spaced not more than 24 inches (610 mm) on center. External pins shall have full lateral bearing on the sill plate and the top plate or roof- or floor-bearing element, and shall be tightly tied through the wall to an opposing pin with ties spaced not more than 32 inches (762 mm) apart and not more than 6 inches (381 mm) from each end of the pin.

105.4.2.3 Internal pins shall be installed vertically within the center third of the bales, at spacing not exceeding 24 inches (610 mm) and shall extend from top course to bottom course. The bottom course shall be similarly connected to its support and the top course

shall be similarly connected to the roof- or floor-bearing member above with pins or other *approved* means. Internal pins shall be continuous or shall overlap through not less than one bale course.

105.5 Connection of light-frame walls to strawbale walls. Light-frame walls perpendicular to, or at an angle to a straw bale wall assembly, shall be fastened to the bottom and top wood members of the strawbale wall in accordance with requirements for wood or cold-formed steel light-frame walls in the *International Building Code*, or the abutting stud shall be connected to alternating straw bale courses with a 1/2 inch (13mm) diameter steel, 3/4" diameter (19 mm) wood, or 5/8" diameter (16 mm) bamboo dowel, with minimum 8 inch (203 mm) penetration.

105.6 Moisture control. Strawbale walls shall be protected from moisture intrusion and damage in accordance with 105.6.1 through 105.6.7.

105.6.1 Water-resistive barriers and vapor permeance ratings. Plastered bale walls shall be constructed without any membrane barrier between straw and plaster to facilitate transpiration of moisture from the bales, and to secure a structural bond between straw and plaster, except as permitted or required elsewhere in this appendix. Where a water-resistive barrier is placed behind an exterior finish, it shall have a minimum vapor permeance rating of 5 perms, except as permitted or required elsewhere in this appendix.

105.6.2 Vapor retarders. Wall finishes shall have an equivalent vapor permeance rating of a Class III vapor retarder, except that a Class I or Class II vapor retarder shall be provided on the interior of side of exterior strawbale walls in Climate Zones 5, 6, 7, 8 and Marine 4 as defined in Chapter 3 of the *International Energy Conservation Code*. Bales in walls enclosing showers or steam rooms shall be protected on the interior side by a Class I or Class II vapor retarder.

105.6.3 Penetrations in exterior strawbale walls. Penetrations in exterior strawbale walls shall be sealed with an *approved* sealant or gasket on the exterior side of the wall in all Climate Zones, and on the interior sided of the wall in Climate Zones 5, 6, 7, 8 and Marine 4 as defined in Chapter 3 of the *International Energy Conservation Code*.

105.6.4 Horizontal surfaces. Bale walls and other bale elements shall be provided with a moisture barrier at all weather-exposed horizontal surfaces. The moisture barrier shall be of a material and installation that will prevent water from entering the wall system. Horizontal surfaces shall include exterior window sills, sills at exterior niches, and buttresses. The finish material at such surfaces shall be sloped not less than 1 unit vertical in 12 units horizontal (8-percent slope) and shall drain away from all bale walls and elements. Where the moisture barrier is below the finish material, it shall be sloped not less than 1 unit vertical in 12 units horizontal (8-percent slope) and shall drain to the outside surface of the bale's vertical finish.

105.6.5 Bale and concrete separation. A sheet or liquid applied Class II vapor retarder shall be installed between bales and supporting concrete or masonry. The bales shall be separated from the vapor retarder by not less than 3/4 inch (19 mm), and that space shall be filled with an insulating material such as wood or rigid insulation, a material that allows vapor dispersion such as gravel, or other *approved* insulating or vapor dispersion material. Sill plates in structural walls shall comply with Table 106.2 and Table 106.3. Where bales abut a concrete or masonry wall that retains earth, a Class II vapor retarder shall be provided between such wall and the bales.

105.6.6 Separation of bales and earth. Bales shall be separated from earth a minimum of 8" (203 mm).

105.6.7 Separation of exterior plaster and earth. Exterior plaster applied to straw bales shall be located not less than 4 inches (102 mm) above the earth or 2 inches (51 mm) above paved areas.

**SECTION 106
STRAWBALE WALLS - STRUCTURAL**

106.1 General. An *approved* engineered design demonstrating complete vertical and lateral load paths in accordance with this section and the *International Building Code* shall be provided for buildings or portions thereof that use structural strawbale walls.

106.2 Foundations. Foundations shall be in accordance with Chapter 18 of the *International Building Code*.

106.3 Building height and stories. Buildings or portions of buildings constructed with structural strawbale walls shall comply with 106.3.1 through 106.3.3

106.3.1 Building height shall not exceed 35 feet and the limits contained in Table 106.14.

106.3.2 The number of stories above *grade plane* shall not exceed two.

106.3.3 Structural strawbale walls interrupted by floor assemblies shall be designed and detailed by a *registered design professional*.

106.4 Configuration of bales. Bales in structural walls shall be laid flat or on-edge and in a running bond or stack bond, except that bales in structural walls with unreinforced plasters shall be laid in a running bond only.

106.5 Pre-compression of load-bearing strawbale walls. Prior to application of plaster, walls designed to be load-bearing shall be pre-compressed by a uniform load of not less than 100 pounds per linear foot.

106.6 Voids and stuffing. Voids between bales in structural strawbale walls shall not exceed 4 inches (102 mm) in width, and such voids shall be stuffed with flakes of straw or straw-clay, before application of finish.

106.7 Plaster on structural walls. Plaster on loadbearing walls shall be in accordance with Table 106.14. Plaster on shear walls shall be in accordance with Table 106.16.

106.7.1 Compressive strength. The *building official* is authorized to require a 2" cube compression test to demonstrate a minimum compressive strength for plasters on structural walls according to Table 106.7.1.

**TABLE 106.7.1
MINIMUM COMPRESSIVE STRENGTH FOR STRUCTURAL PLASTERS**

PLASTER TYPE	MINIMUM COMPRESSIVE STRENGTH (psi)
Clay	100
Soil-cement	1000
Lime	600
Cement-lime	1000
Cement	1400

106.8 Straightness of plaster. Plaster on structural strawbale walls shall be straight, as a function of the bale wall surfaces they are applied to, according to 106.8.1 through 106.8.3

106.8.1 As measured across the face of a bale, straw bulges shall not protrude more than 3/4 inch (19 mm) across 2 feet (610 mm) of its height or length.

106.8.2 As measured across the face of a bale wall, straw bulges shall not protrude from the vertical plane of a bale wall more than 2 inches (51 mm) over 8 feet (2438 mm).

106.8.3 The vertical faces of adjacent bales shall not be offset more than 1/2 inch (13 mm).

106.9 Plaster and membranes. Structural strawbale walls shall not have a membrane between straw and plaster, or shall have attachment through the bale wall from one plaster skin to the other in accordance with an *approved* engineered design.

106.10 Mesh. Mesh in structural plasters, and where required by Table 105.4, shall be installed in accordance with 106.10.1 through 106.10.4.

106.10.1 Mesh laps. Mesh required by Table 106.14 or Table 105.4 shall be installed with minimum 4-inch (102 mm) laps. Mesh required by Table 106.16 shall run continuous vertically from sill plate to the top plate or roof or floor bearing element, or shall lap not less than 8 inches (203 mm). Horizontal laps in such mesh shall be not less than 4 inches (102 mm).

106.10.2 Mesh attachment. Mesh shall be attached with staples to horizontal boundary elements in accordance with 106.10.2.1 through 106.10.2.3.

106.10.2.1 Staples. Staples shall be pneumatically driven, stainless steel or electro-galvanized, 16 gauge with 1 1/2-inch legs, 7/16-inch crown; or manually driven, galvanized, 15 gauge with 7/8-inch legs. Other staples shall be permitted to be used as designed by a *registered design professional*. Staples into *preservative-treated wood* shall be stainless steel.

106.10.2.2 Staple orientation. Staples shall be firmly driven diagonally across mesh intersections at the required spacing.

106.10.2.3. Staple spacing. Staples at the top plate or roof or floor bearing element shall be at maximum spacing of 2-inches (51 mm) on center or as shown in an *approved* design in accordance with Section 106.11. Staples at sill plates shall be at a maximum spacing of 4-inches (102 mm) on center, unless otherwise required by Table 106.15 or by an *approved* design in accordance with 106.11.

106.10.3 Steel mesh. Steel mesh shall be galvanized, and shall be separated from *preservative-treated wood* by grade D paper, 15# roofing felt, or other *approved* barrier.

106.10.4 Mesh in plaster. Required mesh shall be embedded in middle third of the plaster excluding its finish coat, except where staples fasten the mesh to horizontal boundary elements.

106.11 Transfer of loads to and from plaster skins. Where plastered strawbale walls are used to support superimposed vertical loads, such loads shall be transferred to the plaster skins by continuous direct bearing or by an *approved* engineered design. Where plastered strawbale walls are used to resist in-plane lateral loads, such loads shall be transferred to the reinforcing mesh from the structural member

or assembly above and to the sill plate in accordance with Table 106.16, or by an *approved* engineered design.

106.12 Support of plaster skins. Plaster skins for structural strawbale walls shall be continuously supported along their bottom edge. Acceptable supports include: a concrete or masonry stem wall, a concrete slab on grade, a wood-framed floor adequately blocked with an *approved* engineered design, or a steel angle adequately anchored with an *approved* engineered design. An unsupported weep screed is not an acceptable support.

106.13 Resistance to uplift loads. Where plastered strawbale walls are used to resist vertical uplift loads, such loads shall be transferred to the plaster skins by an *approved* engineered design. In lieu of an *approved* engineered design, plaster mesh in skins complying with Table 106.16, with staples at 2 inches (51 mm) on center, and with associated sill plate and anchoring requirements, shall be considered capable of resisting uplift loads not associated with in-plane shear resistance, of 200 plf (2,918 N/m) per plaster skin.

106.14 Load-bearing strawbale walls. Load-bearing strawbale walls shall be in accordance with Table 106.14 as part of an *approved* engineered design to support superimposed vertical loads. Concentrated loads shall be distributed by a structural element capable of distributing the loads to the bearing wall within the uniform load limits in 106.13. The allowable bearing capacity values in Table 106.14 are in accordance with *allowable stress design*.

**TABLE 106.14
ALLOWABLE SUPERIMPOSED VERTICAL LOADS (LBS/FOOT)
FOR PLASTERED LOAD-BEARING STRAWBALE WALLS**

WALL DESIGNATION	PLASTER ^a (both sides) Minium thickness each side	MESH ^b	STAPLES ^c	ALLOWABLE BEARING CAPACITY ^d (plf)
A	Clay 1-1/2"	None required	None required	400
B	Soil-cement 1"	required	required	800
C	Lime 7/8"	required	required	500
D	Cement-lime 7/8"	required	required	800
E	Cement 7/8"	required	required	800

For SI: 1 inch=25.4mm, 1 pound per foot = 14.5939 N/m.

- a. Plasters shall conform with Sections 104.4.3through 104.4.8, 106.7, 106.8, and 106.12.
- b. Any metal mesh allowed by this appendix and installed in accordance with Section 106.10.
- c. In accordance with Section 106.10.1, except as required to transfer roof or floor loads to the plaster skins in accordance with Section 106.11.
- d. For walls with a different plaster on each side, the lower value shall be used.

106.15 Design coefficients and factors for seismic design. The values in Table 106.14 shall apply to seismic design using strawbale shear walls detailed in accordance with Table 106.16.

106.16 Strawbale shear walls. Strawbale shear walls shall be in accordance with Table 106.16 as part of an *approved* engineered design to resist in-plane lateral loads. Components of strawbale shear walls shall also comply with 106.16.1 through 106.16.3. The allowable shear values in Table 106.16 are in accordance with *allowable stress design*. Design shear wall deflection shall not be more than .0035 times the wall height at the allowable shear wall limits. Other *approved* in-plane lateral load resisting systems

shall be permitted for use in combination with strawbale shear walls with apportionment of design loads as prescribed in the *International Building Code*.

106.16.1 Bale thickness. Bale thickness shall not be less than 15 inches (3810 mm).

106.16.2 Sill plates. Sill plates shall be in accordance with Table 106.16.

106.16.3 Sill plate fasteners. Sill plates shall be fastened with minimum 5/8-inch (16 mm) diameter steel anchor bolts with 3-inch by 3-inch by 3/16-inch steel washers, with not less than 7-inch embedment in a concrete or masonry foundation, or shall be an *approved* equivalent. Anchor bolts or other fasteners into framed floors shall be of an *approved* engineered design.

**TABLE 106.15
DESIGN COEFFICIENTS AND FACTORS FOR SEISMIC-FORCE-RESISTING SYSTEMS**

Seismic-Force-Resisting System	Response Modification Coefficient, R^a	System Overstrength Factor, Ω^b	Deflection Amplification Factor, C_d	Structural System Limitations and Building Height (ft) Limits				
				Seismic Design Category				
				B	C	D	E	F
A. Bearing Wall Systems								
Strawbale shear walls	3.5	3	3	25	25	15	15	NP
B. Building Frame Systems								
Strawbale shear walls	4	3	3.5	35	35	25	15	NP

^a R reduces forces to a strength level, not an allowable stress level

^b The tabulated value of the overstrength factor is permitted to be reduced by subtracting 0.5 for structures with flexible diaphragms, but shall not be taken as less than 2.0 for any structure.

**TABLE 106.16
ALLOWABLE SHEAR (POUNDS PER FOOT) FOR PLASTERED STRAWBALE SHEAR WALLS**

WALL DESIGNATION	PLASTER ^a (both sides)		SILL PLATES ^b (nominal size in inches)	ANCHOR BOLT ^c SPACING (on center)	MESH ^d	STAPLE SPACING ^e (on center)	ALLOWABLE SHEAR ^{f,g,h} (plf)
	TYPE	THICKNESS (minimum, each side)					
A1	Clay	1.5 in.	2 x 4	32 in.	None	None	60
A2	Clay	1.5 in.	2 x 4	32 in.	2 in. by 2 in. high-density polypropylene	2 inches	140
A3	Clay	1.5 in.	2 x 4	32 in.	2 in. by 2 in. by 14ga ⁱ	4 inches	180
B	Soil-cement	1 in.	4 x 4	24 in.	2 in. by 2 in. by 14ga ⁱ	2 inches	520
C1	Lime	7/8 in.	2 x 4	32 in.	17 ga woven wire	3 inches	330
C2	Lime	7/8 in.	4 x 4	24 in.	2 in. by 2 in. by 14ga ⁱ	2 inches	450
D1	Cement-lime	7/8 in.	4 x 4	32 in.	17 ga woven wire	2 inches	380
D2	Cement-lime	7/8 in.	4 x 4	24 in.	2 in. by 2 in. by 14ga ⁱ	2 inches	520

E1	Cement	7/8 in.	4 x 4	32 in.	2 in. by 2 in. by 14ga ⁱ	2 inches	540
E2	Cement	1.5 in.	4 x 4	24 in.	2 in. by 2 in. by 14ga ⁱ	2 inches	680

SI: 1 inch=25.4 mm, 1 pound per foot = 14.5939 N/m

- a. Plasters shall conform with Sections 104.4.3 through 104.4.8, 106.7, 106.8, and 106.12.
- b. Sill plates shall be Douglas fir-larch or southern pine and shall be *preservative-treated* where required by the *International Building Code*. Multiply allowable shear value by .82 for other species with specific gravity of .42 or greater, or by .65 for all other species.
- c. Anchor bolts shall be in accordance with Section 106.16.3 at the spacing shown in this table.
- d. Installed in accordance with Section 106.10.
- e. Staples shall be in accordance with Section 106.10.2 at the spacing shown in this table.
- f. Values shown are for aspect ratios of 1:1 or less. Reduce values shown to 50% for the limit of a 2:1 aspect ratio. Linear interpolation shall be permitted for aspect ratios between 1:1 and 2:1. The full value shown shall be used for aspect ratios greater than 1:1, where an additional layer of mesh is installed at the base of the wall to a height where the remainder of the wall has an aspect ratio of 1:1 or less, and the second layer of mesh is fastened to the sill plate with the required stapling, and the sill bolt spacing is decreased with linear interpolation between 1:1 and 2:1.
- g. For walls with a plaster Type A on one side and any other plaster type on the other side, a *registered design professional* shall show transfer of the design lateral load into the stiffer Type B, C, D, or E plaster only, and 50% of the allowable shear value shown for that wall designation shall be used.
- h. These values are permitted to be increased 40 percent for wind design.
- i. 16 gauge mesh shall be permitted to be used with a reduction to 0.60 of the allowable shear values shown.

SECTION 107 FIRE RESISTANCE

107.1 Fire-resistance rating. Strawbale walls shall be considered to be non-rated, except for walls constructed in accordance with Section 107.1.1 or 107.1.2. Alternately, fire-resistance ratings of strawbale walls shall be determined in accordance with Section 703.2 or 703.3 of the *International Building Code*.

107.1.1 1-hour rated clay plastered wall. 1-hour fire-resistance-rated non-load-bearing clay plastered strawbale walls shall comply with 107.1.1.1 through 107.1.1.5.

107.1.1.1 Bales shall be laid flat or on-edge in a running bond.

107.1.1.2 Bales shall maintain thickness of not less than 18 inches (457 mm).

107.1.1.3 Gaps shall be fire-stopped with straw-clay.

107.1.1.4 Clay plaster on each side of the wall shall be not less than 1 inch (25 mm) thick and shall be comprised of a mixture of 3 parts clay, 2 parts chopped straw, and 6 parts sand, or an alternative *approved* clay plaster.

107.1.1.5 Plaster application shall be in accordance with 104.4.3.3 for the number and thickness of coats.

107.1.2 2-hour rated cement plastered wall. 2-hour fire-resistance-rated non-load-bearing cement plastered strawbale walls shall comply with 107.1.2.1 through 107.1.1.6.

107.1.2.1 Bales shall be laid flat or on-edge in a running bond.

107.1.2.2 Bales shall maintain a thickness of not less than 14 inches (356 mm).

107.1.2.3 Gaps shall be fire-stopped with straw-clay.

107.1.2.4 1 1/2 inch (38 mm) by 17 gauge galvanized woven wire mesh shall be attached to wood members with 1 1/2 inch (38 mm) staples at 6 inches (406 mm) on center. 9 gauge U-pins with minimum 8 inch (203 mm) legs shall be installed in the field at 18 inches (457 mm) on center.

107.1.2.5 Cement plaster on each side of the wall shall be not less than 1 inch (25 mm) thick.

107.1.2.6 Plaster application shall be in accordance with 104.4.8 for the number and thickness of coats.

107.2 Openings in rated walls. Openings and penetrations in bale walls required to have a fire-resistance rating shall satisfy the same requirements for openings and penetrations as prescribed in the *International Building Code*.

107.3 Clearance to fireplaces and chimneys. Strawbale surfaces adjacent to fireplaces or chimneys shall be finished with a minimum 3/8 inch (10 mm) thick plaster of any type permitted by this appendix. Clearance from the face of such plaster to fireplaces and chimneys shall be maintained as required from fireplaces and chimneys to combustibles in *International Building Code* Chapter 21, Sections 2111, 2112, and 2113, or as required by manufacturer's installation instructions, whichever is more restrictive.

107.4 Type of construction. Buildings or portions thereof utilizing strawbale walls in accordance with this appendix shall be classified as Type V-B construction. Strawbale walls constructed in compliance with Section 107.1.1 or 107.1.2 shall be permitted wherever combustible walls of the same fire-resistance are allowed by Chapter 6 of the *International Building Code*. Strawbale walls with any finish allowed by this appendix shall be permitted wherever non-rated combustible walls are allowed by the *International Building Code*.

SECTION 108 THERMAL INSULATION

108.1 R-value. The unit R-value of a strawbale wall with bales laid flat is R-1.3 per inch of bale thickness. The unit R-value of a strawbale wall with bales on-edge is R-2 per inch of bale thickness.

Appendix B

Load-Deformation Plots of Straw Bale and Light-Framed Plywood Sheathed Wall Assemblies

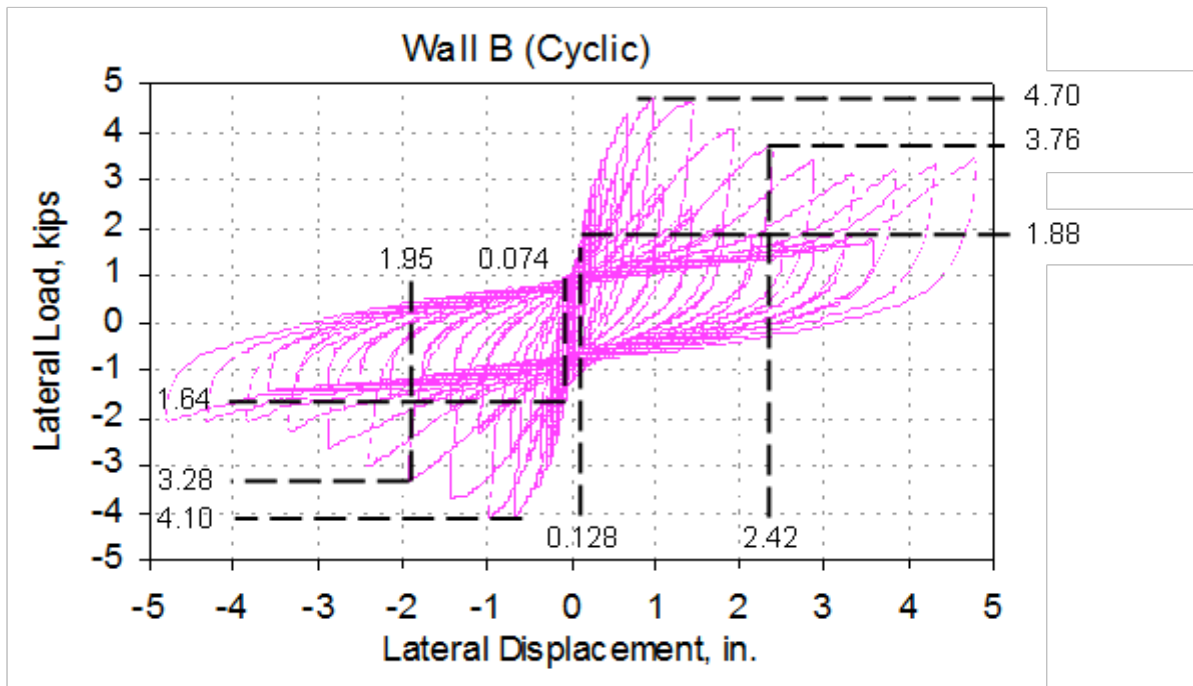


Figure 52: Response of Straw Bale Wall B

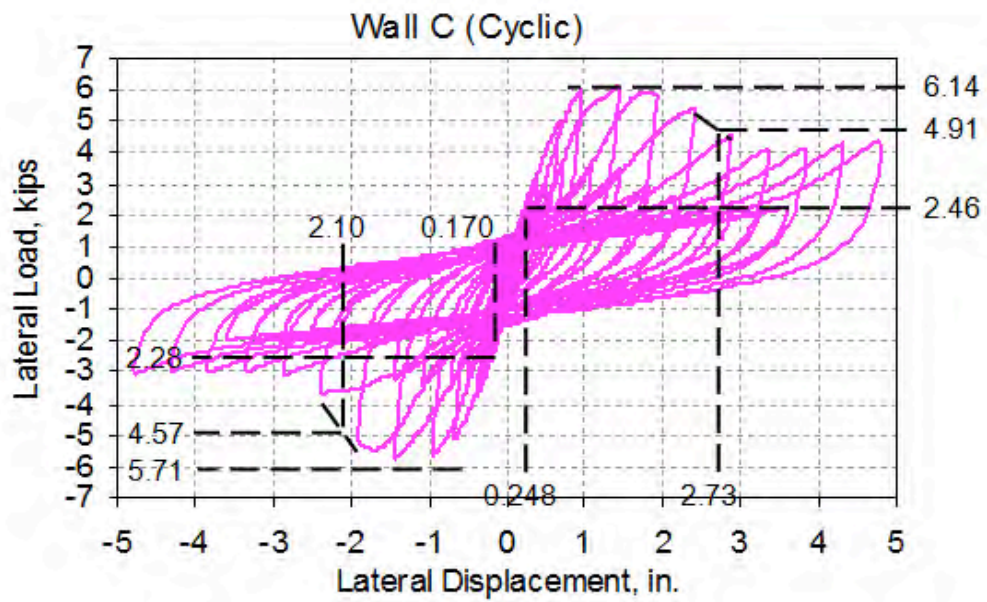


Figure 53: Response of Straw Bale Wall C

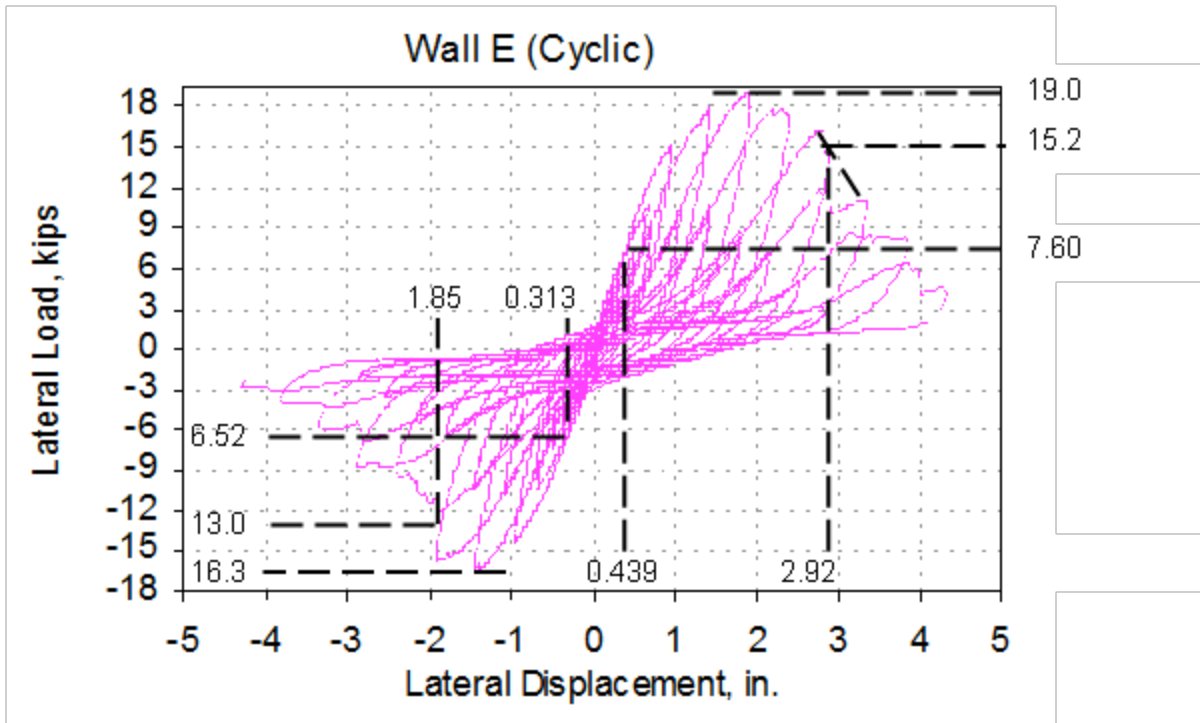


Figure 54: Response of Straw Bale Wall E

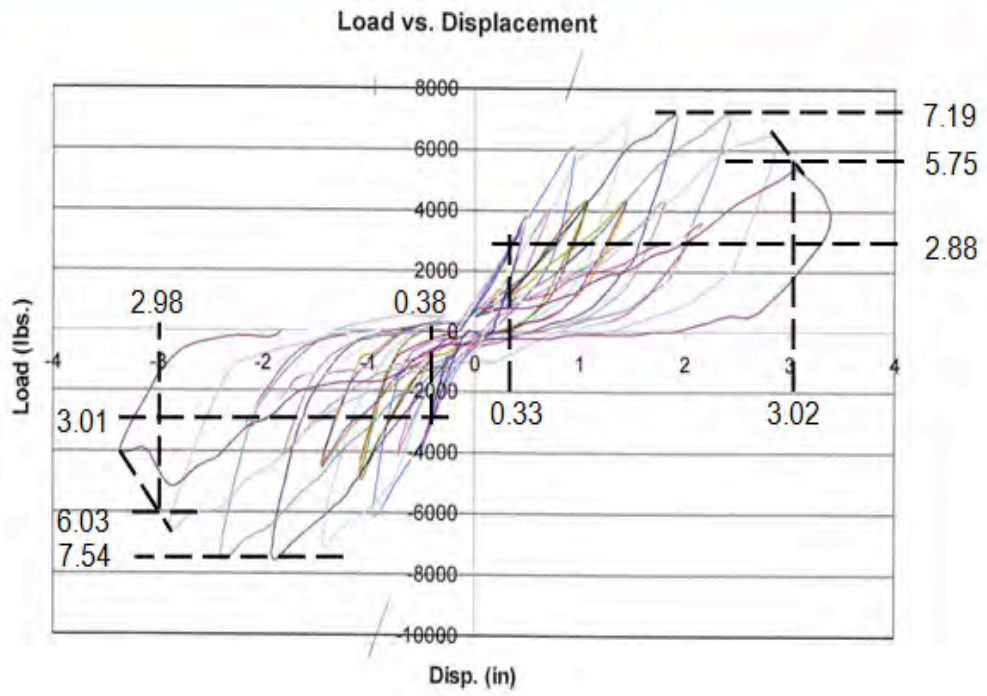


Figure 55: Response of Cal Poly Straw Bale Wall

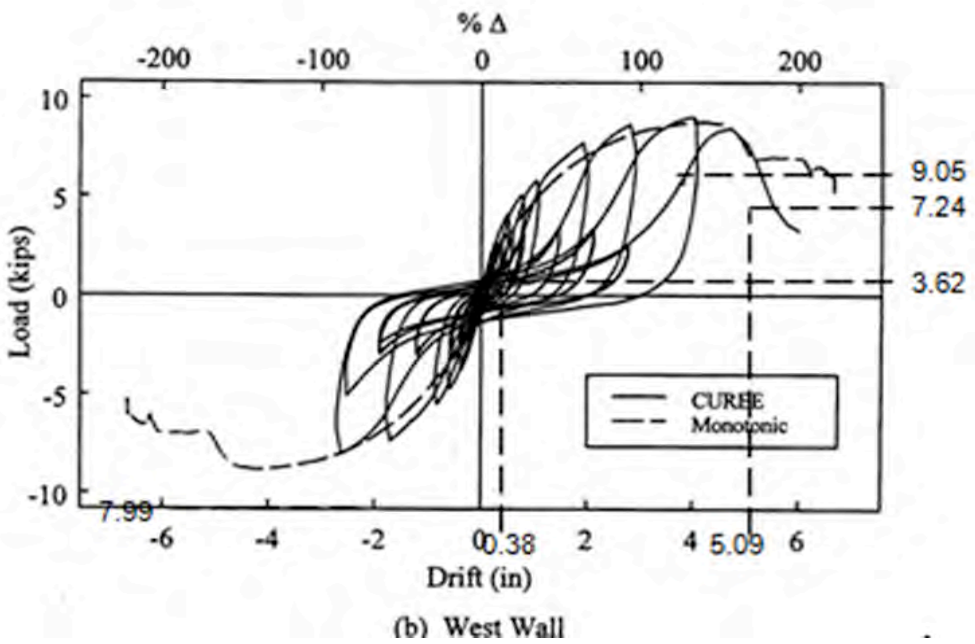
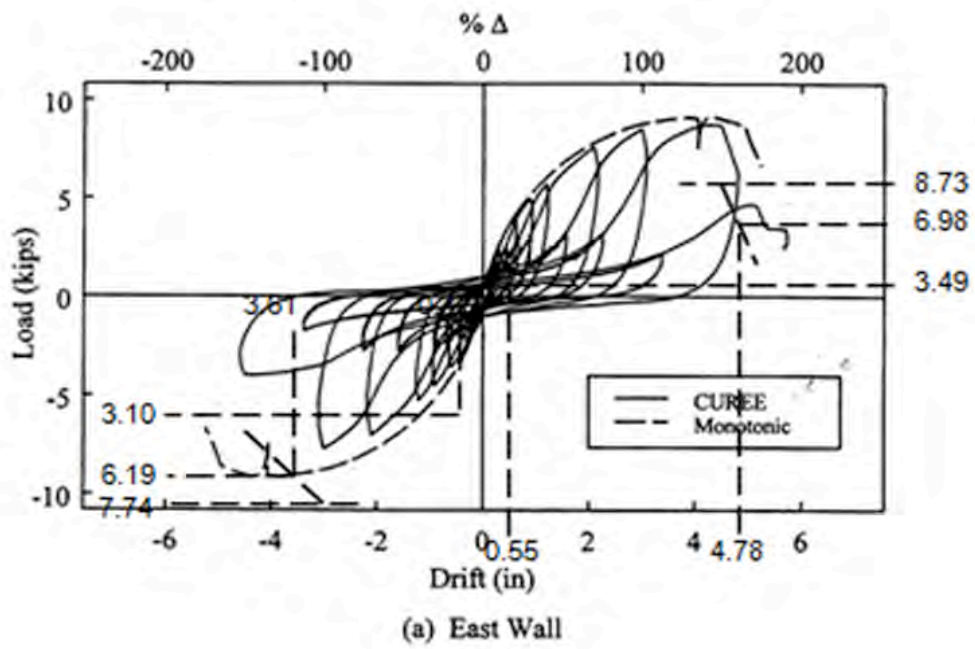


Figure 56: Response of Light-Framed OSB Sheathed Walls (Test 2) under CUREE Protocol.

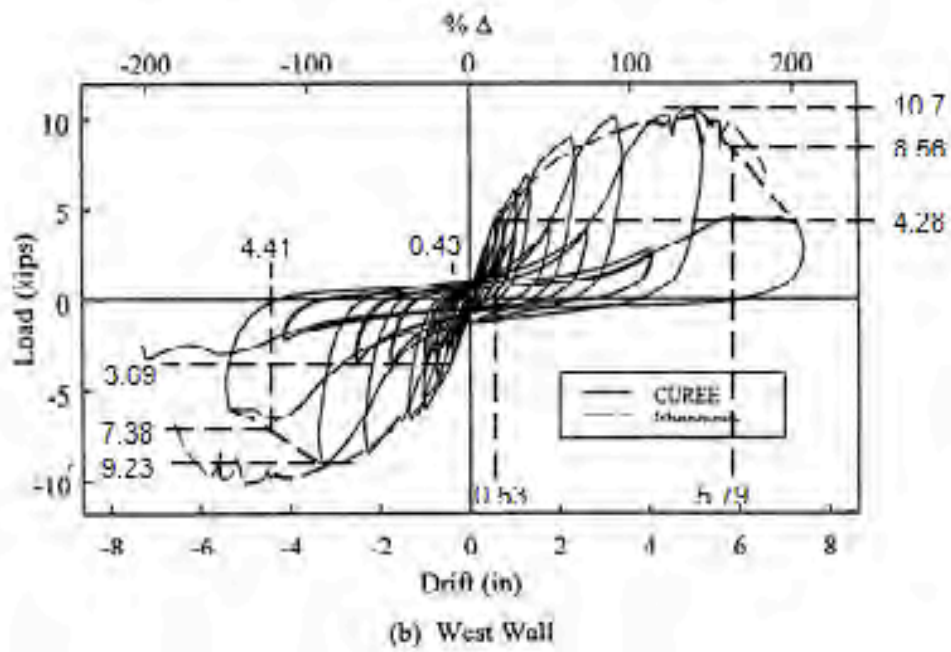
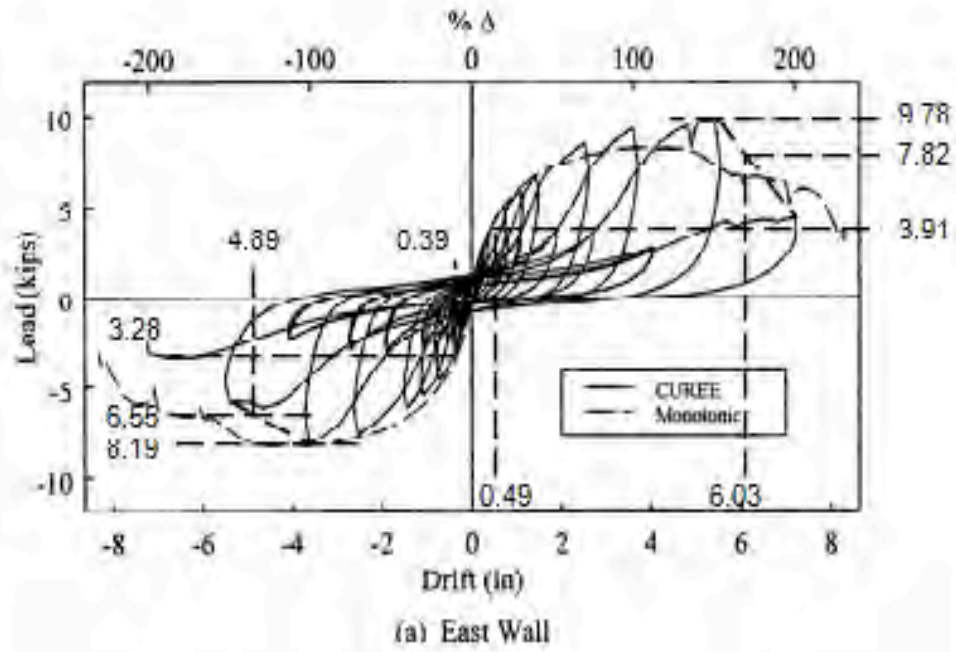


Figure 57: Response of Light-Framed Plywood Sheathed Walls (Test 6) under CUREE Protocol.

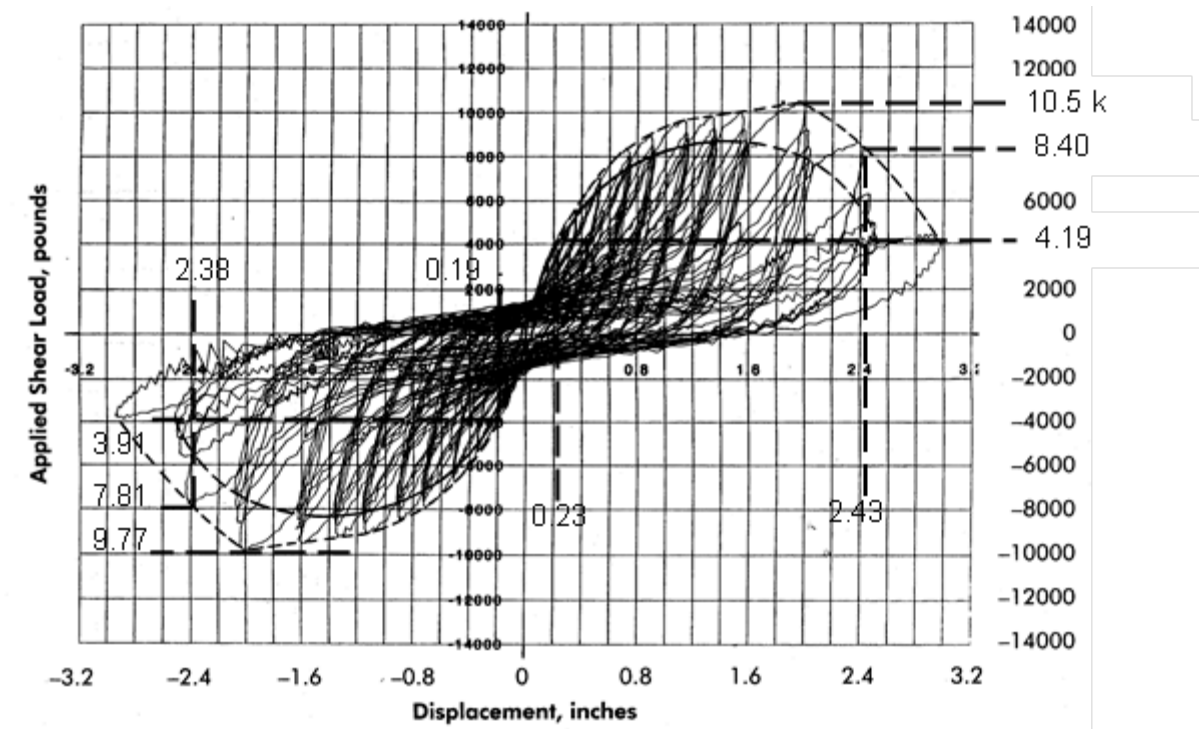


Figure 58: A6: Response of Light-Framed Plywood Sheathed Walls (Test 1A) under Sequential Phased Displacement Protocol.

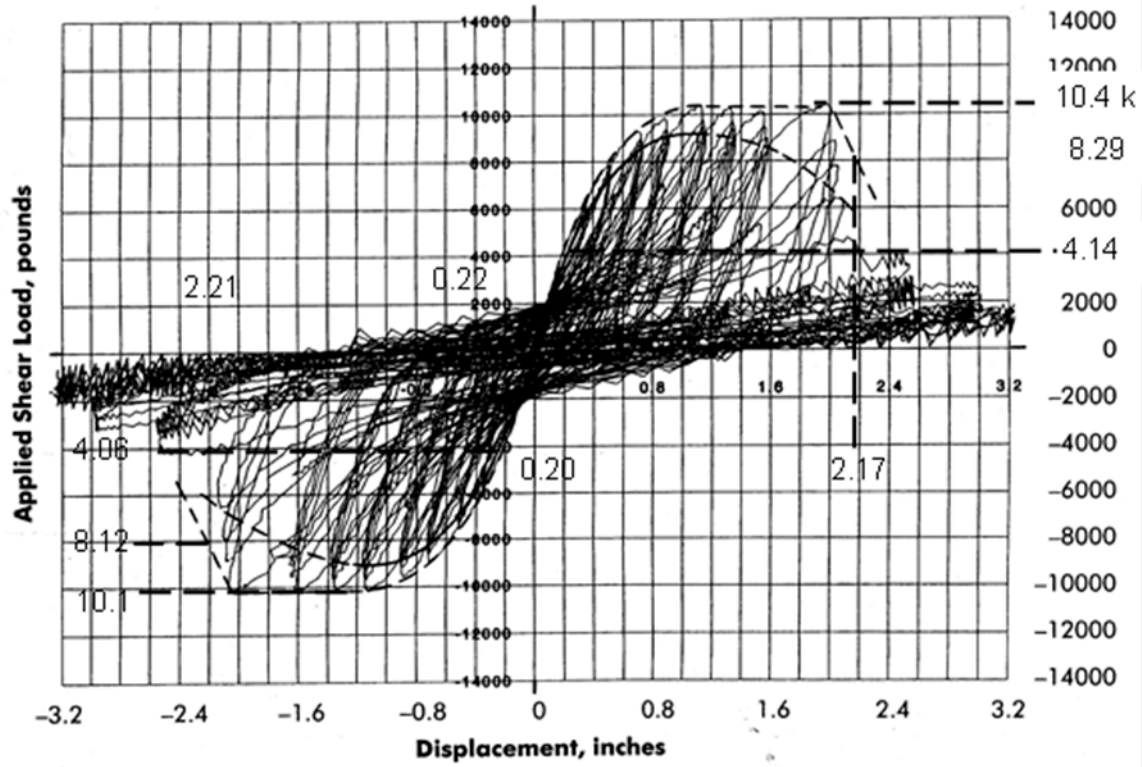


Figure 59: Response of Light-Framed Plywood Sheathed Walls (Test 6A) under Sequential Phased Displacement Protocol.

Appendix C

Index building in three Archetypes

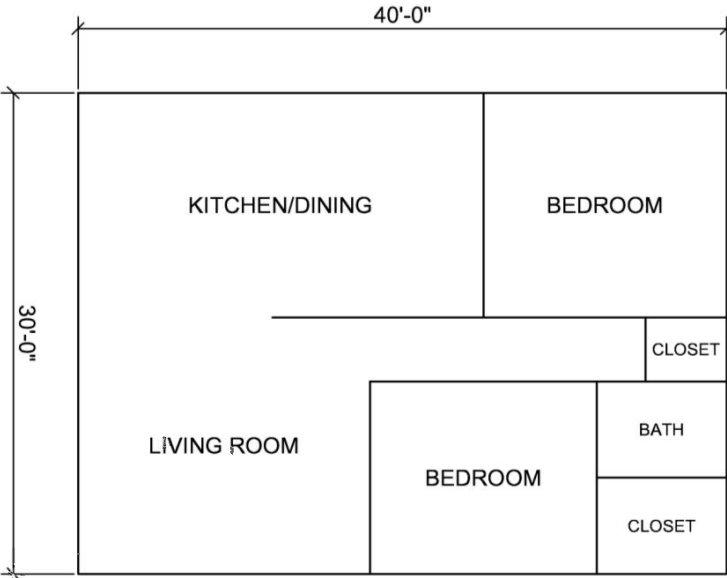


Figure 60: One-family 1200 ft² home (Archetype Configuration #1) [NAHB Report]

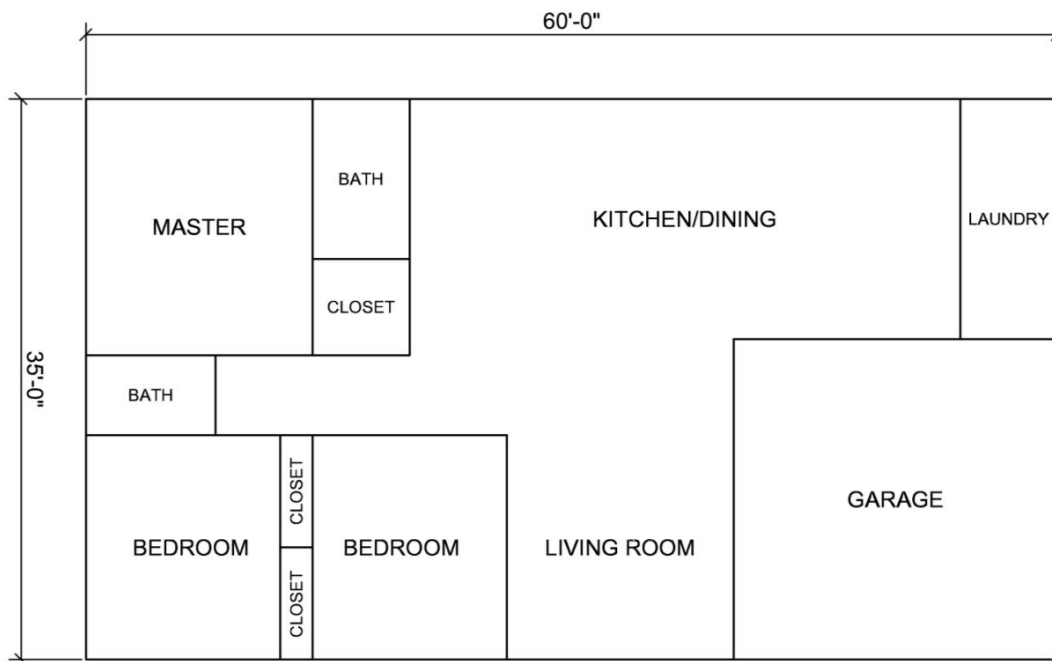
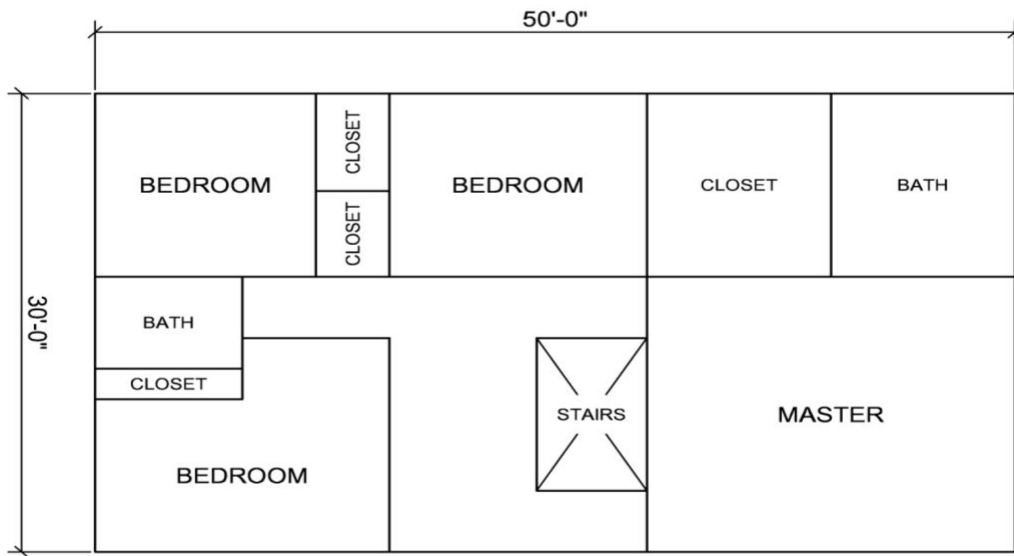
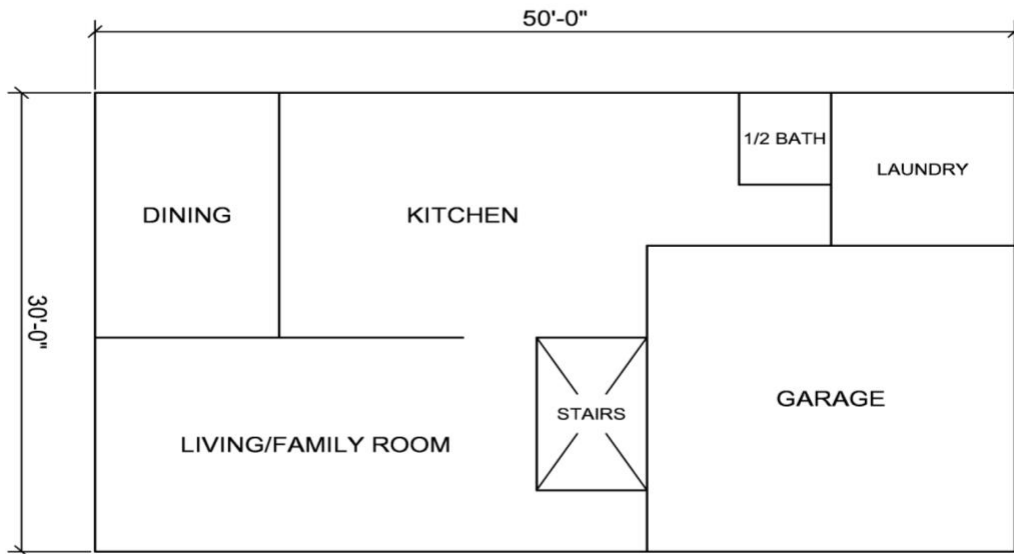


Figure 61: One-family 2100 ft² home (Archetype Configuration #2)[NAHB Report]



2nd Floor Plan



1st Floor Plan

Figure 62: One-family 3000 ft² home (Archetype Configuration #3) [NAHB Report]

Appendix D

Unit area load

Table 31: Unit area load for Wall E⁵

		Design	OpenSees
System	Component	Unit weight (psf)	Unit weight (psf)
Roof	Comp. Shingle	3	3
	1/2" Plywd. Sheating	1.5	1.5
	2x6 rafters @ 24"	1	1
	2x4 clg. Joists @24"	1	1
	R-19 Fiberglass insul.	1	1
	5/8" gyp.bd.	2	2
	Total	9.5	9.5
Floor	1/2" gyp. Bd.	1.5	1.5
	2x10 @16 Joist	6	6
	Misc (Electrical, Plumbing)	1	1
	Total	8.5	8.5
Interior Wall	2x4 Framing	4	4
	Gypsum	4	4
	Total	8	8
Exterior Wall	Straw Bale	13.42	13.42
	1.5" Cement paster both side	35.00	40.83
	Total	48.42	54.25

⁵ As seen in the table the weight of the building in design and modeling in OpenSees are not similar due to the different assumption in thickness of the Strawbale. In design approach the thickness of the wall was assumed to be 1.5" while in modeling the extra ¼" thickness of each plaster skin was added in determining the seismic mass for a conservative approach.

Table 32: Unit area load for Wall B⁶

		Design	OpenSees
System	Component	Unit weight (psf)	Unit weight
Roof	Comp. Shingle	3	3
	1/2" Plywd. Sheating	1.5	1.5
	2x6 rafters @ 24"	1	1
	2x4 clg. Joists @24"	1	1
	R-19 Fiberglass insul.	1	1
	5/8" gyp.bd.	2	2
	Total	9.5	9.5
Floor	1/2" gyp. Bd.	1.5	1.5
	2x10 @16 Joist	6	6
	Misc (Electrical, Plumbing)	1	1
	Total	8.5	8.5
Interior Wall	2x4 Framing	4	4
	Gypsum	4	4
	Total	8	8
Exterior Wall	Straw Bale	13.42	13.42
	1.5" earth paster both side	28.75	33.54
	Total	42.17	46.96

⁶ As seen in the table the weight of the building in design and modeling in OpenSees are not similar due to the different assumption in thickness of the Strawbale. In design approach the thickness of the wall was assumed to be 1.5" while in modeling the extra ¼" thickness of each plaster skin was added in determining the seismic mass for a conservative approach.

Appendix E

Building archetype loading

Table 33: Building Archetype Loading

Building Archetype	Index building ¹					Wall E		Wall B	
	Level	Area (ft^2)				Total Weight (kips)	Shear wall weight (kips)	Total Weight (kips)	Shear wall weight (kips)
		Roof	Floor	Wall					
				Exterior	interior				
1	1	1200		560	400	42	21	38	19
2	2	2100		760	824	64	32	59	29
3	1		1500	1280	1264	85	43	77	38
	2	1500		640	800	52	26	48	24

1- The source data for index information is NAHB Report.

Appendix F

Building archetype Design

Wall B⁷

Table 34: Archetype 1 Small -Single Family 1200 Square feet (30'x40') Wall B

Model	Stories	SDC	Seismic Hazard (S _{DS})	Tributary	Shear Wall Aspect Ratio	Description	Shear Walls								
				Tributary Width (ft)			Story	Tributary Weight (#)	Story Shear Coefficient	ASD Story Shear (#)*	Quantity	Length	Capacity of the wall (plf)	ASD Capacity (#)	Demand/Capacity
B	1	D _{max}	1	15	1	small-Family	1	19207	1.00	3841	4	7.7	140	4300	0.893
B	1	D _{min}	0.50	15	1	small-Family	1	19207	1.00	1916	2	7.7	140	2150	0.891

⁷ In our earliest analysis the allowable shear design was 129 plf, therefore the length of 8 ft of wall was selected for building archetype design, but as the allowable shear design updated to 140 plf the length of the wall adjusted to 7.7 ft (column 13 in above tables). The safety factor for Wall B is 2.5. Therefore (129 plf*2.5*8)=2.58 kips

$$\begin{aligned}
 &0.14*2.5*L/H*L=2.580 \text{ kips} \\
 &L^2/H=2.580/(0.14*2.5) \\
 &L^2/8= \quad 7.37 \\
 &L^2= \quad 58.97 \\
 &L= \quad 7.7 \quad \text{ft}
 \end{aligned}$$

Table 35: Archetype 2 Large- Single Family 2100 Square feet (35'x60') Wall B

Model	Stories	SDC	Seismic Hazard (S_{DS})	Tributary	Shear Wall Aspect Ratio	Description	Shear Walls								
				Tributary Width (ft)			Story	Tributary Weight (#)	Story Shear Coefficient	ASD Story Shear (#)*	Quantity	Length	Capacity of the wall (plf)	ASD Capacity (#)	Demand/ Capacity
B	1	D_{max}	1	17.5	1	Large-Family	1	29500	1.00	5900	6	7.7	140	6451	0.915
B	1	D_{min}	0.50	17.5	1	Large-Family	1	29500	1.00	2942	3	7.7	140	3225	0.912

Table 36: Archetype 3 Townhouse- Family 3000 Square feet (30'x50')Wall B

Model	Stories	SDC	Seismic Hazard (S_{DS})	Tributary	Shear Wall Aspect Ratio	Description	Shear Walls								
				Tributary Width (ft)			Story	Tributary Weight (#)	Story Shear Coefficient	ASD Story Shear (#)	Quantity	Length	Capacity (plf)	ASD Capacity (#)	Demand/ Capacity
B	2	D_{max}	1	15	1	Townhouse	2	23818	0.55	6890	7	7.7	140	7525.699967	0.916
							1	38418	1.00	12447	12	7.7	140	12901.199994	0.965
B	2	D_{min}	0.5	15	1	Townhouse	2	23818	0.55	3445	6	7.7	140	6450.599972	0.534
							1	38418	1.00	6224	6	7.7	140	6450.599972	0.965

- 1- The design required shear wall lengths was greater than the building dimensions for wall B. Therefore Seismic design category D_{max} has not considered for wall B (Townhouse archetype).

$$R = 3.5$$

$$*V = C_s W$$

$$*V = 0.7 C_s W$$

$$V = 0.7 * S_{DS} / (R/I) * W$$

LRFD

ASD

Wall E⁸

Table 37: Archetype 1 Small -Single Family 1200 Square feet (30'x40') Wall E

Model	Stories	SDC	Seismic Hazard (S ₀ s)	Tributary Weight	Shear Wall Aspect Ratio	Description	Shear Walls									
				Tributary Width (ft)			Story	Tributary Weight (#)	Story Shear Coefficient	ASD Story Shear (#)*	Quantity	Length	Capacity of the wall (plf)	Aspect Ratio Adjustment ^a	Capacity (#)	Demand/Capacity
E	1	D _{max}	1	15	1.00	small Family	1	20957	1.00	5868	2	7.56	680	1.00	10279	0.571
E	1	D _{min}	0.50	15	1.00	small Family	1	20957	1.00	2926	1	7.56	680	1.00	5139	0.569

Table 38: Archetype 2 Large- Single Family 2100 Square feet (35'x60') Wall E

Model	Stories	SDC	Seismic Hazard (S ₀ s)	Tributary Weight	Shear Wall Aspect Ratio	Description	Shear Walls									
				Tributary Width (ft)			Story	Tributary Weight (#)	Story Shear Coefficient	LRFD Story Shear (#)*	Quantity	Length	Capacity of the wall (plf)	Aspect Ratio Adjustment ^a	Capacity (#)	Demand/Capacity
E	1	D _{max}	1	17.5	1.00	Large Family	1	31875	1.00	8925	2	7.56	680	1.00	10279	0.868
E	1	D _{min}	0.50	17.5	1.00	Large Family	1	31875	1.00	4463	1	7.56	680	1.00	5139	0.868

⁸ In our earliest analysis the allowable shear design was 607 plf, therefore the length of 8 ft of wall was selected for building archetype design, but as the allowable shear design updated to 680 plf the length of the wall adjusted to 7.6 ft (column 13 in above tables). The safety factor for Wall E is 2.9. Therefore (607 plf*2.9*8)=14.08 kips

$$0.68 * 2.9 * L / H * L = 14.08 \text{ kips}$$

$$L^2 / H = 14.08 / (0.68 * 2.9)$$

$$L^2 / 8 = 7.141176$$

$$L^2 = 57.12941$$

$$L = 7.56 \text{ ft}$$

Table 39: Archetype 3 Townhouse- Family 3000 Square feet (30'x50') Wall E

Model	Stories	SDC	Seismic Hazard (S_{DS})	Tributary Tributary Width (ft)	Shear Wall Aspect Ratio	Description	Shear Walls									
							Story	Tributary Weight (#)	Story Shear Coefficient	ASD Story Shear (#)	Quantity	Length	Capacity (plf)	Aspect Ratio Adjustment ^a	ASD Capacity (#)	Demand/Capacity
E	2	D_{max}	1	15	1	Townhouse	2	25818	0.55	10489	3	7.6	680	1.00	15419.14	0.680
							1	42418	1.00	19106	4	7.6	680	1.00	20558.85	0.929
E	2	D_{min}	0.5	15	1	Townhouse	2	25818	0.55	5245	2	7.6	680	1.00	10279.42	0.510
							1	42418	1.00	9553	2	7.6	680	1.00	10279.42	0.929

R= 2.5

* $V=C_sW$

* $V=0.7C_sW$

$V=0.7*S_{DS}/R/I)*W$

LRFD

ASD

Appendix G

Sample OpenSees SAWS data file

#Wall B Archetype ID 1

```
model BasicBuilder -ndm 2 -ndf 3;          # Define the model builder,
ndm=#dimension, ndf=#dofs
# wallB1 8x8
# define GEOMETRY -----
node 1 0 0;
node 2 0 0;
node 3 480 0;
node 4 480 0;
node 5 480 360;
node 6 0 360;
node 7 0 360;
puts "Node"
# Single point constraints -- Boundary Conditions
fix 1 1 1 1;          # node DX DY RZ
fix 2 0 0 1;
fix 3 1 1 1;
fix 4 0 0 1;
fix 5 0 0 1;
fix 6 1 1 1;
fix 7 0 0 1;
puts "Fix";
#rigidLink $type $masterNodeTag $slaveNodeTag
rigidLink bar 2 4 5 7
puts "Diaphragm";
# Total dead load of the bulding    total weight 41097 lbs /4= 10274 lbs
Mass: (10274/1000)/386= 0.02661658031
mass 2 0.02661658031 0.02661658031 0;
mass 4 0.02661658031 0.02661658031 0;
mass 5 0.02661658031 0.02661658031 0;
mass 7 0.02661658031 0.02661658031 0;
puts "Mass";
## Materials
set F0 1.924 ;# kip
set FI 0.384 ;# kip
set DU 1.264;# in
```

```

set S0 9.869 ;# kip/in
set R1 0.01
set R2 -0.024
set R3 1.0
set R4 0.01
set alph 0.75
set bet 1.1
uniaxialMaterial SAWS 1 $F0 $FI $DU $S0 $R1 $R2 $R3 $R4 $alph $bet
puts "Saws";
## Transformation
geomTransf Linear 1
## Define Model
element zeroLength 1 1 2 -mat 1 -dir 2 2 # direction 2 means shear walls on
vertical axis
element zeroLength 11 1 2 -mat 1 -dir 2 2
element zeroLength 20 1 2 -mat 1 -dir 2 2
element zeroLength 22 1 2 -mat 1 -dir 2 2

element zeroLength 2 3 4 -mat 1 -dir 2 2
element zeroLength 12 3 4 -mat 1 -dir 2 2
element zeroLength 19 3 4 -mat 1 -dir 2 2
element zeroLength 21 3 4 -mat 1 -dir 2 2

element zeroLength 3 6 7 -mat 1 -dir 1 1
element zeroLength 13 6 7 -mat 1 -dir 1 1
element zeroLength 15 6 7 -mat 1 -dir 1 1
element zeroLength 17 6 7 -mat 1 -dir 1 1

element zeroLength 4 1 2 -mat 1 -dir 1 1 # direction 1 means shear wall on
horizontal axis
element zeroLength 14 1 2 -mat 1 -dir 1 1
element zeroLength 16 1 2 -mat 1 -dir 1 1
element zeroLength 18 1 2 -mat 1 -dir 1 1

puts "Material";
# Rigid Diaphragm Element Node Area Modulus
element elasticBeamColumn 5 2 5 1000 100000.0 1e6 1
element elasticBeamColumn 6 4 7 1000 100000.0 1e6 1
element elasticBeamColumn 7 2 7 1000 100000.0 1e6 1
element elasticBeamColumn 8 5 7 1000 100000.0 1e6 1
element elasticBeamColumn 9 4 5 1000 100000.0 1e6 1
element elasticBeamColumn 10 2 4 1000 100000.0 1e6 1

```

#Wall B Archetype ID 3

```
model BasicBuilder -ndm 2 -ndf 3;          # Define the model builder,
ndm=#dimension, ndf=#dofs
# wallB2 8x8
# define GEOMETRY -----
node 1 0 0;
node 2 0 0;
node 3 720 0;
node 4 720 0;
node 5 720 420;
node 6 0 420;
node 7 0 420;
puts "Node"
# Single point constraints -- Boundary Conditions
fix 1 1 1 1;          # node DX DY RZ
fix 2 0 0 1;
fix 3 1 1 1;
fix 4 0 0 1;
fix 5 0 0 1;
fix 6 1 1 1;
fix 7 0 0 1;
puts "Fix";
#rigidLink $type $masterNodeTag $slaveNodeTag
rigidLink bar 2 4 5 7
puts "Diaphragm";
# Total dead load of the bulding    total weight 62642 lbs /4= 15661 lbs
Mass: (15661/1000)/386= 0.0405714594

mass 2 0.0405714594 0.0405714594 0;
mass 4 0.0405714594 0.0405714594 0;
mass 5 0.0405714594 0.0405714594 0;
mass 7 0.0405714594 0.0405714594 0;
puts "Mass";
## Materials
set F0 1.924 ;# kip
set FI 0.384 ;# kip
set DU 1.264;# in
set S0 9.869 ;# kip/in
set R1 0.01
set R2 -0.024
set R3 1.0
set R4 0.01
set alph 0.75
set bet 1.1
```

```

uniaxialMaterial SAWS 1 $F0 $FI $DU $S0 $R1 $R2 $R3 $R4 $alph $bet
puts "Saws";
## Transformation
geomTransf Linear 1
## Define Model
element zeroLength 1 1 2 -mat 1 -dir 2 2 # direction 2 means shear walls on
vertical axis
element zeroLength 11 1 2 -mat 1 -dir 2 2
element zeroLength 20 1 2 -mat 1 -dir 2 2
element zeroLength 22 1 2 -mat 1 -dir 2 2
element zeroLength 28 1 2 -mat 1 -dir 2 2
element zeroLength 30 1 2 -mat 1 -dir 2 2

element zeroLength 2 3 4 -mat 1 -dir 2 2
element zeroLength 12 3 4 -mat 1 -dir 2 2
element zeroLength 19 3 4 -mat 1 -dir 2 2
element zeroLength 21 3 4 -mat 1 -dir 2 2
element zeroLength 27 3 4 -mat 1 -dir 2 2
element zeroLength 29 3 4 -mat 1 -dir 2 2

element zeroLength 3 6 7 -mat 1 -dir 1 1
element zeroLength 13 6 7 -mat 1 -dir 1 1
element zeroLength 15 6 7 -mat 1 -dir 1 1
element zeroLength 17 6 7 -mat 1 -dir 1 1
element zeroLength 23 6 7 -mat 1 -dir 1 1
element zeroLength 25 6 7 -mat 1 -dir 1 1

element zeroLength 4 1 2 -mat 1 -dir 1 1 # direction 1 means shear wall on
horizontal axis
element zeroLength 14 1 2 -mat 1 -dir 1 1
element zeroLength 16 1 2 -mat 1 -dir 1 1
element zeroLength 18 1 2 -mat 1 -dir 1 1
element zeroLength 24 1 2 -mat 1 -dir 1 1
element zeroLength 26 1 2 -mat 1 -dir 1 1

puts "Material";
# Rigid Diaphragm Element Node Area Modulus
element elasticBeamColumn 5 2 5 1000 100000.0 1e6 1
element elasticBeamColumn 6 4 7 1000 100000.0 1e6 1
element elasticBeamColumn 7 2 7 1000 100000.0 1e6 1
element elasticBeamColumn 8 5 7 1000 100000.0 1e6 1
element elasticBeamColumn 9 4 5 1000 100000.0 1e6 1
element elasticBeamColumn 10 2 4 1000 100000.0 1e6 1

```

#Wall E Archetype ID 1

```
model BasicBuilder -ndm 2 -ndf 3;          # Define the model builder,
ndm=#dimension, ndf=#dofs
# define GEOMETRY -----
node 1 0 0;
node 2 0 0;
node 3 480 0;
node 4 480 0;
node 5 480 360;
node 6 0 360;
node 7 0 360;
puts "Node"

# Single point constraints -- Boundary Conditions
fix 1 1 1 1;          # node DX DY RZ
fix 2 0 0 1;
fix 3 1 1 1;
fix 4 0 0 1;
fix 5 0 0 1;
fix 6 1 1 1;
fix 7 0 0 1;
puts "Fix";

#rigidLink $type $masterNodeTag $slaveNodeTag
rigidLink bar 2 4 5 7
puts "Diaphragm";

# Total dead load of the bulding    total weight 45180 lbs /4= 11295 lbs
Mass: (11295/1000)/386= 0.029261658

mass 2 0.029261658 0.029261658 0;
mass 4 0.029261658 0.029261658 0;
mass 5 0.029261658 0.029261658 0;
mass 7 0.029261658 0.029261658 0;
puts "Mass";
# Wall E 8x8
## Materials ;
set F0 10.966 ;# kip
set FI 1.1 ;# kip
set DU 2.58 ;# in
set S0 30.314 ;# kip/in    stiffness original model is 13.6 kip/in
set R1 0.01
set R2 -0.07
set R3 1.0
set R4 0.01
```

```

set alph 0.75
set bet 1.1
uniaxialMaterial SAWS 1 $F0 $FI $DU $S0 $R1 $R2 $R3 $R4 $alph $bet
puts "Saws";

## Transformation
geomTransf Linear 1
## Define Model
element zeroLength 1 1 2 -mat 1 -dir 2 2 # direction 2 means shear walls on
vertical axis
element zeroLength 2 3 4 -mat 1 -dir 2 2
element zeroLength 3 6 7 -mat 1 -dir 1 1
element zeroLength 4 1 2 -mat 1 -dir 1 1 # direction 1 means shear wall on
horizontal axis
element zeroLength 11 1 2 -mat 1 -dir 2 2
element zeroLength 12 3 4 -mat 1 -dir 2 2
element zeroLength 13 6 7 -mat 1 -dir 1 1
element zeroLength 14 1 2 -mat 1 -dir 1 1
puts "Material";
# Rigid Diaphragm Element Node Area Modulus
element elasticBeamColumn 5 2 5 1000 100000.0 1e6 1
element elasticBeamColumn 6 4 7 1000 100000.0 1e6 1
element elasticBeamColumn 7 2 7 1000 100000.0 1e6 1
element elasticBeamColumn 8 5 7 1000 100000.0 1e6 1
element elasticBeamColumn 9 4 5 1000 100000.0 1e6 1
element elasticBeamColumn 10 2 4 1000 100000.0 1e6 1

```

#Wall E Archetype ID 3

```
model BasicBuilder -ndm 2 -ndf 3;          # Define the model builder,
ndm=#dimension, ndf=#dofs
# define GEOMETRY -----
node 1 0 0;
node 2 0 0;
node 3 720 0;
node 4 720 0;
node 5 720 420;
node 6 0 420;
node 7 0 420;
puts "Node"

# Single point constraints -- Boundary Conditions
fix 1 1 1 1;          # node DX DY RZ
fix 2 0 0 1;
fix 3 1 1 1;
fix 4 0 0 1;
fix 5 0 0 1;
fix 6 1 1 1;
fix 7 0 0 1;
puts "Fix";

#rigidLink $type $masterNodeTag $slaveNodeTag
rigidLink bar 2 4 5 7
puts "Diaphragm";

# Total dead load of the bulding      total weight 68184 lbs /4= 17046 lbs
Mass: (17046/1000)/386= 0.04416

mass 2 0.04416 0.04416 0;
mass 4 0.04416 0.04416 0;
mass 5 0.04416 0.04416 0;
mass 7 0.04416 0.04416 0;
puts "Mass";
# Wall E 8x8
## Materials ;
set F0 10.966 ;# kip
set FI 1.1 ;# kip
set DU 2.58 ;# in
set S0 30.314 ;# kip/in      stiffness original model is 13.6 kip/in
set R1 0.01
set R2 -0.07
set R3 1.0
set R4 0.01
```

```

set alph 0.75
set bet 1.1

uniaxialMaterial SAWS 1 $F0 $FI $DU $S0 $R1 $R2 $R3 $R4 $alph $bet
puts "Saws";

## Transformation
geomTransf Linear 1
## Define Model
element zeroLength 1 1 2 -mat 1 -dir 2 2 # direction 2- means shear walls on
vertical axis
element zeroLength 2 3 4 -mat 1 -dir 2 2
element zeroLength 3 6 7 -mat 1 -dir 1 1
element zeroLength 4 1 2 -mat 1 -dir 1 1 # direction 1- means shear wall on
horizontal axis
element zeroLength 11 1 2 -mat 1 -dir 2 2
element zeroLength 12 3 4 -mat 1 -dir 2 2
element zeroLength 13 6 7 -mat 1 -dir 1 1
element zeroLength 14 1 2 -mat 1 -dir 1 1
puts "Material";
# Rigid Diaphragm Element Node Area Modulus
element elasticBeamColumn 5 2 5 1000 100000.0 1e6 1
element elasticBeamColumn 6 4 7 1000 100000.0 1e6 1
element elasticBeamColumn 7 2 7 1000 100000.0 1e6 1
element elasticBeamColumn 8 5 7 1000 100000.0 1e6 1
element elasticBeamColumn 9 4 5 1000 100000.0 1e6 1
element elasticBeamColumn 10 2 4 1000 100000.0 1e6 1

```

#Wall E Archetype ID 5

```
model BasicBuilder -ndm 2 -ndf 3;          # Define the model builder,
ndm=#dimension, ndf=#dofs

# define GEOMETRY -----
# Floor
node 1 0 0;
node 2 0 0;
node 3 600 0;
node 4 600 0;
node 5 600 360;
node 6 0 360;
node 7 0 360;
# Roof
node 8 600 0;
node 9 1200 0;
node 10 1200 360 ;
node 11 600 360;
puts "Node"
# Single point constraints -- Boundary Conditions
# Floor
fix 1 1 1 1;          # node DX DY RZ
fix 2 0 0 1;
fix 3 1 1 1;
fix 4 0 0 1;
fix 5 0 0 1;
fix 6 1 1 1;
fix 7 0 0 1;

# Roof
fix 8 0 1 1;
fix 9 0 0 1;
fix 10 0 0 1 ;
fix 11 0 1 1;

puts "Fix";

#rigidLink $type $masterNodeTag $slaveNodeTag
rigidLink bar 2 4 5 7
puts "FloorRigid";
rigidLink bar 8 9 10 11
puts "RoofRigid";

# Total dead load of the first floor   firstfloor weight 92.30 kips /4= 23.0755
kips          Mass: 23.0755/386= 0.05978 kips.in^2/sec
```

```

mass 2 0.05978 0.05978 0;
mass 4 0.05978 0.05978 0;
mass 5 0.05978 0.05978 0;
mass 7 0.05978 0.05978 0;
# Total dead load of the roof      roof weight 55.37 kips /4= 13.8425 kips
Mass: 13.8425/386= 0.0358614 kips.in^2/sec
mass 8 0.0358614 0.0358614 0;
mass 9 0.0358614 0.0358614 0;
mass 10 0.0358614 0.0358614 0;
mass 11 0.0358614 0.0358614 0;
puts "Mass";
# Wall E 8x8
## Materials ;
set F0 10.966 ;# kip
set FI 1.1 ;# kip
set DU 2.58 ;# in
set S0 30.314 ;# kip/in      stiffness original model is 13.6 kip/in
set R1 0.01
set R2 -0.07
set R3 1.0
set R4 0.01
set alph 0.75
set bet 1.1

uniaxialMaterial SAWS 1 $F0 $FI $DU $S0 $R1 $R2 $R3 $R4 $alph $bet
puts "Saws";

## Transformation
geomTransf Linear 1
## Define Model
element zeroLength 200 1 2 -mat 1 -dir 2 2      # direction 2->1 means shear
walls on vertical axis
element zeroLength 400 3 4 -mat 1 -dir 2 2

element zeroLength 201 1 2 -mat 1 -dir 1 1
element zeroLength 202 1 2 -mat 1 -dir 1 1
element zeroLength 203 1 2 -mat 1 -dir 1 1
element zeroLength 204 1 2 -mat 1 -dir 1 1

element zeroLength 701 6 7 -mat 1 -dir 1 1
element zeroLength 702 6 7 -mat 1 -dir 1 1
element zeroLength 703 6 7 -mat 1 -dir 1 1
element zeroLength 704 6 7 -mat 1 -dir 1 1

puts "floorMaterial";

```

```
element zeroLength 801 4 8 -mat 1 -dir 1 1
element zeroLength 802 4 8 -mat 1 -dir 1 1
element zeroLength 803 4 8 -mat 1 -dir 1 1
```

```
element zeroLength 1101 5 11 -mat 1 -dir 1 1
element zeroLength 1102 5 11 -mat 1 -dir 1 1
element zeroLength 1103 5 11 -mat 1 -dir 1 1
```

```
puts "roofMaterial";
```

```
# Rigid Diaphragm Element Node Area Modulus
element elasticBeamColumn 1 2 4 1000 100000.0 1e6 1
element elasticBeamColumn 2 4 5 1000 100000.0 1e6 1
element elasticBeamColumn 3 5 7 1000 100000.0 1e6 1
element elasticBeamColumn 4 2 7 1000 100000.0 1e6 1
element elasticBeamColumn 5 2 5 1000 100000.0 1e6 1
element elasticBeamColumn 6 4 7 1000 100000.0 1e6 1
```

```
element elasticBeamColumn 7 8 9 1000 100000.0 1e6 1
element elasticBeamColumn 8 9 10 1000 100000.0 1e6 1
element elasticBeamColumn 9 10 11 1000 100000.0 1e6 1
element elasticBeamColumn 10 8 11 1000 100000.0 1e6 1
element elasticBeamColumn 11 8 10 1000 100000.0 1e6 1
element elasticBeamColumn 12 9 11 1000 100000.0 1e6 1
```

Appendix H

Sample OpenSees Pinching4 data file

```
#Wall E Archetype ID 5

model BasicBuilder -ndm 2 -ndf 3;          # Define the model builder,
ndm=#dimension, ndf=#dofs

# define GEOMETRY -----
# Floor
node 1 0 0;
node 2 0 0;
node 3 600 0;
node 4 600 0;
node 5 600 360;
node 6 0 360;
node 7 0 360;
# Roof
node 8 600 0;
node 9 1200 0;
node 10 1200 360 ;
node 11 600 360;

puts "Node"

# Single point constraints -- Boundary Conditions
# Floor
fix 1 1 1 1;          # node DX DY RZ
fix 2 0 0 1;          # node DX DY RZ
fix 3 1 1 1;
fix 4 0 0 1;          # node DX DY RZ
fix 5 0 0 1;          # node DX DY RZ
fix 6 1 1 1;
fix 7 0 0 1;

# Roof
fix 8 0 1 1;
fix 9 0 0 1;
fix 10 0 0 1 ;
fix 11 0 1 1;

puts "Fix";

#rigidLink $type $masterNodeTag $slaveNodeTag
rigidLink bar 2 4 5 7
puts "FloorRigid";
rigidLink bar 8 9 10 11
puts "RoofRigid";
```

```
# Total dead load of the first floor    first floor weight 84.84.30 kips /4= 21.20883
kips      Mass: 21.20883/386= 0.05495 kips.in^2/sec
# the weight has been revised based on (11/2) thickness of Cement Plaster. July
03/2012
```

```
mass 2 0.05495 0.05495 0;
mass 4 0.05495 0.05495 0;
mass 5 0.05495 0.05495 0;
mass 7 0.05495 0.05495 0;
```

```
# Total dead load of the roof    roof weight 51.64 kips /4= 12.90917 kips
Mass: 12.90917/386= 0.03344 kips.in^2/sec
```

```
mass 8 0.03344 0.03344 0;
mass 9 0.03344 0.03344 0;
mass 10 0.03344 0.03344 0;
mass 11 0.03344 0.03344 0;
puts "Mass";
# Wall E 8x8
```

```
## please keep the following procedures on the same path
```

```
source procUniaxialPinching.tcl
```

```
#source procRCycDAns.tcl
```

```
##### Positive/Negative envelope Stress/Load
```

```
### stress1 stress2 stress3 stress4
```

```
set pEnvelopeStress [list 6.0 17.2 18.2 6.35]
```

```
set nEnvelopeStress [list -6.0 -17.2 -18.2 -6.35]
```

```
##### Positive/Negative envelope Strain/Deformation
```

```
### strain1 strain2 strain3 strain4
```

```
set pEnvelopeStrain [list 0.14 1.3 3.7 5.3]
```

```
set nEnvelopeStrain [list -0.14 -1.3 -3.7 -5.3]
```

```
##### Ratio of maximum deformation at which reloading begins
```

```
### Pos_env. Neg_env.
```

```
set rDisp [list 0.8 0.8]
```

```
##### Ratio of envelope force (corresponding to maximum deformation) at which
reloading begins
```

```
### Pos_env. Neg_env.
```

```
set rForce [list 0.20 0.20]
```

```
##### Ratio of monotonic strength developed upon unloading
```

```
### Pos_env. Neg_env.
```

```
set uForce [list 0.05 0.05]
```

```
##### Coefficients for Unloading Stiffness degradation
```

```
### gammaK1 gammaK2 gammaK3 gammaK4 gammaKLimit
```

```
set gammaK [list 0.8 0.15 0.05 0.0 0.8]
```

```
##### Coefficients for Reloading Stiffness degradation
```

```
### gammaD1 gammaD2 gammaD3 gammaD4 gammaDLimit
```

```
set gammaD [list 0.5 0.0 2.0 0.0 0.0]
```

```
##### Coefficients for Strength degradation
```

```

### gammaF1 gammaF2 gammaF3 gammaF4 gammaFLimit
set gammaF [list 1.5 0.0 2.0 0.0 0.68]
set gammaE 10
# material ID
set matID 1
# damage type (option: "energy", "cycle")
set dam "energy"
# add the material to domain through the use of a procedure
procUniaxialPinching $matID $pEnvelopeStress $nEnvelopeStress $pEnvelopeStrain
$nEnvelopeStrain $rDisp $rForce $uForce $gammaK $gammaD $gammaF $gammaE
$dam

## Transformation
geomTransf Linear 1
## Define Model
element zeroLength 200 1 2 -mat 1 -dir 2 2
element zeroLength 400 3 4 -mat 1 -dir 2 2

element zeroLength 201 1 2 -mat 1 -dir 1 1
element zeroLength 202 1 2 -mat 1 -dir 1 1
element zeroLength 203 1 2 -mat 1 -dir 1 1
element zeroLength 204 1 2 -mat 1 -dir 1 1

element zeroLength 701 6 7 -mat 1 -dir 1 1
element zeroLength 702 6 7 -mat 1 -dir 1 1
element zeroLength 703 6 7 -mat 1 -dir 1 1
element zeroLength 704 6 7 -mat 1 -dir 1 1

puts "floorMaterial";

element zeroLength 801 4 8 -mat 1 -dir 1 1
element zeroLength 802 4 8 -mat 1 -dir 1 1
element zeroLength 803 4 8 -mat 1 -dir 1 1

element zeroLength 1101 5 11 -mat 1 -dir 1 1
element zeroLength 1102 5 11 -mat 1 -dir 1 1
element zeroLength 1103 5 11 -mat 1 -dir 1 1

puts "roofMaterial";

# Rigid Diaphragm Element Node Area Modulus
element elasticBeamColumn 1 2 4 1000 100000.0 1e6 1
element elasticBeamColumn 2 4 5 1000 100000.0 1e6 1
element elasticBeamColumn 3 5 7 1000 100000.0 1e6 1
element elasticBeamColumn 4 2 7 1000 100000.0 1e6 1
element elasticBeamColumn 5 2 5 1000 100000.0 1e6 1
element elasticBeamColumn 6 4 7 1000 100000.0 1e6 1
puts "floorDiaphragm"
element elasticBeamColumn 7 8 9 1000 100000.0 1e6 1
element elasticBeamColumn 8 9 10 1000 100000.0 1e6 1
element elasticBeamColumn 9 10 11 1000 100000.0 1e6 1
element elasticBeamColumn 10 8 11 1000 100000.0 1e6 1

```

```
element elasticBeamColumn 11 8 10 1000 100000.0 1e6 1  
element elasticBeamColumn 12 9 11 1000 100000.0 1e6 1
```

```
puts "roofDiaphragm"
```

Appendix I

Sample C# Program File

```
using System;
using System.Collections.Generic;
using System.Linq;
using System.Text;
using System.IO;
namespace GrounMotion2
{
    class Program
    {
        // public static string path = @"C:\Thesis\SAWS\";
        public static string path = @"C:\Thesis\Pinching4\";

        # region FileNames

        static void Main(string[] args)
        {
            //varlistScaleFactorsByFileNames
            GetListScaleFactorsByFileNamesForWallB1DesignFourWall8x8();
            //varlistScaleFactorsByFileNames
            GetListScaleFactorsByFileNamesForWalle2DesignDouble8x8();
            //var
            listScaleFactorsByFileNames
            GetListScaleFactorsByFileNamesForForWalle3Max();
            //var
            listScaleFactorsByFileNames
            GetListScaleFactorsByFileNamesForPinchingE3Max();

            var listNormalizationFactors = GetListNormalizationFactorsByFileNames();
            var listDeltaTs = GetListDeltaTsByFileNames();
            var listNPoints = GetListNPointsByFileNames();

            //CalculatePGV();
            //CalculatePGA(listScaleFactorsByFileNames);

            # region InputFiles
            //CreateInputFilesForWallB1DesignFourWall8x8(listScaleFactorsByFileNames,
            listNormalizationFactors, listDeltaTs, listNPoints);

            //CreateInputFilesForWalle2DesignDouble8x8(listScaleFactorsByFileNames,
            listNormalizationFactors, listDeltaTs, listNPoints);

            //CreateInputFilesForWalle3Max(listScaleFactorsByFileNames,listNormalizationFacto
            rs, listDeltaTs, listNPoints);
```

```

//CreateInputFilesForPinchingE3Max(listScaleFactorsByFileNames,
listNormalizationFactors, listDeltaTs, listNPoints);

#endregion

CreateLaunchFile(listScaleFactorsByFileNames);

//PostProcess

// CalculateDMax(listScaleFactorsByFileNames);
// CalculateDMaxForTwoStories(listScaleFactorsByFileNames);
// MakeFinalOutput();

}

static void MakeFinalOutput()
{
    List<string[]> result = new List<string[]>();
    List<string> list = new List<string>();
    using (var s = File.OpenText(Path.Combine(path, @"DispMax.txt")))
    {
        var line = s.ReadLine().Split();
        var current = line[0];
        while (!s.EndOfStream)
        {
            line = s.ReadLine().Split();
            if (line[0] != current)
            {
                current = line[0];
                result.Add(list.ToArray());
                list = new List<string>();
            }
            list.Add(line[0] + line[1] + line[2] + line[3] + line[4] + line[5]);
        }
        result.Add(list.ToArray());
    }

    int maxLength = (from item in result select item.Length).Max();
    using (var writer = File.CreateText(Path.Combine(path, @"Final.csv")))
    {
        var counter = 0;
        writer.WriteLine();
        while (counter < maxLength)
        {
            var resultLine = "";
            foreach (var item in result)
            {
                if (counter >= item.Length)
                {
                    resultLine += ", " + ", " + ", " , , , ";
                }
            }
        }
    }
}

```



```

//a.Add("7b_NGA_no_1111_NIS090.AT2", GetListScalesByMax(3.4));

//a.Add("20a_NGA-1485-CHICHITCU045-EAT2.AT2", GetListScalesByMax(3.4));

//a.Add("3a_NGA_no_1602_BOL000.AT2", GetListScalesByMax(3.6));

//a.Add("17b_NGA_no_725_B-POE360.AT2", GetListScalesByMax(3.6));
//a.Add("6a_NGA_no_174_H-E11140.AT2", GetListScalesByMax(3.6));

//a.Add("20b_NGA-1485-CHICHITCU045-NAT2.AT2", GetListScalesByMax(3.8);
//a.Add("2b_NGA_no_960_LOS270.AT2", GetListScalesByMax(3.8));

//a.Add("4a_NGA_no_1787_HEC000.AT2", GetListScalesByMax(3.8));
//a.Add("22a_NGA_no_125_A-TMZ000.AT2", GetListScalesByMax(4.0));
//a.Add("13b_NGA_no_752_CAP090.AT2", GetListScalesByMax(4.6));
//a.Add("8b_NGA_no_1116_SHI090.AT2", GetListScalesByMax(4.5));

//a.Add("9a_NGA_no_1158_DZC180.AT2", GetListScalesByMax(4.4));

//a.Add("10b_NGA_no_1148_ARC090.AT2", GetListScalesByMax(4.9));
//a.Add("15a_NGA-no-1633-MANJILABBARL.AT2", GetListScalesByMax(4.5));

//a.Add("21b_NGA_no_68_PEL180.AT2", GetListScalesByMax(4.4));
//a.Add("16b_NGA_no_721_B-ICC090.AT2", GetListScalesByMax(4.4));

//a.Add("11b_NGA_no_900_YER360.AT2", GetListScalesByMax(5.3));
//a.Add("12a-NGA-848-LanderCoolwaterLN.AT2", GetListScalesByMax(5.6));

//a.Add("6b_NGA_no_174_H-E11230.AT2", GetListScalesByMax(5.0));
//a.Add("18b_NGA_no_829_RIO360.AT2", GetListScalesByMax(5.8));

//a.Add("19a_NGA_no_1244_CHY101-E.AT2", GetListScalesByMax(5.7));

//a.Add("10a_NGA_no_1148_ARC000.AT2", GetListScalesByMax(8.7));

//a.Add("14a_NGA_no_767_G03000.AT2", GetListScalesByMax(6.8));

return a;
}

```

```

static Dictionary<string, List<double>>
GetListScaleFactorsByFileNamesForWallE2DesignDouble8x8()
{
    var a = new Dictionary<string, List<double>>();

    //a.Add("12b-NGA-848-LanderCoolwaterTR.AT2", GetListScalesByMax(1.9));
    //a.Add("22b_NGA_no_125_A-TMZ270.AT2", GetListScalesByMax(3.0));
    //a.Add("3b_NGA_no_1602_BOL090.AT2", GetListScalesByMax(2.5));
    //a.Add("13a_NGA_no_752_CAP000.AT2", GetListScalesByMax(2.4));
    //a.Add("1b_NGA_no_953_MUL279.AT2", GetListScalesByMax(2.4));
    //a.Add("13b_NGA_no_752_CAP090.AT2", GetListScalesByMax(2.5));
    //a.Add("21a_NGA_no_68_PEL090.AT2", GetListScalesByMax(2.6));
}

```

```

        //a.Add("2a_NGA_no_960_LOS000.AT2", GetListScalesByMax(2.6));
        //a.Add("20b_NGA-1485-CHICHITCU045-NAT2.AT2",
GetListScalesByMax(2.7));
        //a.Add("1a_NGA_no_953_MUL009.AT2", GetListScalesByMax(2.8));
        //a.Add("7a_NGA_no_1111_NIS000.AT2", GetListScalesByMax(3.0));
        //a.Add("4b_NGA_no_1787_HEC090.AT2", GetListScalesByMax(3.0));
        //a.Add("20a_NGA-1485-CHICHITCU045-EAT2.AT2", GetListScalesByMax(3.0));
        //a.Add("8a_NGA_no_1116_SHI000.AT2", GetListScalesByMax(2.8));
        //a.Add("11a_NGA_no_900_YER270.AT2", GetListScalesByMax(3.1));
        //a.Add("18a_NGA_no_829_RIO270.AT2", GetListScalesByMax(3.3));
        //a.Add("17a_NGA_no_725_B-POE270.AT2", GetListScalesByMax(3.4));
        //a.Add("7b_NGA_no_1111_NIS090.AT2", GetListScalesByMax(3.4));
        //a.Add("15b_NGA-no-1633-MANJILABBAR.AT2", GetListScalesByMax(3.4));
        //a.Add("2b_NGA_no_960_LOS270.AT2", GetListScalesByMax(3.6));
        //a.Add("5a_NGA_no_169_H-DLT262.AT2", GetListScalesByMax(3.6));
        //a.Add("3a_NGA_no_1602_BOL000.AT2", GetListScalesByMax(3.8));
        //a.Add("17b_NGA_no_725_B-POE360.AT2", GetListScalesByMax(4.0));
        //a.Add("6a_NGA_no_174_H-E11140.AT2", GetListScalesByMax(4.1));
        //a.Add("19b_NGA_no_1244_CHY101-N.AT2", GetListScalesByMax(4.2));
        //a.Add("8b_NGA_no_1116_SHI090.AT2", GetListScalesByMax(4.2));
        //a.Add("16a_NGA_no_721_B-ICC000.AT2", GetListScalesByMax(4.2));
        //a.Add("9b_NGA_no_1158_DZC270.AT2", GetListScalesByMax(4.4));
        //a.Add("14b_NGA_no_767_G03090.AT2", GetListScalesByMax(4.4));
        //a.Add("4a_NGA_no_1787_HEC000.AT2", GetListScalesByMax(4.6));
        //a.Add("15a_NGA-no-1633-MANJILABBARL.AT2", GetListScalesByMax(4.6));
        //a.Add("16b_NGA_no_721_B-ICC090.AT2", GetListScalesByMax(4.8));
        //a.Add("9a_NGA_no_1158_DZC180.AT2", GetListScalesByMax(4.8));
        //a.Add("12a_NGA-848-LanderCoolwaterLN.AT2", GetListScalesByMax(5.0));
        //a.Add("21b_NGA_no_68_PEL180.AT2", GetListScalesByMax(5.0));
        //a.Add("22a_NGA_no_125_A-TMZ000.AT2", GetListScalesByMax(5.0));
        //a.Add("6b_NGA_no_174_H-E11230.AT2", GetListScalesByMax(5.2));
        //a.Add("18b_NGA_no_829_RIO360.AT2", GetListScalesByMax(5.4));
        //a.Add("11b_NGA_no_900_YER360.AT2", GetListScalesByMax(5.6));
        //a.Add("14a_NGA_no_767_G03000.AT2", GetListScalesByMax(6.2));
        // a.Add("5b_NGA_no_169_H-DLT352.AT2", GetListScalesByMax(2.8));
        //a.Add("19a_NGA_no_1244_CHY101-E.AT2", GetListScalesByMax(6.2));
        //a.Add("10a_NGA_no_1148_ARC000.AT2", GetListScalesByMax(7.0));
        //a.Add("10b_NGA_no_1148_ARC090.AT2", GetListScalesByMax(6.4));
    return a;
}

```

```

static Dictionary<string, List<double>>
GetListScaleFactorsByFileNamesForPinchingE3Max()
{
    var a = new Dictionary<string, List<double>>();

    //a.Add("10b_NGA_no_1148_ARC090.AT2", GetListScalesByMax(8.0));
    //a.Add("14b_NGA_no_767_G03090.AT2", GetListScalesByMax(5.0));
    //a.Add("19a_NGA_no_1244_CHY101-E.AT2", GetListScalesByMax(8.0));
    //a.Add("4b_NGA_no_1787_HEC090.AT2", GetListScalesByMax(5.0));
    //a.Add("5a_NGA_no_169_H-DLT262.AT2", GetListScalesByMax(5.0));
}

```

```

//a.Add("12b-NGA-848-LanderCoolwaterTR.AT2", GetListScalesByMax(5.0));
//a.Add("5b_NGA_no_169_H-DLT352.AT2", GetListScalesByMax(5.0));
//a.Add("1b_NGA_no_953_MUL279.AT2", GetListScalesByMax(5.0));
//a.Add("3b_NGA_no_1602_BOL090.AT2", GetListScalesByMax(5.0));
//a.Add("7b_NGA_no_1111_NIS090.AT2", GetListScalesByMax(5.0));
//a.Add("1a_NGA_no_953_MUL009.AT2", GetListScalesByMax(5.0));
//a.Add("21a_NGA_no_68_PEL090.AT2", GetListScalesByMax(5.0));
//a.Add("13b_NGA_no_752_CAP090.AT2", GetListScalesByMax(5.0));
//a.Add("8a_NGA_no_1116_SHI000.AT2", GetListScalesByMax(5.0));
//a.Add("11a_NGA_no_900_YER270.AT2", GetListScalesByMax(5.0));
//a.Add("15b_NGA-no-1633-MANJILABBAR.AT2", GetListScalesByMax(5.0));
//a.Add("18a_NGA_no_829_RIO270.AT2", GetListScalesByMax(5.0));
//a.Add("2a_NGA_no_960_LOS000.AT2", GetListScalesByMax(5.0));
//a.Add("2b_NGA_no_960_LOS270.AT2", GetListScalesByMax(5.0));
//a.Add("3a_NGA_no_1602_BOL000.AT2", GetListScalesByMax(4.0));
//a.Add("20a_NGA-1485-CHICHITCU045-EAT2.AT2", GetListScalesByMax(4.0));
//a.Add("22b_NGA_no_125_A-TMZ270.AT2", GetListScalesByMax(5.0));
//a.Add("17a_NGA_no_725_B-POE270.AT2", GetListScalesByMax(4.0));
//a.Add("13a_NGA_no_752_CAP000.AT2", GetListScalesByMax(5.0));
//a.Add("7a_NGA_no_1111_NIS000.AT2", GetListScalesByMax(5.0));
//a.Add("6a_NGA_no_174_H-E11140.AT2", GetListScalesByMax(5.0));
//a.Add("8b_NGA_no_1116_SHI090.AT2", GetListScalesByMax(5.0));
//a.Add("17b_NGA_no_725_B-POE360.AT2", GetListScalesByMax(5.0));
//a.Add("19b_NGA_no_1244_CHY101-N.AT2", GetListScalesByMax(5.0));
//a.Add("16a_NGA_no_721_B-ICC000.AT2", GetListScalesByMax(5.0));
//a.Add("4a_NGA_no_1787_HEC000.AT2", GetListScalesByMax(5.0));
//a.Add("6b_NGA_no_174_H-E11230.AT2", GetListScalesByMax(5.0));
//a.Add("20b_NGA-1485-CHICHITCU045-NAT2.AT2",
GetListScalesByMax(5.0));
//a.Add("9b_NGA_no_1158_DZC270.AT2", GetListScalesByMax(5.0));
//a.Add("18b_NGA_no_829_RIO360.AT2", GetListScalesByMax(5.0));
//a.Add("9a_NGA_no_1158_DZC180.AT2", GetListScalesByMax(5.0));
//a.Add("15a_NGA-no-1633-MANJILABBARL.AT2", GetListScalesByMax(5.0));
//a.Add("16b_NGA_no_721_B-ICC090.AT2", GetListScalesByMax(5.0));
//a.Add("11b_NGA_no_900_YER360.AT2", GetListScalesByMax(5.0));
//a.Add("22a_NGA_no_125_A-TMZ000.AT2", GetListScalesByMax(5.0));
//a.Add("12a-NGA-848-LanderCoolwaterLN.AT2", GetListScalesByMax(5.0));
//a.Add("21b_NGA_no_68_PEL180.AT2", GetListScalesByMax(5.0));
//a.Add("14a_NGA_no_767_G03000.AT2", GetListScalesByMax(5.0));
//a.Add("10a_NGA_no_1148_ARC000.AT2", GetListScalesByMax(6.03));

return a;
}

static Dictionary<string, List<double>>
GetListScaleFactorsByFileNamesForForWalle3Max()
{
var a = new Dictionary<string, List<double>>();

//a.Add("4b_NGA_no_1787_HEC090.AT2", GetListScalesByMax(2.65));
//a.Add("12b-NGA-848-LanderCoolwaterTR.AT2", GetListScalesByMax(1.6));

```

```

//a.Add("13a_NGA_no_752_CAP000.AT2", GetListScalesByMax(2.0));
//a.Add("5b_NGA_no_169_H-DLT352.AT2", GetListScalesByMax(2.1));
//a.Add("1b_NGA_no_953_MUL279.AT2", GetListScalesByMax(2.1));
//a.Add("3b_NGA_no_1602_BOL090.AT2", GetListScalesByMax(2.2));
//a.Add("22b_NGA_no_125_A-TMZ270.AT2", GetListScalesByMax(2.2));
//a.Add("20b_NGA-1485-CHICHITCU045-NAT2.AT2", GetListScalesByMax(2.2));
//a.Add("7b_NGA_no_1111_NIS090.AT2", GetListScalesByMax(2.2));
//a.Add("1a_NGA_no_953_MUL009.AT2", GetListScalesByMax(2.4));
//a.Add("21a_NGA_no_68_PEL090.AT2", GetListScalesByMax(2.32));
//a.Add("13b_NGA_no_752_CAP090.AT2", GetListScalesByMax(2.4));
//a.Add("8a_NGA_no_1116_SHI000.AT2", GetListScalesByMax(2.4));
//a.Add("11a_NGA_no_900_YER270.AT2", GetListScalesByMax(2.6));
//a.Add("20a_NGA-1485-CHICHITCU045-EAT2.AT2", GetListScalesByMax(2.6));
//a.Add("15b_NGA-no-1633-MANJILABBAR.AT2", GetListScalesByMax(2.8));
//a.Add("18a_NGA_no_829_RIO270.AT2", GetListScalesByMax(2.8));
//a.Add("2a_NGA_no_960_LOS000.AT2", GetListScalesByMax(2.45));
//a.Add("5a_NGA_no_169_H-DLT262.AT2", GetListScalesByMax(2.8));
//a.Add("7a_NGA_no_1111_NIS000.AT2", GetListScalesByMax(2.8));
//a.Add("6a_NGA_no_174_H-E11140.AT2", GetListScalesByMax(3.2));
//a.Add("2b_NGA_no_960_LOS270.AT2", GetListScalesByMax(3.2));
//a.Add("3a_NGA_no_1602_BOL000.AT2", GetListScalesByMax(3.4));
//a.Add("17a_NGA_no_725_B-POE270.AT2", GetListScalesByMax(3.4));
//a.Add("8b_NGA_no_1116_SHI090.AT2", GetListScalesByMax(3.4));
//a.Add("17b_NGA_no_725_B-POE360.AT2", GetListScalesByMax(3.4));
//a.Add("14b_NGA_no_767_G03090.AT2", GetListScalesByMax(3.6));
//a.Add("19b_NGA_no_1244_CHY101-N.AT2", GetListScalesByMax(3.6));
//a.Add("16a_NGA_no_721_B-ICC000.AT2", GetListScalesByMax(3.6));
//a.Add("4a_NGA_no_1787_HEC000.AT2", GetListScalesByMax(3.6));
//a.Add("9b_NGA_no_1158_DZC270.AT2", GetListScalesByMax(3.8));
//a.Add("18b_NGA_no_829_RIO360.AT2", GetListScalesByMax(3.8));
//a.Add("9a_NGA_no_1158_DZC180.AT2", GetListScalesByMax(4.2));
//a.Add("15a_NGA-no-1633-MANJILABBARL.AT2", GetListScalesByMax(4.2));
//a.Add("16b_NGA_no_721_B-ICC090.AT2", GetListScalesByMax(4.2));
//a.Add("11b_NGA_no_900_YER360.AT2", GetListScalesByMax(4.4));
//a.Add("10b_NGA_no_1148_ARC090.AT2", GetListScalesByMax(4.55));
//a.Add("6b_NGA_no_174_H-E11230.AT2", GetListScalesByMax(4.4));
//a.Add("22a_NGA_no_125_A-TMZ000.AT2", GetListScalesByMax(4.4));
//a.Add("12a-NGA-848-LanderCoolwaterLN.AT2", GetListScalesByMax(4.4));
//a.Add("21b_NGA_no_68_PEL180.AT2", GetListScalesByMax(4.5));
//a.Add("14a_NGA_no_767_G03000.AT2", GetListScalesByMax(5.2));
//a.Add("19a_NGA_no_1244_CHY101-E.AT2", GetListScalesByMax(5.8));
//a.Add("10a_NGA_no_1148_ARC000.AT2", GetListScalesByMax(8.8));

return a;
}

#endregion

static List<double> GetListScalesByMax(double max)
{
    var result = new List<double>();

```

```

var step = 0.1;
var length = max / step;
var scale = 0.0;

for (int i = 0; i < length; i++)
{
    scale = (i + 1) * step;
    result.Add(scale);
}

return result;
}

static Dictionary<string, double> GetListNormalizationFactorsByFileNames()
{
    #region Nms
    var a = new Dictionary<string, double>();

    a.Add("1a_NGA_no_953_MUL009.AT2", 0.65);
    a.Add("1b_NGA_no_953_MUL279.AT2", 0.65);
    a.Add("2a_NGA_no_960_LOS000.AT2", 0.83);
    a.Add("2b_NGA_no_960_LOS270.AT2", 0.83);
    a.Add("3a_NGA_no_1602_BOL000.AT2", 0.63);
    a.Add("3b_NGA_no_1602_BOL090.AT2", 0.63);
    a.Add("4a_NGA_no_1787_HEC000.AT2", 1.09);
    a.Add("4b_NGA_no_1787_HEC090.AT2", 1.09);
    a.Add("5a_NGA_no_169_H-DLT262.AT2", 1.31);
    a.Add("5b_NGA_no_169_H-DLT352.AT2", 1.31);
    a.Add("6a_NGA_no_174_H-E11140.AT2", 1.01);
    a.Add("6b_NGA_no_174_H-E11230.AT2", 1.01);
    a.Add("7a_NGA_no_1111_NIS000.AT2", 1.03);
    a.Add("7b_NGA_no_1111_NIS090.AT2", 1.03);
    a.Add("8a_NGA_no_1116_SHI000.AT2", 1.1);
    a.Add("8b_NGA_no_1116_SHI090.AT2", 1.1);
    a.Add("9a_NGA_no_1158_DZC180.AT2", 0.69);
    a.Add("9b_NGA_no_1158_DZC270.AT2", 0.69);
    a.Add("10a_NGA_no_1148_ARC000.AT2", 1.36);
    a.Add("10b_NGA_no_1148_ARC090.AT2", 1.36);
    a.Add("11a_NGA_no_900_YER270.AT2", 0.99);
    a.Add("11b_NGA_no_900_YER360.AT2", 0.99);
    a.Add("12a-NGA-848-LanderCoolwaterLN.AT2", 1.15);
    a.Add("12b-NGA-848-LanderCoolwaterTR.AT2", 1.15);
    a.Add("13a_NGA_no_752_CAP000.AT2", 1.09);
    a.Add("13b_NGA_no_752_CAP090.AT2", 1.09);
    a.Add("14a_NGA_no_767_G03000.AT2", 0.88);
    a.Add("14b_NGA_no_767_G03090.AT2", 0.88);
    a.Add("15a_NGA-no-1633-MANJILABBARL.AT2", 0.79);
    a.Add("15b_NGA-no-1633-MANJILABBAR.AT2", 0.79);
    a.Add("16a_NGA_no_721_B-ICC000.AT2", 0.87);
    a.Add("16b_NGA_no_721_B-ICC090.AT2", 0.87);
    a.Add("17a_NGA_no_725_B-POE270.AT2", 1.17);
    a.Add("17b_NGA_no_725_B-POE360.AT2", 1.17);

```

```

a.Add("18a_NGA_no_829_RIO270.AT2", 0.82);
a.Add("18b_NGA_no_829_RIO360.AT2", 0.82);
a.Add("19a_NGA_no_1244_CHY101-E.AT2", 0.41);
a.Add("19b_NGA_no_1244_CHY101-N.AT2", 0.41);
a.Add("20a_NGA-1485-CHICHITCU045-EAT2.AT2", 0.96);
a.Add("20b_NGA-1485-CHICHITCU045-NAT2.AT2", 0.96);
a.Add("21a_NGA_no_68_PEL090.AT2", 2.1);
a.Add("21b_NGA_no_68_PEL180.AT2", 2.1);
a.Add("22a_NGA_no_125_A-TMZ000.AT2", 1.44);
a.Add("22b_NGA_no_125_A-TMZ270.AT2", 1.44);

#endregion

return a;
}

static Dictionary<string, double> GetListDeltaTsByFileNames()
{
    #region Deltats
    var a = new Dictionary<string, double>();

    a.Add("1a_NGA_no_953_MUL009.AT2", 0.01);
    a.Add("1b_NGA_no_953_MUL279.AT2", 0.01);
    a.Add("2a_NGA_no_960_LOS000.AT2", 0.01);
    a.Add("2b_NGA_no_960_LOS270.AT2", 0.01);
    a.Add("3a_NGA_no_1602_BOL000.AT2", 0.01);
    a.Add("3b_NGA_no_1602_BOL090.AT2", 0.01);
    a.Add("4a_NGA_no_1787_HEC000.AT2", 0.01);
    a.Add("4b_NGA_no_1787_HEC090.AT2", 0.01);
    a.Add("5a_NGA_no_169_H-DLT262.AT2", 0.01);
    a.Add("5b_NGA_no_169_H-DLT352.AT2", 0.01);
    a.Add("6a_NGA_no_174_H-E11140.AT2", 0.005);
    a.Add("6b_NGA_no_174_H-E11230.AT2", 0.005);
    a.Add("7a_NGA_no_1111_NIS000.AT2", 0.01);
    a.Add("7b_NGA_no_1111_NIS090.AT2", 0.01);
    a.Add("8a_NGA_no_1116_SHI000.AT2", 0.01);
    a.Add("8b_NGA_no_1116_SHI090.AT2", 0.01);
    a.Add("9a_NGA_no_1158_DZC180.AT2", 0.005);
    a.Add("9b_NGA_no_1158_DZC270.AT2", 0.005);
    a.Add("10a_NGA_no_1148_ARC000.AT2", 0.005);
    a.Add("10b_NGA_no_1148_ARC090.AT2", 0.005);
    a.Add("11a_NGA_no_900_YER270.AT2", 0.02);
    a.Add("11b_NGA_no_900_YER360.AT2", 0.02);
    a.Add("12a-NGA-848-LanderCoolwaterLN.AT2", 0.0025);
    a.Add("12b-NGA-848-LanderCoolwaterTR.AT2", 0.0025);
    a.Add("13a_NGA_no_752_CAP000.AT2", 0.005);
    a.Add("13b_NGA_no_752_CAP090.AT2", 0.005);
    a.Add("14a_NGA_no_767_G03000.AT2", 0.005);
    a.Add("14b_NGA_no_767_G03090.AT2", 0.005);
    a.Add("15a_NGA-no-1633-MANJILABBARL.AT2", 0.02);
    a.Add("15b_NGA-no-1633-MANJILABBAR.AT2", 0.02);
    a.Add("16a_NGA_no_721_B-ICC000.AT2", 0.005);

```

```

a.Add("16b_NGA_no_721_B-ICC090.AT2", 0.005);
a.Add("17a_NGA_no_725_B-POE270.AT2", 0.01);
a.Add("17b_NGA_no_725_B-POE360.AT2", 0.01);
a.Add("18a_NGA_no_829_RIO270.AT2", 0.02);
a.Add("18b_NGA_no_829_RIO360.AT2", 0.02);
a.Add("19a_NGA_no_1244_CHY101-E.AT2", 0.005);
a.Add("19b_NGA_no_1244_CHY101-N.AT2", 0.005);
a.Add("20a_NGA-1485-CHICHITCU045-EAT2.AT2", 0.005);
a.Add("20b_NGA-1485-CHICHITCU045-NAT2.AT2", 0.005);
a.Add("21a_NGA_no_68_PEL090.AT2", 0.01);
a.Add("21b_NGA_no_68_PEL180.AT2", 0.01);
a.Add("22a_NGA_no_125_A-TMZ000.AT2", 0.005);
a.Add("22b_NGA_no_125_A-TMZ270.AT2", 0.005);

#endregion

return a;
}

static Dictionary<string, int> GetListNPointsByFileNames()
{
    #region NPoints
    var a = new Dictionary<string, int>();

    a.Add("1a_NGA_no_953_MUL009.AT2", 2999);
    a.Add("1b_NGA_no_953_MUL279.AT2", 2999);
    a.Add("2a_NGA_no_960_LOS000.AT2", 1999);
    a.Add("2b_NGA_no_960_LOS270.AT2", 1999);
    a.Add("3a_NGA_no_1602_BOL000.AT2", 5590);
    a.Add("3b_NGA_no_1602_BOL090.AT2", 5590);
    a.Add("4a_NGA_no_1787_HEC000.AT2", 4531);
    a.Add("4b_NGA_no_1787_HEC090.AT2", 4531);
    a.Add("5a_NGA_no_169_H-DLT262.AT2", 9992);
    a.Add("5b_NGA_no_169_H-DLT352.AT2", 9992);
    a.Add("6a_NGA_no_174_H-E11140.AT2", 7807);
    a.Add("6b_NGA_no_174_H-E11230.AT2", 7807);
    a.Add("7a_NGA_no_1111_NIS000.AT2", 4096);
    a.Add("7b_NGA_no_1111_NIS090.AT2", 4096);
    a.Add("8a_NGA_no_1116_SHI000.AT2", 4096);
    a.Add("8b_NGA_no_1116_SHI090.AT2", 4096);
    a.Add("9a_NGA_no_1158_DZC180.AT2", 5437);
    a.Add("9b_NGA_no_1158_DZC270.AT2", 5437);
    a.Add("10a_NGA_no_1148_ARC000.AT2", 6000);
    a.Add("10b_NGA_no_1148_ARC090.AT2", 6000);
    a.Add("11a_NGA_no_900_YER270.AT2", 2200);
    a.Add("11b_NGA_no_900_YER360.AT2", 2200);
    a.Add("12a-NGA-848-LanderCoolwaterLN.AT2", 11186);
    a.Add("12b-NGA-848-LanderCoolwaterTR.AT2", 11186);
    a.Add("13a_NGA_no_752_CAP000.AT2", 7991);
    a.Add("13b_NGA_no_752_CAP090.AT2", 7991);
    a.Add("14a_NGA_no_767_G03000.AT2", 7989);
    a.Add("14b_NGA_no_767_G03090.AT2", 7989);

```

```

a.Add("15a_NGA-no-1633-MANJILABBARL.AT2", 2676);
a.Add("15b_NGA-no-1633-MANJILABBAR.AT2", 2676);
a.Add("16a_NGA_no_721_B-ICC000.AT2", 8000);
a.Add("16b_NGA_no_721_B-ICC090.AT2", 8000);
a.Add("17a_NGA_no_725_B-POE270.AT2", 2230);
a.Add("17b_NGA_no_725_B-POE360.AT2", 2230);
a.Add("18a_NGA_no_829_RIO270.AT2", 1800);
a.Add("18b_NGA_no_829_RIO360.AT2", 1800);
a.Add("19a_NGA_no_1244_CHY101-E.AT2", 18000);
a.Add("19b_NGA_no_1244_CHY101-N.AT2", 18000);
a.Add("20a_NGA-1485-CHICHITCU045-EAT2.AT2", 18000);
a.Add("20b_NGA-1485-CHICHITCU045-NAT2.AT2", 18000);
a.Add("21a_NGA_no_68_PEL090.AT2", 2800);
a.Add("21b_NGA_no_68_PEL180.AT2", 2800);
a.Add("22a_NGA_no_125_A-TMZ000.AT2", 7269);
a.Add("22b_NGA_no_125_A-TMZ270.AT2", 7269);

#endregion

return a;
}

static List<double> GetListDeltaTs()
{
#region Deltats
var res = new List<double> {0.010 ,0.010 ,0.010 ,0.010 ,0.010 ,0.010 ,0.010
,0.010 ,0.01 ,0.01 ,
0.005 ,0.005 ,0.010 ,0.010 ,0.010 ,0.010 ,0.005 ,0.005
,0.005 ,0.005 ,
0.020 ,0.020 ,0.0025,0.0025,0.005 ,0.005 ,0.005
,0.005 ,0.020 ,0.020 ,0.005 ,0.005 ,
0.010 ,0.010 ,0.020 ,0.020 ,0.005 ,0.005 ,0.005, 0.005,
0.010 ,0.010 ,0.005 ,0.005};

#endregion

return res;
}

#region Archetype 1

static void CreateInputFilesForWallB1DesignFourWall8x8(Dictionary<string,
List<double>> listScaleFactorsByFileNames, Dictionary<string, double>
listNormalizationFactorsByFileName, Dictionary<string, double>
listDeltaTsByFileName, Dictionary<string, int> listNPointsByFileName)
{
foreach (var fileName in listScaleFactorsByFileNames.Keys)
{
foreach (var scaleFactor in listScaleFactorsByFileNames[fileName])

```

```

    {
        const double g = 32.2 * 12; //in. sec2
        var factor = listNormalizationFactorsByFileName[fileName] * scaleFactor
    * g;

        #region inputString
        var inputString = @"source WallB1DesignFourWall8x8.tcl;
# Define RECORDERS -----
recorder Node -file Results\OutDisp_" + fileName + "_" + scaleFactor + @".out -time -
node 2 4 5 7 -dof 1 disp;                # displacements of free nodes
recorder Node -file Results\OutRBase_" + fileName + "_" + scaleFactor + ".out -time -
node 1 3 6 -dof 1 reaction;            # support reaction \n\r" +
"puts Recorder \n\r" +
"## Units kips-inches \n\r" +
"# DYNAMIC ground-motion analysis -----
- \n\r" +
"# create load pattern \n\r" +
"set accelSeries \"Series -dt " + listDeltaTsByFileName[fileName] + @" -filePath eq/" +
fileName + @" -factor " + factor + "\";    # define acceleration vector from file
(dt=0.01 is associated with the input file gm) \n\r" +
@"pattern UniformExcitation 400 1 -accel $accelSeries;
rayleigh 2.723 0.0 0. 0.;                # set damping based on first eigen mode

# create the analysis
wipeAnalysis;                            # clear previously-define analysis
parameters                               # how it handles boundary conditions
constraints Plain;                        # renumber dof's to minimize band-
numberer Plain;                            width (optimization), if you want to
system BandGeneral;                        # how to store and solve the system of
equations in the analysis
test NormDisplIncr 1.0e-8 10;            # determine if convergence
has been achieved at the end of an iteration step
algorithm Newton;                          # use Newton's solution algorithm:
updates tangent stiffness at every iteration
integrator Newmark 0.5 0.25 ;            # determine the next time step for
an analysis
analysis Transient;                        # define type of analysis: time-
dependent
analyze " + listNPointsByFileName[fileName] + " " + listDeltaTsByFileName[fileName]
+ @";                                     # apply 1000 0.02-sec time steps in analysis

puts Done!
wipe;
";

        #endregion

        File.WriteAllText(Path.Combine(path,@"\inputFiles\", fileName + "_" +
scaleFactor.ToString() + ".tcl"), inputString);
    }
}

```

```

}
#endregion

#region Archetype 2

static void CreateInputFilesForWalle2DesignDouble8x8(Dictionary<string,
List<double>> listScaleFactorsByFileNames, Dictionary<string, double>
listNormalizationFactorsByFileName, Dictionary<string, double>
listDeltaTsByFileName, Dictionary<string, int> listNPointsByFileName)

{
    foreach (var fileName in listScaleFactorsByFileNames.Keys)
    {
        foreach (var scaleFactor in listScaleFactorsByFileNames[fileName])
        {
            const double g = 32.2 * 12; //in. sec2
            var factor = listNormalizationFactorsByFileName[fileName] * scaleFactor
* g;

            #region inputString
            var inputString = @"source E2DesignDouble8x8.tcl;
# Define RECORDERS -----
recorder Node -file Results\OutDisp_" + fileName + "_" + scaleFactor + @".out -time -
node 2 4 5 7 -dof 1 disp; # displacements of free nodes
recorder Node -file Results\OutRBase_" + fileName + "_" + scaleFactor + @".out -time -
node 1 3 6 -dof 1 reaction; # support reaction \n\r" +
"puts Recorder \n\r" +
"## Units kips-inches \n\r" +
"# DYNAMIC ground-motion analysis -----
- \n\r" +
"# create load pattern \n\r" +
"set accelSeries \"Series -dt " + listDeltaTsByFileName[fileName] + @" -filePath eq/" +
fileName + @" -factor " + factor + "\"; # define acceleration vector from file
(dt=0.01 is associated with the input file gm) \n\r" +
@"pattern UniformExcitation 400 1 -accel $accelSeries;
rayleigh 2.62 0.0 0.0; # set damping based on first eigen mode

# create the analysis
wipeAnalysis; # clear previously-define analysis
parameters # how it handles boundary conditions
constraints Plain; # renumber dof's to minimize band-
numberer Plain; width (optimization), if you want to
system BandGeneral; # how to store and solve the system of
equations in the analysis
test NormDispIncr 1.0e-8 10; # determine if convergence
has been achieved at the end of an iteration step
algorithm Newton; # use Newton's solution algorithm:
updates tangent stiffness at every iteration
integrator Newmark 0.5 0.25 ; # determine the next time step for
an analysis

```

```

analysis Transient;                                # define type of analysis: time-
dependent
analyze " + listNPointsByFileName[fileName] + " " + listDeltaTsByFileName[fileName]
+ @";                                             # apply 1000 0.02-sec time steps in analysis

puts Done!
wipe;
";

        #endregion

        File.WriteAllText(Path.Combine(path,@"\inputFiles\", fileName + "_" +
scaleFactor.ToString() + ".tcl"), inputString);

    }
}
}
#endregion

#region Archetype 3

    static void CreateInputFilesForPinchingE3Max(Dictionary<string, List<double>>
listScaleFactorsByFileNames, Dictionary<string, double>
listNormalizationFactorsByFileName, Dictionary<string, double>
listDeltaTsByFileName, Dictionary<string, int> listNPointsByFileName)

{
    foreach (var fileName in listScaleFactorsByFileNames.Keys)
    {
        foreach (var scaleFactor in listScaleFactorsByFileNames[fileName])
        {
            const double g = 32.2 * 12; //in. sec2
            var factor = listNormalizationFactorsByFileName[fileName] * scaleFactor
* g;

            #region inputString
            var inputString = @"source PinchingE3Max.tcl;
# Define RECORDERS -----
recorder Node -file Results\OutDisp_" + fileName + "_" + scaleFactor + @".out -time -
node 2 4 5 7 8 9 10 11 -dof 1 disp;           # displacements of free nodes
recorder Node -file Results\OutRBase_" + fileName + "_" + scaleFactor + ".out -time -
node 1 3 6 -dof 1 reaction;           # support reaction \n\r" +
"puts Recorder \n\r" +
"## Units kips-inches \n\r" +
"# DYNAMIC ground-motion analysis -----
- \n\r" +
"# create load pattern \n\r" +
"set accelSeries \"Series -dt " + listDeltaTsByFileName[fileName] + @" -filePath eq/" +
fileName + @" -factor " + factor + "\";      # define acceleration vector from file
(dt=0.01 is associated with the input file gm) \n\r" +
@"pattern UniformExcitation 400 1 -accel $accelSeries;
rayleigh 1.65 0.0 0.0.;           # set damping based on first eigen mode

```

```

# create the analysis
wipeAnalysis;                                # clear previously-define analysis
parameters                                  # how it handles boundary conditions
constraints Plain;                           # renumber dof's to minimize band-
numberer Plain;                               width (optimization), if you want to
width (optimization), if you want to         # how to store and solve the system of
system BandGeneral;                          equations in the analysis
equations in the analysis                    # determine if convergence
test NormDispIncr 1.0e-8 10;                 # has been achieved at the end of an iteration step
has been achieved at the end of an iteration # use Newton's solution algorithm:
step algorithm Newton;                       updates tangent stiffness at every iteration
algorithm Newton;                             # determine the next time step for
updates tangent stiffness at every iteration  # define type of analysis: time-
integrator Newmark 0.5 0.25 ;                dependent
integrator Newmark 0.5 0.25 ;                 analyze " + listNPointsByFileName[fileName] + " " + listDeltaTsByFileName[fileName]
an analysis analysis Transient;              + @";
dependent                                     # apply 1000 0.02-sec time steps in analysis

puts Done!
wipe;
";

#endregion

File.WriteAllText(Path.Combine(path, @"inputFiles\", fileName + "_" +
scaleFactor.ToString() + ".tcl"), inputString);

}
}
}

static void CreateInputFilesForWalleE3Max(Dictionary<string, List<double>>
listScaleFactorsByFileNames, Dictionary<string, double>
listNormalizationFactorsByFileName, Dictionary<string, double>
listDeltaTsByFileName, Dictionary<string, int> listNPointsByFileName)
{
    foreach (var fileName in listScaleFactorsByFileNames.Keys)
    {
        foreach (var scaleFactor in listScaleFactorsByFileNames[fileName])
        {
            const double g = 32.2 * 12; //in. sec2
            var factor = listNormalizationFactorsByFileName[fileName] * scaleFactor
* g;

            #region inputString
            var inputString = @"source E3TownhouseMax.tcl;
# Define RECORDERS -----
recorder Node -file Results\OutDisp_" + fileName + "_" + scaleFactor + @".out -time -
node 2 4 5 7 8 9 10 11 -dof 1 disp; # displacements of free nodes
recorder Node -file Results\OutRBase_" + fileName + "_" + scaleFactor + ".out -time -
node 1 3 6 -dof 1 reaction; # support reaction \n\r" +
"puts Recorder \n\r" +

```

```

"## Units kips-inches \n\r" +
"# DYNAMIC ground-motion analysis -----
- \n\r" +
"# create load pattern \n\r" +
"set accelSeries \"Series -dt \" + listDeltaTsByFileName[fileName] + @\" -filePath eq/\" +
fileName + @\" -factor \" + factor + "\";      # define acceleration vector from file
(dt=0.01 is associated with the input file gm) \n\r" +
@\"pattern UniformExcitation 400 1 -accel $accelSeries;
rayleigh 1.59 0.0 0. 0.;          # set damping based on first eigen mode

# create the analysis
wipeAnalysis;                    # clear previously-define analysis
parameters                       # how it handles boundary conditions
constraints Plain;               # renumber dof's to minimize band-
numberer Plain;                 # width (optimization), if you want to
width (optimization), if you want to
system BandGeneral;            # how to store and solve the system of
equations in the analysis
test NormDispIncr 1.0e-8 10;    # determine if convergence
has been achieved at the end of an iteration step
algorithm Newton;              # use Newton's solution algorithm:
updates tangent stiffness at every iteration
integrator Newmark 0.5 0.25 ;  # determine the next time step for
an analysis
analysis Transient;           # define type of analysis: time-
dependent
analyze \" + listNPointsByFileName[fileName] + \" \" + listDeltaTsByFileName[fileName]
+ @\";                          # apply 1000 0.02-sec time steps in analysis

puts Done!
wipe;
\";

#endregion

File.WriteAllText(Path.Combine(path, @\"inputFiles\", fileName + \"_\" +
scaleFactor.ToString() + \".tcl\"), inputString);

}
}
}

# endregion

static void CreateLaunchFile(Dictionary<string, List<double>>
listScaleFactorsByFileNames)
{
    var res = \"\";
    foreach (var item in listScaleFactorsByFileNames)
    {
        foreach (var scaleFactor in item.Value)
        {

```

```

        res += "source \"InputFiles/\" + item.Key + @"_" + scaleFactor.ToString() +
".tcl \"\n\r";
        // res += "wipe \n\r";
        res += "puts \"\" \n\r";
        res += "puts \"" + item.Key + @"_" + scaleFactor.ToString() + ".tcl \"\n\r";
        res += "puts \"\" \n\r";
    }
}
File.WriteAllText(Path.Combine(path, "go.tcl"), res);
}

static void CalculatePGV(Dictionary<string, List<double>>
listScaleFactorsByFileNames)
{
    const double g = 32.2 * 12; //in. sec2

    var listPgv = new Dictionary<string, double>();

    foreach (var fileName in listScaleFactorsByFileNames.Keys)
    {
        var pgv = 0.0;
        using (var s = File.OpenText(Path.Combine(@"C:\users\Sara\downloads\",
fileName)))
        {
            // Reads header
            for (int i = 0; i < 3; i++)
                s.ReadLine();

            var info = s.ReadLine().Split();
            var numberOfPoints = info[0];
            var deltaT = Convert.ToDouble(info[4]);

            var velocity = 0.0;

            while (!s.EndOfStream)
            {
                var line = s.ReadLine().Trim().Split(' ');
                foreach (var item in line)
                {
                    if (item != "")
                        velocity += Convert.ToDouble(item) * deltaT;

                    if (Math.Abs(velocity) > pgv)
                        pgv = Math.Abs(velocity);
                }
            }
        }

        listPgv.Add(fileName, pgv * g);
    }
}

```

```

var sortedDict = (from entry in listPgv orderby entry.Value ascending select
entry).ToDictionary(x => x.Key, x => x.Value);

var median = 0.0;
var counter = 0;
if (sortedDict.Count / 2.5 == Math.Floor(sortedDict.Count / 2.0))
{
    counter = (int)(sortedDict.Count / 2);
    median = 0.5 * (sortedDict.ElementAt(counter).Value +
sortedDict.ElementAt(counter + 1).Value);
}
else
{
    counter = (int)((sortedDict.Count + 1) / 2);
    median = sortedDict.ElementAt(counter).Value;
}

using (var writer = File.CreateText(Path.Combine(path, @"\Results.txt")))
{
    foreach (var item in listPgv)
    {
        writer.WriteLine(item.Key + " , " + item.Value);
    }
}

}

static void CalculatePGA(Dictionary<string, List<double>>
listScaleFactorsByFileNames)
{
    // const double g = 32.2 * 12; //in. sec2

    var listPga = new List<double>();

    foreach (var fileName in listScaleFactorsByFileNames.Keys)
    {
        var pga = 0.0;
        using (var s = File.OpenText(Path.Combine(path, @"\eq", fileName)))
        {
            var acceleration = 0.0;

            while (!s.EndOfStream)
            {
                var line = s.ReadLine().Trim().Split(' ');
                foreach (var item in line)
                {
                    if (item != "")
                        acceleration = Convert.ToDouble(item);

                    if (Math.Abs(acceleration) > pga)
                        pga = Math.Abs(acceleration);
                }
            }
        }
    }
}

```

```

    }
}

listPga.Add(pga);
}

using (var writer = File.CreateText(Path.Combine(path,@"\PGAs.txt")))
{
    foreach (var item in listPga)
        writer.WriteLine(item);
}

}

static void CalculatedDMax(Dictionary<string, List<double>>
listScaleFactorsByFileNames)
{
    var maxDispByFileScale = new Dictionary<string, double>();

    foreach (var item in listScaleFactorsByFileNames)
    {
        foreach (var scaleFactor in item.Value)
        {
            var outPutFileName = "OutDisp_" + item.Key + "_" + scaleFactor;

            var maxDisp = 0.0;
            using (var s = File.OpenText(Path.Combine(path,@"Results",
outPutFileName + ".out")))
            {
                while (!s.EndOfStream)
                {
                    var line = s.ReadLine().Split();
                    var disp = Convert.ToDouble(line[1]);
                    if (Math.Abs(disp) > maxDisp)
                        maxDisp = Math.Abs(disp);
                }
            }
            maxDispByFileScale.Add(item.Key + ", " + scaleFactor, maxDisp);
        }
    }

    using (var writer = File.CreateText(Path.Combine(path,@"DispMax.txt")))
    {
        foreach (var item in maxDispByFileScale)
            writer.WriteLine(item.Key+ ", " + item.Value);
    }
}

static void CalculatedDMaxForTwoStories(Dictionary<string, List<double>>
listScaleFactorsByFileNames)
{
    var maxDispByFileScale = new Dictionary<string, double>();

```

```

foreach (var item in listScaleFactorsByFileNames)
{
    foreach (var scaleFactor in item.Value)
    {
        var outPutFileName = "OutDisp_" + item.Key + "_" + scaleFactor;

        var maxDisp1 = 0.0;
        var maxDisp2 = 0.0;

        using (var s = File.OpenText(Path.Combine(path,@"Results",
outPutFileName + ".out")))
        {
            while (!s.EndOfStream)
            {
                var line = s.ReadLine().Split();
                var disp1 = Convert.ToDouble(line[1]);
                var disp2 = Convert.ToDouble(line[5]);

                if (Math.Abs(disp1) > maxDisp1)
                    maxDisp1 = Math.Abs(disp1);

                if (Math.Abs(disp2-disp1) > maxDisp2) //Interstory drift
                    maxDisp2 = Math.Abs(disp2 - disp1);

            }
        }

        var maxDisp = Math.Max(maxDisp1, maxDisp2);

        maxDispByFileScale.Add(item.Key + " , " + scaleFactor, maxDisp);
    }
}

using (var writer = File.CreateText(Path.Combine(path,@"DispMax.txt")))
{
    foreach (var item in maxDispByFileScale)
        writer.WriteLine(item.Key + " , " + item.Value);
}
}
}

```